STRUCTURAL POLYMERS AND MOLECULAR PATHWAYS THAT INFLUENCE TOMATO FRUIT INTEGRITY AND SURFACE QUALITY TRAITS

A Dissertation

Presented to the Faculty of the Graduate School

of Cornell University

In Partial Fulfillment of the Requirements for the Degree of

Doctor of Philosophy

By

Yonghua He

January 2012

STRUCTURAL POLYMERS AND MOLECULAR PATHWAYS THAT INFLUENCE TOMATO FRUIT INTEGRITY AND SURFACE QUALITY TRAITS

Yonghua He, Ph.D.

Cornell University 2012

Plant cuticles are protective, hydrophobic, waxy coverings produced by the epidermal cells of aerial organs of land plant. The variation in fruit cuticle structure or composition may influence many commercially important fruit traits, such as storability/shelf life, surface glossiness, and resistance to desiccation, microbial infection or cracking. Despite the fundamental importance of the fruit cuticle, current knowledge of its synthesis and metabolism is relatively limited. This work describes the cloning and characterization of four tomato fruit cuticle-related mutants, including three *cutin-deficient* mutants (*cd1*, *cd2* and *cd3*) and one early fruit cracking mutant (*hcr1*), each of which provides new insights into fruit cuticles and associated structural polymers.

In the first part of this thesis, the different aspects of plant cuticle biology, such as cuticle structure, functions, monomer biosynthesis and assembly are briefly reviewed, summarizing present knowledge of the cutin biosynthesis pathway. The second part of this research focuses on the map-based cloning of three *cutin-deficient* mutants. The *cd1* mutant was identified

as having a lesion in a gene in the GDSL-motif lipase/hydrolase family. Further research has demonstrated that the CD1 enzyme catalyzes extracellular cutin polymerization at the cuticle formation site. The *cd2* gene was identified as a putative transcription factor in the IV group of the homeodomain-leucine zipper family (HD-Zip IV). The *cd3* gene was identified as a member of CYP86A group in cytochrome P450 family, with possible catalytic activity of ω-hydroxylation to C16 and C18 fatty acids in the cutin biosynthesis pathway. The last part of this research focuses on the detailed characterization of *hypercracking 1* (*hcr1*) mutant, which exhibits early fruit cracking and subsequent massive suberin deposition on the fruit surface. The *HCR1* gene encodes a 3β-hydroxysteroid dehydrogenase/C-4 decarboxylase (3β-HSD/D1), which is a key enzyme in the sterol biosynthesis pathway. Sterol profiling showed that the mutation results in 11~16% reduction of sterol compositions in *hcr1* mutant fruits. Phenotypic and biochemical analysis of the *hcr1* mutant suggests that early fruit cracking probably results from the severe inhibition of cell division/expansion in pericarp. The possible physiological and molecular mechanisms underlying the abnormal cell expansion/division in *hcr1* fruit are discussed.

BIOGRAPHICAL SKETCH

Yonghua He was born September 23rd, 1964 in Sichuan Province, People's Republic of China. He earned his B.S. in Botany in 1985 from the Department of Biology, Lanzhou University, Lanzhou China. In the same year, he started his career as a botanist at the Chengdu Institute of Biology (CIB), Chinese Academy of Sciences (CAS). During his tenure at the CIB, He was engaged in studies of the systematics and natural resources of Genus *Vitis* and *Rosa*, and studies on restoration and reconstruction of degraded mountain ecosystems. He came to Cornell in 2002, and had worked in Dr. Timothy Fahey's Lab in the Department of Natural Resources for three years. His work involved in some ecological projects related to rhizosphere carbon and nitrogen dynamics in forest ecosystems. In 2006, he joined Dr. Rose's research team in the Department of Plant Biology at Cornell. Since then he has been engaged in genetic and molecular biology studies of tomato. In the spring of 2008, he entered the Ph.D. program in the Department of Plant Biology at Cornell University, where he received his doctorate in the Horticulture field in December, 2011.

ACKNOWLEDGEMENTS

I am very grateful to Dr. Jocelyn K.C. Rose for giving me this incredible opportunity to pursue my Ph.D. degree at Cornell University, and for his mentorship and guidance, and also his generosity, patience and encouragement during my PhD study. My background in molecular biology and genetics was almost zero when I joined his lab. Although I had worked on plant resources and ecology for 15 years at the Chengdu Institute of Biology, Chinese Academy of Sciences, my research capability in tackling challenging scientific issues was weak, due to a lack of professional training. Dr. Rose's training not only built my lab skills but also enhanced my strategic and practical insight for addressing research problems. My interests were broad, which sometimes hindered targeted effort; he always guided me to focus on crucial questions. My English pronunciation is poor, but one of the most memorable scenes in my mind during our academic discussion is that Dr. Rose was very patiently teaching me how to pronounce some English words. In this way, I gained not only a wide range of knowledge in genetics and molecular biology, but also the skills necessary to solve scientific problems more wisely and independently. I am also deeply grateful to Dr. Rose for providing most financial support for my Ph.D. program. I sincerely thank the other two members of my committee, Dr. James Giovannoni and Dr. Christopher Watkins, for their valuable insight, suggestions and feedback that

contributed to the completion of my research work. I also greatly appreciate them for devoting their precious time to read and revise my thesis.

I am very thankful to the members of the Rose lab for their valuable suggestions, comments, and help on research and lab work. I would like to give special thanks to Dr. Tal Isaacson, who initiated the mapping project of *cutin-deficient* mutants in our lab and taught me many molecular and genetic techniques. Also special thanks to Dr. Sang Jik Lee, who helped me with a study of the subcellular localization of HCR1 protein. I am very thankful as well to our collaborator Dr. Sonia Osorio-Algar in Dr. Fernie's lab at the Max-Planck Institute for Molecular Plant Physiology in Germany, who did sterol profile analysis for the project.

I am very grateful to Nancy Eannetta, Yimin Xu, Xiaomin Jiang and Dr. Bin Cong for their kind help and for sharing their experience during map-based cloning in Dr. Tanksley's lab. I also appreciate the members of Dr. Scanlon's lab for their assistance with cytological study. I would like to thank Dr. Zamir for providing all of the tomato mutant seeds for this research. I am grateful to the staff and faculty in the Department of Plant Biology and the Department of Horticulture for providing an exciting and collaborative academic and research environment.

Finally, I want to thank my wife Hui Jiang, my daughter Xinyu He and my parents for their generosity, love, and unconditional support. No words can fully express my gratitude to them.

TABLE OF CONTENTS

CHAPTER ONE: LITERATURE REVIEW

Plant Surface Lipid Barrier: Function, Structure, Synthesis and Assembly

The plant cuticle, defined as an extracellular lipid-rich membrane covering aerial organs of plants, is a crucial adaptation of terrestrial plants to their harsh environment on land (Riederer, 2006). The cuticle can also be considered as a cutinized cell wall, because of the nature of its cutin-rich composition and intensive interaction with the underlying polysaccharide cell wall (Dominguez, 2011). The plant cuticle serves mainly as a physical barrier to minimize water loss and pathogen infection, and also to protect the plant against other physical, chemical and biological threats. However, despite its biological importance, some aspects of cuticle biology remain obscure. The studies of plant cuticle biology have been recently reviewed and discussed in detail in several papers (Pollard et al., 2008; Kerstin Koch et al., 2008; Buschhaus and Jetter, 2011; Dominguez, 2011; Javelle, 2011). The different aspects of plant cuticle biology, such as structure, potential functions, monomer biosynthesis and assembly will be summarized in this review.

1.1 The Structure and Composition of Plant Cuticles

1.1.1 The structure of plant cuticle

The plant cuticle is a hydrophobic lipid layer secreted by epidermal cells on their outer surfaces (Fig. 1.1). The biochemical composition of plant cuticles varies among species or organs, but they are basically composed of two main components: cutin and waxes (Jeffree, 2006; Nawrath, 2006). Moreover, the structural organization of the components also follows a similar pattern: a thin epicuticular wax layer on the outer surface, beneath which is a cutin matrix, infiltrated with intracuticular waxes, phenolics and polysaccharides (Jeffree, 2006; Dominguez, et al., 2010) (Fig. 1.1D). Epicuticular waxes are deposited as a relatively uniform and amorphous layer, or in crystal form. The matrix underneath is mainly composed of cutin (accounting for 40–80% by weight). The thickness of this cutin matrix can range from less than 1 μm to 10 μm or more, depending on the species. Intracuticular waxes and phenolic compounds are embedded or trapped in the cutin matrix. On the inner side of the cuticle, cutin is mixed with polysaccharides, such as cellulose, hemicellulose and pectin, which are secreted into the epidermal cell wall. The nature of the interconnections between cutin and cuticle polysaccharides, including specific intermolecular, is currently unclear.

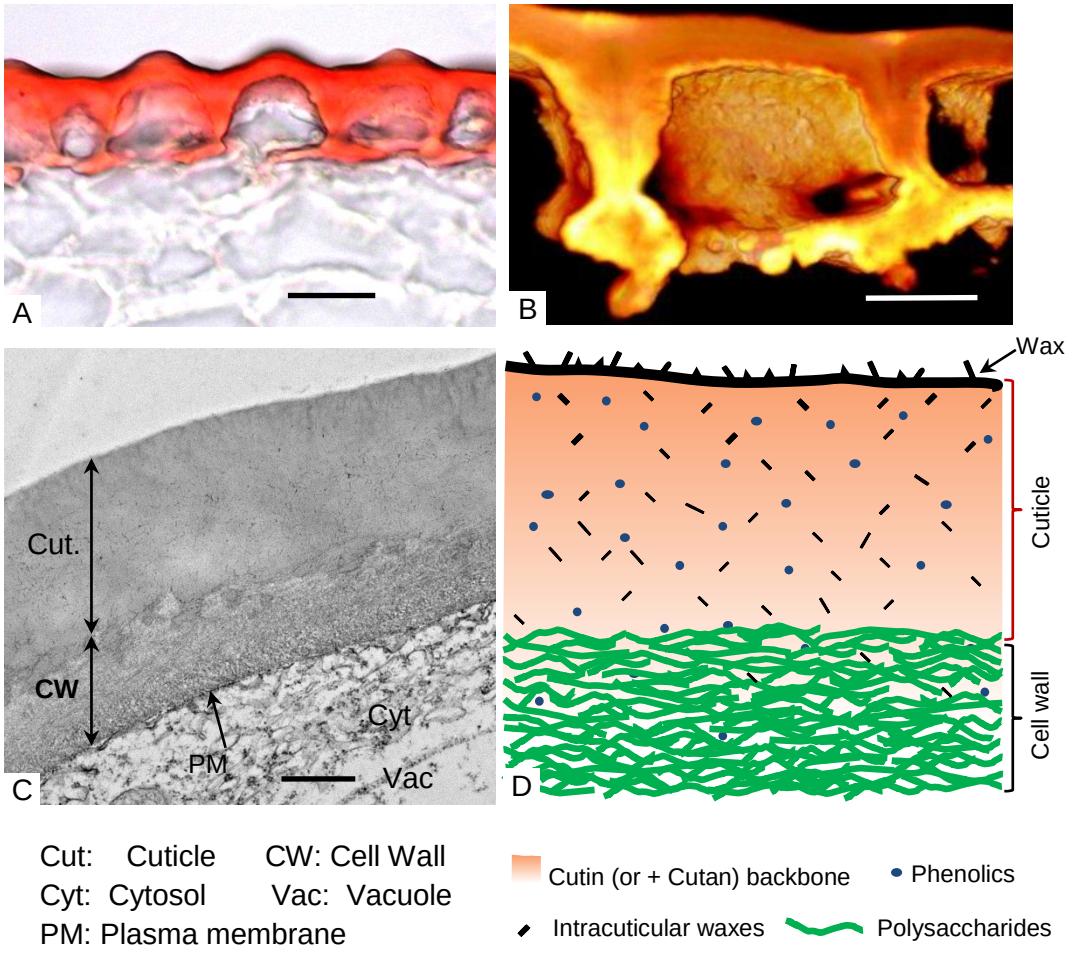

Figure 1.1 The structure of plant cuticle. (A) Light micrograph of the cuticle of tomato fruit (cv. M82) stained with Sudan IV. Scale bar = 20 μm. (B) A 3-D rendering of the tomato fruit cuticle. Scale bar = 10 μm. (C) Transmission electron micrograph of the tomato fruit (cv. M82) cuticle. Scale bar = 500 nm. (D) Structural model of a transverse section of plant cuticle, showing the different components (adapted from Dominguez et al., 2011).

1.1.2 The major compositions of plant cuticle

Cutin, a biological polymer which is cross-linked mainly by ester bonds between its monomers, serves as the structural backbone of the plant cuticle (Nawrath, 2006; Dominguez, et al., 2011) (Fig. 1.2B). Overall, the dominant aliphatic monomers of plant cutin are C16 and C18 ω-hydroxylated fatty acids or dicarboxylic acids (DCA), with or without mid-chain oxygenated substitutions, such as hydroxyl or epoxy groups (Fig. 1.2A). In most plants, the C16 cutin monomers are typically composed of 16-hydroxy-hexadecanoic acid and 9(10), 16- dihydroxyhexadecanoic acid. The main components of the C18 cutin monomers are 9, 10, 18-trihydroxyoctadecanoic acid and 18-hydroxy-9, 10-epoxyoctadecanoic acid, together with their monounsaturated homologs (Fig. 1.2A) (Pollard et al., 2008; Dominguez, et al., 2010). In *Arabidopsis thaliana*, however, dicarboxylic acids (DCA) and glycerol are the predominant cutin monomers. Some very long chain ω-hydroxy fatty acids (C20–C28) have also been identified in the cutin of this model plant (Pollard et al., 2008).

Although the polymerization models of cutin monomers have been proposed (Kolattukudy, 1977; Ramirez et al., 1992), several important aspects of cutin polymer structure are still unclear (Pollard et al., 2008). For instance, it is unknown if cutin exists as discrete polymer molecules or as a highly cross-linked continuum. In some plants, the dominant cutin monomers are

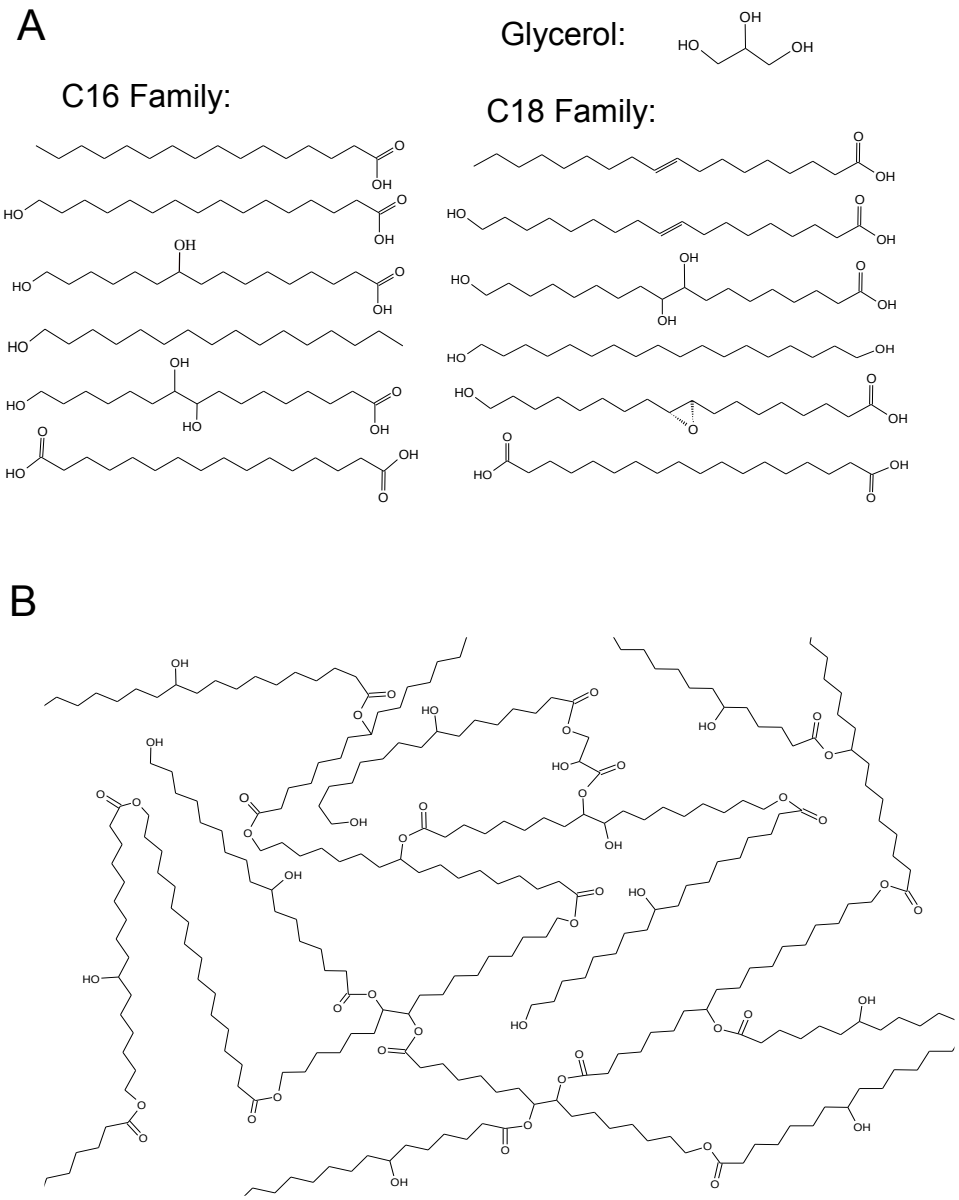

Figure 1.2 Cutin monomers and proposed cutin networking.
(A) Major cutin monomers of C16 and C18 in the plant cuticle.
(B) Proposed schematic networking of a cutin polymer.
(Adapted from Dominguez et al., 2011)

ω-hydroxy fatty acids, where self-polymerization will produce a linear polyester chain. In the case of ω-hydroxy fatty acids with mid-chain oxygen-containing functional groups (epoxy, hydroxy or vicinal diol), the mid-chain hydroxyls may be esterified to create a branched structure on the linear polyester chain (Kolattukudy 2001) (Fig. 1.2B). In *Arabidopsis*, glycerol has been found in the cutin matrix, prompting speculation that the glycerol is probably directly esterified with DCAs or ω-hydroxy fatty acids to produce a crosslinked domain or dendrimer structure. However, this kind of polymerization of cutin monomers is considered as an atypical or non-representative pattern in the majority of plants (Graca et al., 2002; Franke et al., 2005; Pollard et al., 2008).

Waxes are collectively a structurally diverse mixture of discrete hydrophobic compounds that are primarily composed of aliphatic lipids and their derivatives (Nawrath, 2002; Kunst and Samuels, 2003; Kerstin Koch et al., 2008). Generally, both epicuticular and intracuticular waxes are a mixture of primary and secondary alcohols, *n*-aldehydes, *n*-alkanes, ketones, wax esters and very long chain fatty acids (VLCFAs) with chain lengths typically in the range C20 to C34, and in the case of wax esters (two connected chains), about 60 carbons. Several reviews have addressed the chemical composition of plant waxes in detail, and a long list of rare and uncommon wax compositions has been reported (Baker, 1982; Riederer and Markstadter, 1996; Kunst and Samuels, 2003; Jetter et al., 2006). In addition, other

compounds, such as triterpenoids and phenylpropanoids also can be detected in the wax fraction.

The epicuticular wax may be deposited as a film or in the form of crystals. In contrast, intracuticular waxes are consider to be embedded into cutin and can be extracted by organic solvents. Direct evidence has suggested that the compositional differences between epicuticular and intracuticular waxes are significant in both quality and quantity. The mechanism causing this wax fractionation difference remains unclear but it may be influenced, at least in part, by spontaneous partitioning due to the physicochemical properties of the wax compounds and interactions with other intracuticular polymers (Buschhaus and Jetter, 2011). In addition, it has been observed that the wax composition of the plant cuticle is highly variable among the organs or plant species, and may also be significantly altered by some environmental factors (Jetter and Schaffer, 2001; Cameron et al., 2006).

Cutan is non-saponifiable lipid polymer existing in the cuticle of some plants, either as a substitute for, or in combination with cutin (Kolattukudy, 1996). A common characteristic of cutan polymers is their resistance to de-esterification by alkaline hydrolysis (e.g. hot BF_3/methanol). Cutan is often considered to be composed of poly-unsaturated fatty acid derivatives, typically linked to each other by ether bonds, as distinct from the ester bonds that exist in cutin polymers (Villena et al., 1999).

Cutan is present in varying amounts in the cuticle of different plants or organs, and can account for at least as much mass as cutin in some species (Fernandez et al., 2011). Many cutan-rich plants, such as some crassulacean acid metabolism (CAM) plants, have a certain degree of adaptation to drought. This suggests that cutan may enhance the hydrophobic nature of the cuticle, thus more effectively preventing water loss from the plant organs (Boom et al., 2005). Little is known about cutan biosynthesis and assembly, and its functional roles to protect plants from harsh environmental conditions.

Phenolics only account for a small portion (typically a few percent) of the plant cuticle and are principally composed of cinnamic acids, flavonoids or lignin-like chemicals, and (Hunt and Baker, 1980; Reina et al., 2001). The phenolic compounds can absorb UV light, thus providing a protective function against UV radiation. Their distribution in the flower cuticle may increase pollinating insect attraction (Kolb and Pfundel, 2005; Koch et al., 2008).

1.2 The Function of the Plant Cuticle

The highly hydrophobic cuticle layer plays important roles in plant growth and development, essentially as a barrier to control the movement of water, gases and solutes, and to protect against pathogen infection. The plant cuticle is also involved in other functions, such as preventing organ fusion, protecting against mechanical injury and attenuating UV light absorption

(Kerstiens, 1996; Riederer, 2006). Here, the major physiological functions of plant cuticles will be discussed.

1.2.1 An efficient diffusion barrier for water, gases and other molecules

The primary and most important function of the plant cuticle is considered to be as an efficient barrier for restricting the diffusion of water, gases or solutes across aerial plant organ surfaces (Schreiber, 2010). This idea is supported by the fact that mutants with severe defects in cuticle biosynthesis often do not survive under normal growth conditions, but may be rescued under conditions of high humidity (Tanaka et al., 2001; Yang et al., 2008).

The relative importance of cutin or waxes in restricting water loss is still debatable. Some *Arabidopsis* cutin-defect mutants, such as the *gpat4*/*gpat8* double mutant, exhibit a high permeability to water but display a normal wax profile (Li et al., 2007). In contrast, the high epidermal permeability of the *wax2* mutant cuticle is likely associated with a major reduction of its wax load (Chen et al., 2003; Rowland et al., 2007). As I report here, although three tomato cutin-deficient (*cd*) mutants all exhibited dramatic (95–98%) reductions in cutin content, transpirational water loss from the fruit at room temperature in high humidity conditions increased markedly only in *cd1* (Fig. 1.3), but slightly in *cd2* and *cd3*, compared with the wild type (Isaacson et al., 2009). This result suggests that there is probably no simple linear relationship between the

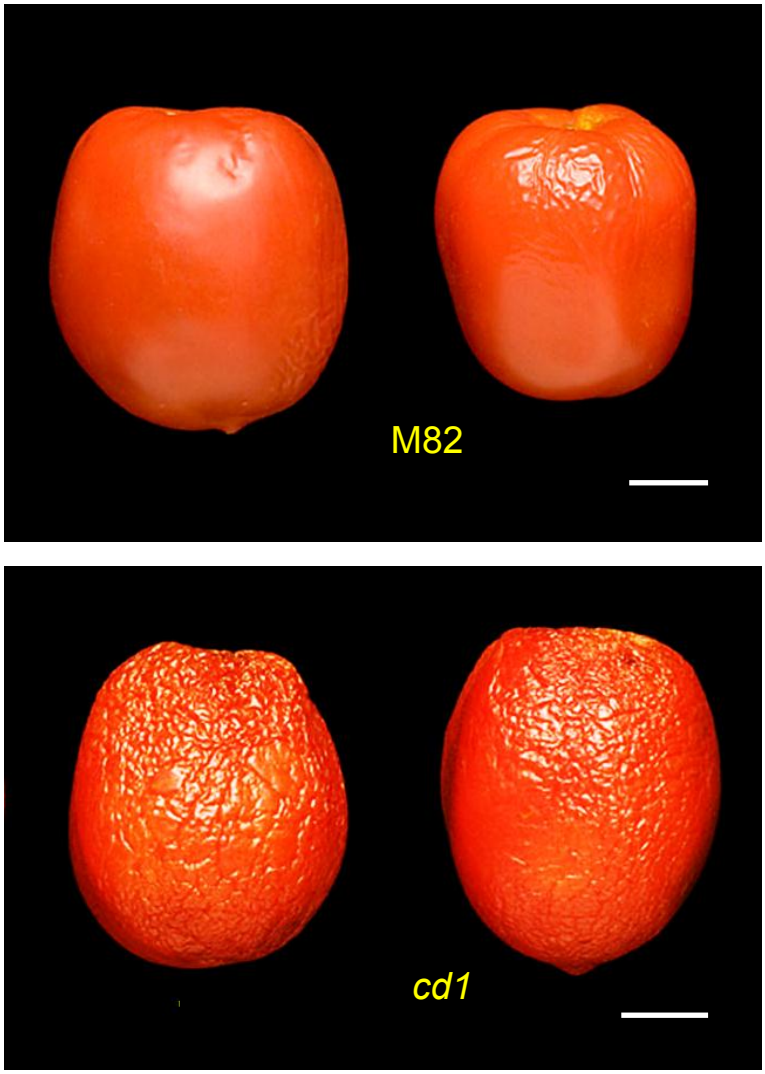

Figure 1.3 The function of plant cuticle: protecting against water loss. Differential water loss of tomato fruits between wild-type (M82) and *cd1* mutant after storage for 21 days at room temperature (about 20°C). Scale bars = 1 cm.

amount of cutin and transpirational water loss in the fruit. Nevertheless, cuticular permeability is likely not only correlated to its physical thickness, chemical composition and structural assembly (Burghardt and Riederer, 2006), but also influenced by environmental factors, such as temperature and humidity (Shepherd and Griffiths, 2006).

1.2.2 A physical barrier to resist pathogen infection

The plant cuticle provides a physical barrier that resists penetration by virus particles, bacterial cells, and the spores or growing filaments of fungi. The function of the cuticle in resisting pathogen infection has been deduced from the following observations: some cuticular-defect mutants exhibit an increase in sensitivity to pathogens (Li et al., 2007; Lee et al., 2009), and some fungal pathogens secrete cutinases (a cutin hydrolases) to facilitate their penetration of the plant cuticle during colonization (Kolattukudy et al., 1995).

Interestingly, an *Arabidopsis* cutin defective mutant, *sma4*, displays an enhanced susceptibility to the avirulent strains of *Pseudomonas syringae pv tomato*, normal susceptibility to the biotrophic fungal pathogen *Erysiphe cichoracearum*, and an enhanced resistance to a necrotrophic fungal pathogen *Botrytis cinerea* (Tang et al., 2007). Similarly, other three *Arabidopsis* cutin-defective mutants, *att1*, *bodyguard* and *lacerate*, were also reported to show increased resistance to *B. cinerea* in the same experiment. This unexpected phenomenon might be explained by an enhanced perception

of putative elicitors leading to the production of antifungal compounds in those cutin-defective mutants, or by activating compensatory defense pathways, such as increased wax biosynthesis or the up-regulation of defense genes (Bessire et al., 2007; Chassot et al., 2007). In our studies, fruits of the tomato cutin-defective mutants (*cd1*, *cd2* and *cd3*) displayed an enhanced susceptibility to *B. cinerea* under controlled inoculation conditions (Fig. 1.4), suggesting that the increased susceptibility of *cd* mutants probably resulted from a massive reduction in cutin load (Isaacson et al., 2009).

It is clear that the plant cuticle plays important roles in resistance against microbial infection. However, some aspects, such as the roles of cuticle composition and structure, and the interaction between pathogens and plants through cuticle, are still not well understood.

1.2.3 A physical barrier to prevent organs from fusion

The plant cuticle provides a highly hydrophobic barrier, which physically defines organ boundaries (Javelle et al., 2011) and without which organ fusion can occur. Organ fusion phenotypes have been observed in many cuticle-defective mutants, such as *fdh, lcr, hth, wax2*, *ad1, wbc11*, *wsl1*and *bgd* (Lolle et al., 1998; Sinha and Lynch, 1998; Krolikowski et al., 2003; Bird et al., 2007; Yu et al., 2008). A typical organ fusion mutant, *fdh*, is characterized by the fusion of leaves, floral organs and ovules, even though the epidermal cell layer of these organs is intact (Lolle et al., 1992) (Fig. 1.5). Genetic studies showed

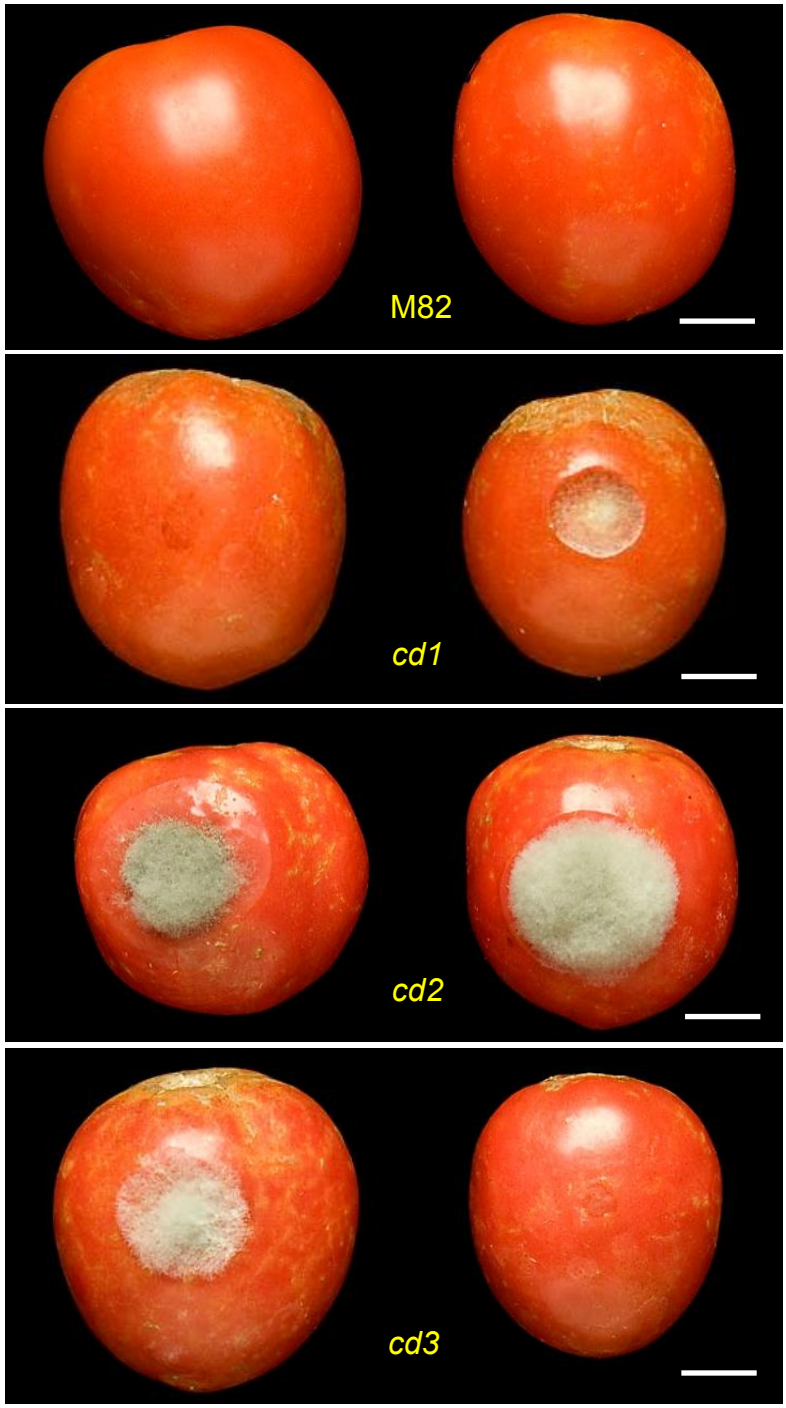

Figure 1.4 The function of plant cuticle: protecting against pathogen infection. The appearance of the ripe fruits of M82 and *cd* mutants after storage for 7 days following infection with *Botrytis cinerea*. (Pictures provided by Dr. Tal Isaacson. Scale bars = 1cm)

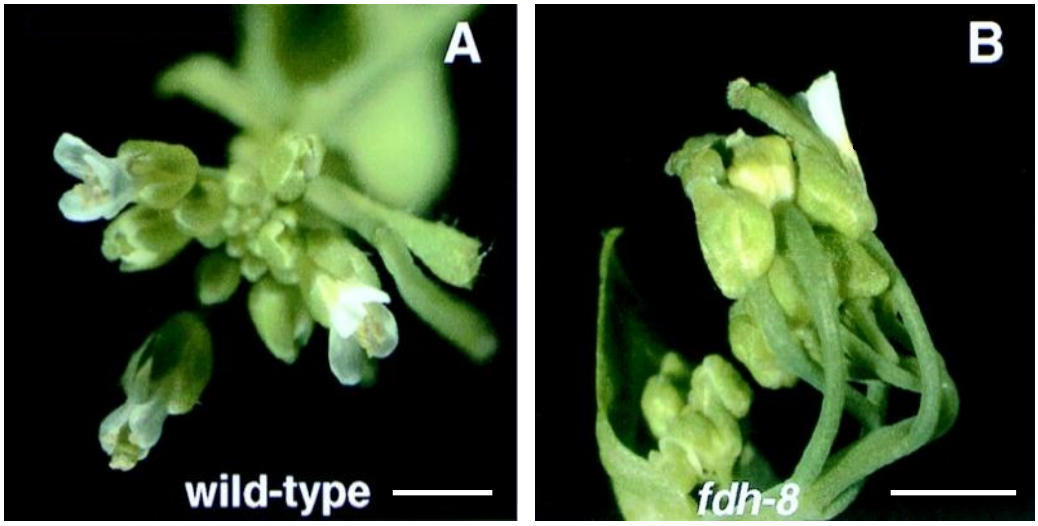

Figure 1.5 The function of plant cuticle: protecting against organ fusion. Light micrographs of the *fiddlehead* (*fdh*) mutant (B) (from Pruitt et al., 2000) and wild-type (A) *Arabidopsis*, showing the fusion phenotype of the inflorescences in the mutant. (Scale bars = 0.5cm.)

that the *fdh* gene encodes a subunit of a fatty acid elongase complex (FAE), 3-ketoacyl CoA synthase (KCS), which is a key enzyme involved in cuticle monomer biosynthesis. Together, these results suggest that the organ fusion of *fdh* results from defective cuticle formation (Fig. 1.5) (Pruitt et al., 2000). It should be mentioned that many cuticle-defective mutants do not exhibit an organ fusion phenotype. In addition, the respective roles of wax and cutin on organ separation and the precise mechanism underlying plant organ fusion are still obscure (Nawrath, 2002; Pighin et al., 2004).

1.2.4 Reducing water wettability of plant organs

Due to the hydrophobic nature of the plant cuticle, water on the surface of leaves or other organs often gathers into droplets and easily runs off, rather than forming extended films. An excellent example is the self-cleaning behavior of lotus (*Nelumbo nucifera*) leaves (also called the “lotus effect”). The exceptional water repellency of the lotus leaf relies on several features, such as the robustness and the unique properties of the epicuticular wax, and the unique surface topography (Hans Ensikat, et al., 2011).

The reduced wettability of leaf surface can help to keep stomata unclogged by water and facilitate the uptake of carbon dioxide after rain or during the morning hours following the formation of dew. Furthermore, the hydrophobicity of cuticles may also reduce the likelihood of pathogen infection because fungal spores have fewer opportunities for germination. It has been shown that the presence of a dense layer of epicuticular wax crystals, waxy trichomes and papillose epidermal cells may strongly increase the water repellency of leaf surface.

1.2.5 Protecting against UV light damage

The precise role of the cuticle in providing protection against UV radiation at the plant surface is still not well understood (Zhang et al., 2007, Javelle et al., 2011), although it has been suggested that the light-scattering properties of the cuticular layer may contribute to reducing UV-light absorption

by the plant (Shepherd and Griffiths, 2006). Some studies have indicated that cuticular phenolic compounds (e.g. cinnamic acids and flavonoids) can absorb or scatter UV light, thereby reducing UV radiation damage to the plant (Solovchenko and Merzlyak, 2003; Kolb and Pfundel, 2005).

1.2.6 Other roles of cuticle in plant development

Some mutants impaired in cuticle biosynthesis exhibit not only a deficiency in those cuticular chemical compounds but also a variety of developmental abnormalities, including embryo/seedling lethality and crinkled organs. This phenomenon suggests that plant cuticle may play other roles in plant development, or that those genes may be indirectly related to other important physiological processes.

Some cuticle-defective mutants are also affected in stomatal density or patterning, or altered in trichome density or its distribution (Kurata et al., 2003; Aharoni et al., 2004; Sturaro et al., 2005). One possible explanation for this is that cuticular permeability changes can alter a physiological signal network which globally regulates water balance.

1.3 Cuticle Monomer Biosynthesis

It is estimated that over half of the fatty acids produced in stem epidermal cells of *Arabidopsis thaliana* are exported into the cuticular layer for cutin and wax load, underlining the importance of cuticle biosynthesis in

epidermal cell metabolism (Suh et al., 2005). Many biosynthetic enzymes of the plant cuticle have been identified by comparing the lipid profiles of cuticle defective mutants to their wild-types (Neuffer et al., 1997; Pollard et al., 2008; Samuels et al., 2008; Kunst and Samuels, 2009, Javelle et al., 2011). Following a brief summary of current knowledge regarding wax biosynthesis and associated cutin monomer biosynthesis is presented.

1.3.1 Wax biosynthesis

The successive steps of enzymatic reactions in wax biosynthesis in *Arabidopsis thaliana* are well studied and have been described in several review papers (Nawrath, 2006; Samuels et al., 2008; Dominguez et al., 2011; Javelle et al., 2011). A schematic overview of wax biosynthesis pathways is illustrated in Figure 1.6. In brief, the elongation of C16–C18 fatty acids (FAs) into VLCFAs (C20 to C34) is catalyzed in the endoplasmic reticulum (ER) by a fatty acid elongase (FAE) complex, which is composed of four distinct enzymes: 3-ketoacyl- CoA synthase (KCS), 3-ketoacyl reductase (KCR), 3-hydroxyacyl-CoA dehydratase (HCD) and enoyl-CoA reductase (ECR) (Bach and Faure, 2010). The major wax products are synthesized from VLCFAs via two pathways: the alkane pathway and the wax ester pathway (Kunst and Samuels, 2003). In the alkane pathway, VLCFAs are reduced to aldehydes by an unknown long-chain-fatty-acyl-CoA reductase, and then decarbonylated into odd-numbered alkanes by a fatty aldehyde decarbonylase (CER1).

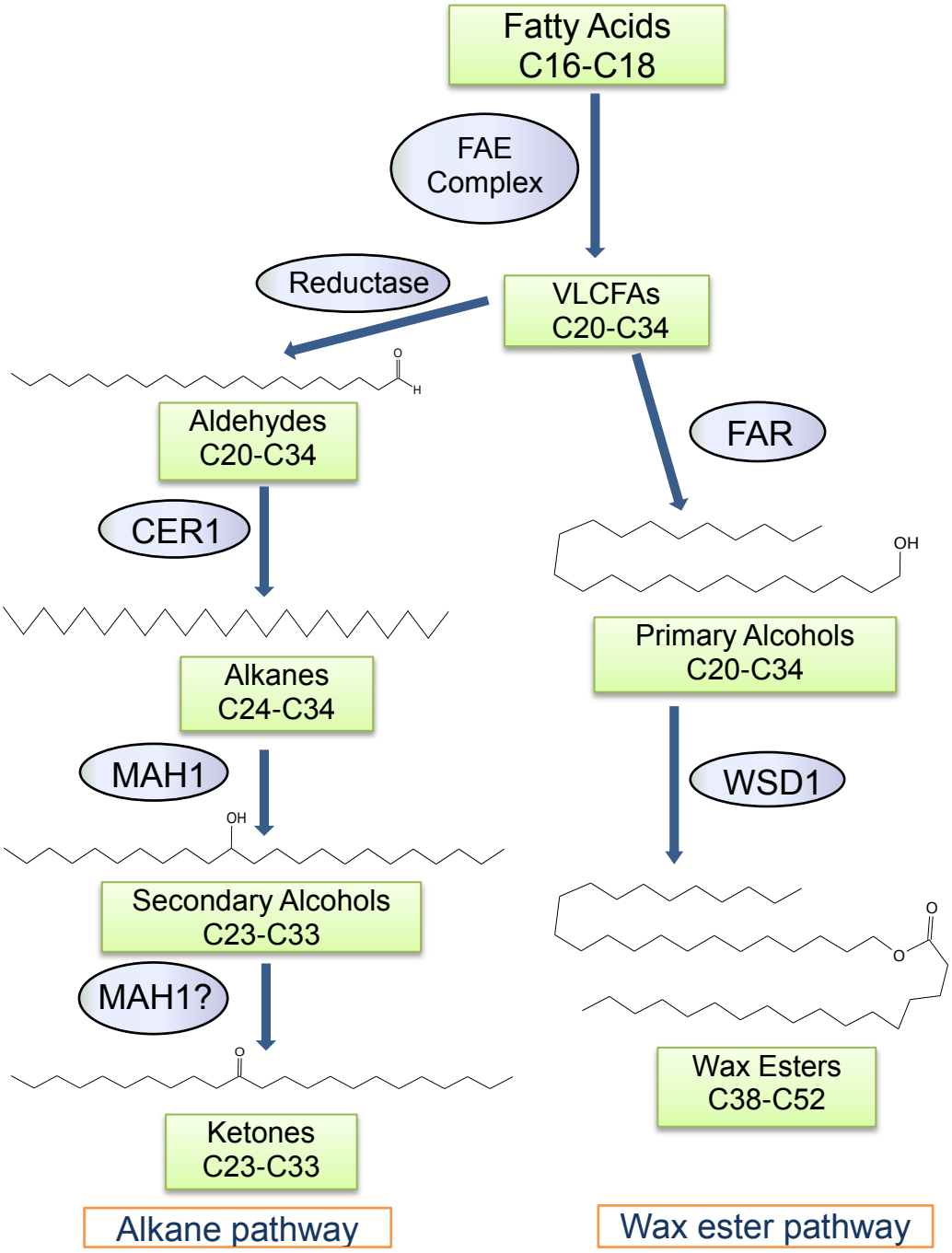

Figure 1.6 Biosynthetic pathways of major cuticular wax molecules.
CER1: fatty aldehyde decarbonylase; **FAE Complex**: fatty acid elongase complex; **FAR**: fatty acid reductase; **MAH1**: midchain alkanes hydroxylase; **WSD1**: wax ester synthase/acyl-coa: diacylglycerol acyltransferase

Subsequently, they are synthesized into corresponding secondary alcohols and ketones via a mid-chain alkane hydroxylase (MAH1) enzymatic reaction (Greer et al., 2007; Samuels et al., 2008). In the wax ester pathway, VLCFAs are reduced to primary alcohols by fatty acyl-CoA reductase (FAR), and subsequently condensed with C16/C18 fatty acids into wax esters by wax ester synthase (WSD1) (Rowland et al., 2006; Li et al., 2008).

1.3.2 Cutin monomer biosynthesis

To date, considerable progress has been made in the elucidation of the biosynthetic pathway of cutin monomers and the major enzymes involved in cutin monomer biosynthesis have been identified by forward or reverse genetic analysis and biochemical analysis of the corresponding recombinant proteins (Kolattukudy, 2001; Herecdia, 2003; Pollards, 2008; Reina-Pinto and Yephremov 2009; Pinot and Beisson, 2011). Common cutin monomers of the plant cuticle, such as 10, 16-dihydroxy C16 acid, 9,10,18-trihydroxy C18 acid and 18-hydroxy-9,10 epoxy C18 acid (Fig. 1.2A), are synthesized in the epidermal cells from the corresponding C16 and C18 fatty acids by ω-hydroxylation, in-chain hydroxylation, epoxidation and epoxide hydration. The oxygenation reactions of fatty acids are mainly catalyzed by the enzymes in the cytochrome P450 family (P450s), which represents one of the largest superfamilies of plant proteins (Pinot and Beisson 2011).

It should be noted that most cutin monomer substrates (fatty acids) are first conjugated to acyl-CoA by long-chain acyl-Coenzyme A synthetase (LACS), which is a key activation step for the subsequent oxidation reaction of FAs. Multiple substrate oxidation events may result in a complex pathway, depending on their relative sequence. The simplified biosynthetic steps of the major cutin monomers are depicted in Figure 1.7.

ω-hydroxylation: Three enzymes with alkane 1-monooxygenase activity (CYP86A8, CYP86A2 and CYP86A4) in the CYP86A subfamily, have been confirmed to be involved in the ω-hydroxylation of cutin monomers in *Arabidopsis* (Wellesen et al., 2001; Duan and Schuler 2005; Molina et al., 2008; Pinot and Beisson 2011). It reported that YP86A8 (LCR) can catalyze ω-hydroxylation of fatty acids ranging from C12 to C18:1, but that 9, 10-epoxystearate is not an efficient substrate for this enzyme (Wellesen et al., 2001). In contrast, CYP94C1 has the highest ω-hydroxylase activity with 9,10-epoxystearic acid; meanwhile, it can also catalyze ω-hydroxylation of lauric acid (C12:0) and C18 unsaturated fatty acids (Kandel et al., 2007). It has also been demonstrated that another gene *CYP704B1*, which is essential for pollen exine development of *Arabidopsis*, encodes a *ω*-hydroxylase that can catalyze ω-hydroxylation of long-chain fatty acids when expressed in yeast cells (Dobritsa, et al., 2009).

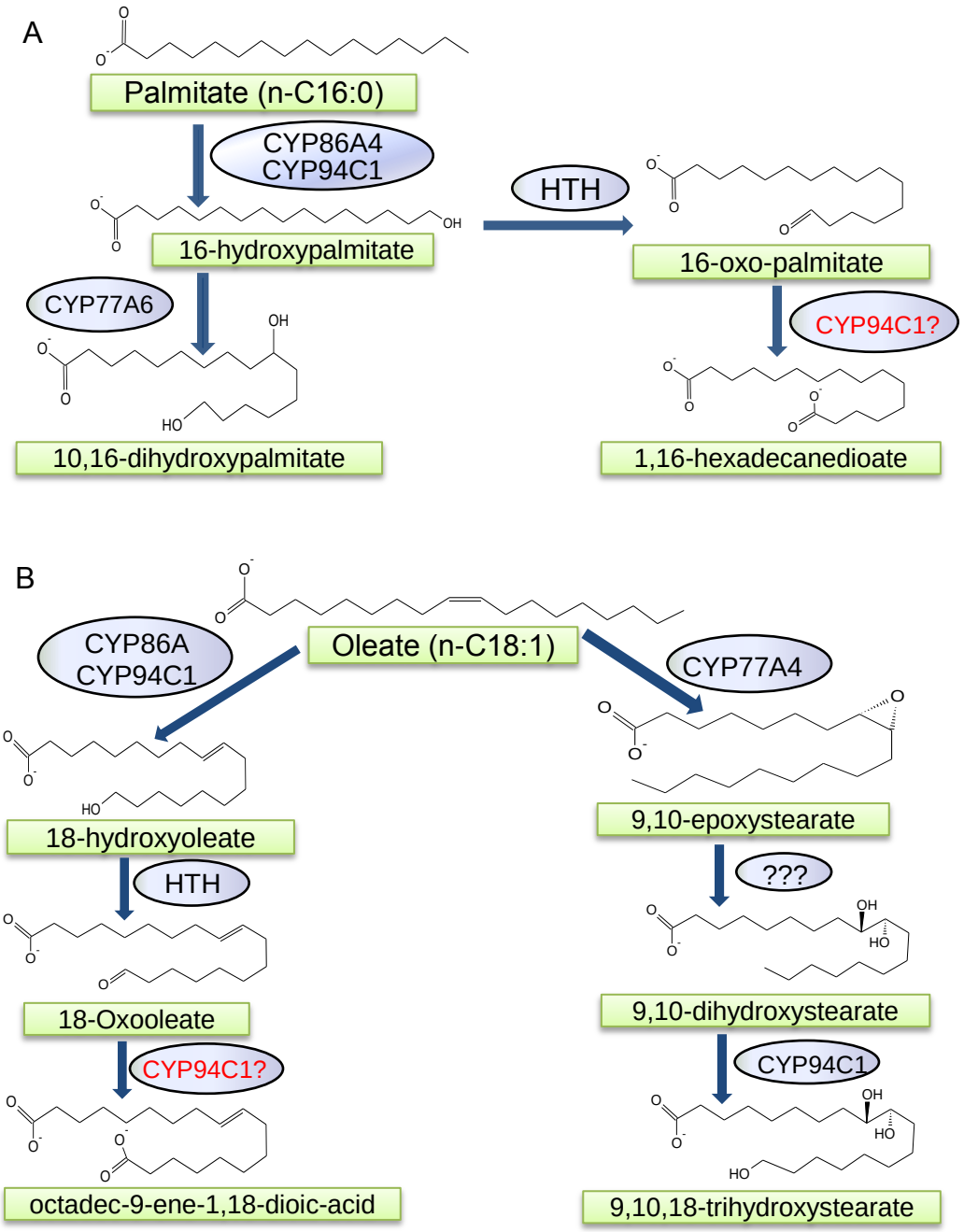

Figure 1.7 The biosynthetic pathways of major cutin monomers. (A) The biosynthesis of C16 cutin monomers. (B) The biosynthesis of C18 cutin monomers. Note: Fatty acids are first activated to Acyl-CoAs, followed by other synthesis steps. **HTH**: *hothead/adhesion of calix edge*. Other **CYP** enzymes in the blue spheres belong to Cytochrome P450 superfamily (abbreviated as CYP), which are found in *Arabidopsis*.

In-chain hydroxylation: It has been suggested that the introduction of in-chain hydroxyl group into ω-hydroxy FAs allows cross-linking between cutin monomers, leading to a reticulation structure and strengthening of the polymeric envelope (Pinot and Beisson 2011). Recently, the *Arabidopsis* gene *CYP77A6*, which encodes an in-chain hydroxylase, was cloned from a mutant lacking nanoridges on the surface of the flowers. Biochemical activity analysis using CYP77A6-expressing yeast microsomes demonstrated that 10, 16 dihydroxypalmitates can be synthesized by CYP77A6 from 16-hydroxy-palmitate (Li-Beisson et al., 2009).

Epoxidation: The 9, 10-dihydroxy FAs are derived from unsaturated FAs (such as oleic acid, linoleic acid) by the epoxidation of their double bonds, followed by the hydroxylation of the epoxide to produce oxygenated FAs (Pinot et al., 1992, 1999; Osman, 1995; Kolattukudy, 2001). It has been reported that CYP77A4 enzyme from *Arabidopsis* is able to synthesize epoxides by epoxidating the double bond of unsaturated fatty acids, after which further synthesis to the corresponding diols is accomplished by an unidentified epoxide hydrolase (Sauveplane et al., 2009).

Dicarboxylic acid (DCA) synthesis: DCAs are thought to make a significant contribution to the formation of the cross-linked domain in cutin biosynthesis. The *Arabidopsis* organ fusion mutant *hothead* (*hth*) shows decreased α-, ω-dicarboxylic fatty acid content in the leaf cuticle polyesters, suggesting that HTH may function as an enzyme in ω-oxidation pathway to

oxidize long-chain ω-hydroxyl fatty acids into ω-oxo fatty acids. The HTH protein shows high sequence similarity to long-chain FA ω-alcohol dehydrogenases from *Candida* species, prompting speculation that it may catalyze the next step after ω-hydroxylases in the ω-oxidation pathway (Fig. 1.8) (Kurdyukov et al., 2006).

From research on synthesizing dicarboxylic fatty acid *in vitro*, dodecadioic acid (a diacid) can be synthesized from a 12-hydroxylauric acid substrate by incubating recombinant microsomes of yeasts transformed with CYP94C1 plasmid, but not with a control plasmid. This suggests the possible involvement of the CYP94C1 enzyme in the biosynthesis of diacids in *Arabidopsis* (Kandel et al., 2007). In a prior study, it was found that the enzyme CYP94A5 from *Nicotiana tabacum* can catalyze the oxidation of fatty acids to produce the ω-alcohol, then to the corresponding diacid (Bouquin et al., 2001).

It is worth noting that much of the summarized knowledge of FA oxidation comes from biochemical studies performed after heterologous expression in yeast. Moreover, the activity measurements were performed with free FA, not natural substrates (e.g. acyl-CoAs or glycerolipids etc). Therefore, the exact enzymatic reactions of some oxidation steps of FAs, such as epoxide hydration and oxidation of ω-hydroxyl, may require further elucidation.

1.4 Cutin Monomer Export and Assembly

Based on subcellular localization studies, the majority of biosynthetic enzymes of wax and cutin monomers reside in the ER, suggesting that the final monomers of the plant cuticle are probably synthesized in this compartment (Rowland et al., 2006; Greer et al., 2007; Li et al., 2008; Reina-Pinto and Yephremov 2009). The mechanisms behind the export and assembly of wax and cutin monomers to the outer cuticle remain poorly understood. Several reviews have discussed and proposed the possible transport paths of cuticular lipids (Pollard, 2008; Samuels et al., 2008; Kunst and Samuels, 2009). Here, I will shed light on recent progress in the export and assembly of cutin molecules.

1.4.1 *sn*-2-monoacylglycerol (2-MAG), the major transport substrate and acyl donor in cutin biosynthesis

Cutin monomers must traffic from their synthetic site to the plasma membrane (PM); move across the PM, and cross the polysaccharide rich cell wall in the hydrophilic apoplastic environment, before reaching to their assembly site, the cuticle. Although direct experimental evidence identifying the actual transport substrates of the cutin components is still lacking, indirect evidence suggests that 2-monoacylglycerol (2-MAG) may serve as a transport substrate and acyl donor in the cutin biosynthesis pathway. It has been demonstrated that two acyltransferases, GPAT4 and GPAT6, which are

required for cutin formation in *Arabidopsis,* can esterify acyl groups of FAs predominantly to the *sn*-2 position of G3P, resulting in the *sn*2-MAG as a major product (Yang et al., 2010). The authors speculated that 2-MAG might serve as a cutin precursor for export and assembly.

A detailed biosynthetic pathway of 2-MAG and cutin polymer is illustrated in Figure 1.8. Briefly, ω-hydroxy fatty acid is first activated by long-chain acyl-CoA synthetase (LACS) to produce corresponding ω-hydroxy fatty acyl-CoA (Schnurr et al., 2004), then 2-MAG is synthesized via esterifying the acyl groups of ω-hydroxy FA to the *sn*-2 position of G3P by acyltransferases (GPAT4 or GPAT6) (Yang et al., 2010). At a cutin synthesis site, the acyl group of 2-MAG (acyl donor) is presumably then esterified to the growing cutin polymer.

1.4.2 Export of cutin monomers

The synthetic site of cutin monomers: The biosynthesis site of the cutin monomer (2-MAG) remains uncertain, because experimental evidence is still inadequate regarding subcellular localization of two acyltransferases, GPAT4 and GPAT6, which are required for 2-MAG biosynthesis (Yang et al., 2010). GPAT8, the closest homolog of GPAT4, has been demonstrated to be localized in the ER with both N and C termini in the cytosol (Li et al., 2007; Gidda et al., 2009). Moreover, the C-termini of GPAT4 and GPAT6 contain

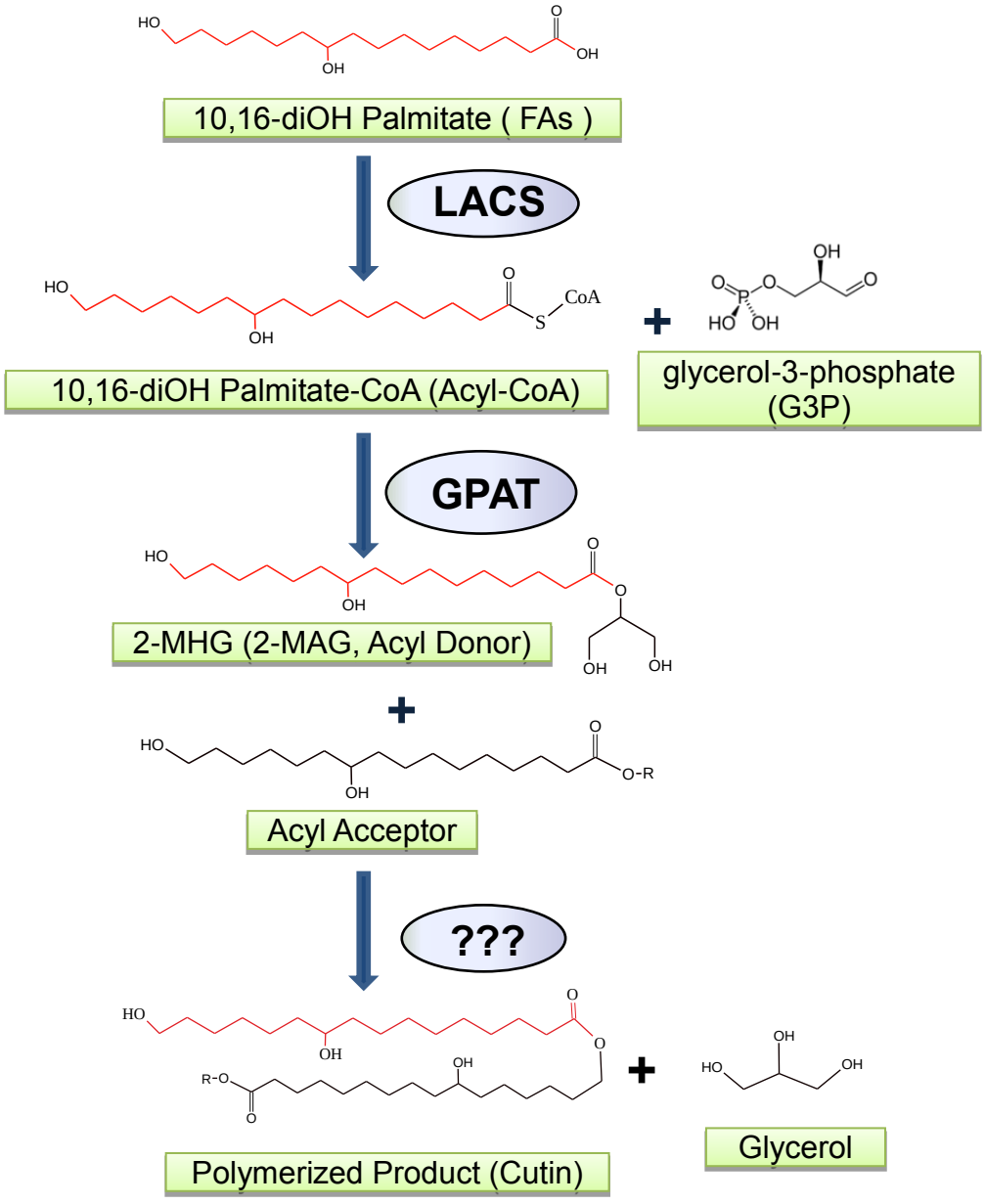

Figure 1.8 Cutin polymerization pathway.
GPAT: glycerol phosphate acyltransferase
LACS: long-chain acyl-CoA synthetase

diverged-type dilysine motifs (–KXKXXX–COOH and –KKXKX–COOH, respectively). Accordingly, a reasonable hypothesis is that GPAT4 and GPAT6 reside in the ER, although whether the two diverged dilysine sequences function as ER retrieval signals remains to be experimentally tested.

ABC transporter: The cutin monomers must be transported from the synthesis site to the apoplastic assembly site in the plant cuticle. During this process, they must cross the PM, a process that is most likely mediated by ATP-binding cassette G subfamily transporters (ABCG transporter) (Bird et al., 2007; Verrier et al., 2008; Panikashvili and Aharoni 2008; Bessire et al., 2011; Chen et al., 2011; Panikashvili et al., 2011). The ABC transporter subfamily G includes both white-brown complex (WBC) 'half-size transporters' and pleiotropic drug resistance (PDR) 'full-length transporters', with more than 40 members in both *Arabidopsis* and rice (Verrier et al., 2008). ABCG family half-transporters (WBC), with 28 genes annotated in the *Arabidopsis* genome, must dimerize to form a full-length, functional ABC transporter (Verrier et al., 2008). *abcg11/wbc11/ desperado/cof1*, a well-characterized ABC half-size transporter mutant, displays an array of cuticle defects and a dramatic reduction in the levels of waxes and cutin monomers (Bird et al., 2007; Luo et al., 2007; Panikashvili et al., 2007; Ukitsu et al., 2007; Panikashvili et al., 2010; McFarlane et al., 2010). In contrast, *abcg12/cer5*, another ABCG half-size transporter mutant, is phenotypically normal except for having abnormally

glossy stems, which reflects a reduction of wax components in the cuticle (Rashotte et al., 2001; Pighin et al., 2004). In an *in-vivo* interaction experiment of the two half-size transporters using bimolecular fluorescence complementation (BiFC), it has been reported that ABCG11/ABCG12 heterodimers and ABCG11 homodimers can be detected in the PM of epidermal cells, while ABCG12 homodimers cannot. The protein trafficking assays showed that ABCG11 can travel to the plasma membrane, while, ABCG12 is retained in the ER in the case of ABCG11 knockout. This suggests that ABCG11 is capable of forming flexible dimer partnerships, but that ABCG12 is only capable of forming a dimer with ABCG11 (McFarlane et al., 2010).

Another *Arabidopsis* half-size transporter gene *ABCG13* was recently characterized (Panikashvili et al., 2011) and it was reported that loss of ABCG13 function resulted in cuticle-related phenotypes and caused a significant reduction in levels of cutin monomers in the flowers. This suggests that ABCG13 is probably required for *Arabidopsis* flower cutin monomer secretion.

Evidence is accumulating that full-length subfamily G transporters, known as pleiotropic drug resistance (PDR), also are probably associated with cutin monomer export. The *permeable cuticle 1* (*pec1*) *Arabidopsis* mutant, caused by the knockout of the ATP Binding Cassette G32 (*abcg32*) gene, displays a highly permeable cuticle phenotype. The ABCG32 full-length transporter

shows polar localization in PM regions near the plant surface. Further, cutin profiling data reveal that typical cutin monomers (e.g. ω-hydroxy fatty acids) in *pec1* flowers, are reduced to 40% of wild-type levels, suggesting that ABCG32 likely exports cutin precursors to the plant cuticle (Bessire et al., 2011). A similar result is also found in other plants: the *eibi1* mutant of wild barley, which carries a spontaneous mutation in an ATP-binding cassette (ABC) subfamily G full transporter (HvABCG31), displays a phenotype of cutin disorganization and a low capacity to retain leaf water. Quantification of cuticle components showed that levels of the major cutin monomers in the *eibi1* mutant are reduced to about 50% of those in wild barley, but that there is little difference in the major wax component (1-hexacosanol) between the two lines. This result suggests that HvABCG31 is likely required for cutin load (Chen et al., 2011).

Possible role of transfer proteins: Lipid transfer proteins (LTPs) are abundant in the *Arabidopsis* genome, with about 70 members in total. It has been proposed that LTPs may play a role in the transfer of cuticle components during the cuticle development (Yeats and Rose, 2008). The first convincing evidence of the role of LTPs in the export of cuticular components was from a study of the *ltpg* mutant of *Arabidopsis* (Debono et al., 2009). The *LTPG* gene encodes a glycosylphosphatidyl-inositol-anchored lipid transfer protein. Mutant lines with decreased *LTPG* expression exhibit a reduced total wax load (mainly alkanes) in the cuticle, indicating that LTPG likely contributes to

cuticular wax deposition (Debono et al., 2009, Lee et al., 2009). However, it remains unclear whether LTPG delivers lipids across the cell wall to the cuticle, because LTPG is a PM-bound protein (Kunst and Samuels, 2009).

It is thought that LTPs are probably not capable of facilitating intracellular lipid trafficking due to their extracellular localization feature (Yeats and Rose, 2008). Therefore, the trafficking route and molecular mechanisms by which cuticle lipid precursors move from the ER to the PM in the cytosol remain unknown. Acyl-CoA-binding proteins (ACBPs) have been proposed as candidates for intracellular lipid transfer in plant cells (Xiao and Chye 2009). Six members of the ACBP group have been identified from *Arabidopsis*, and some of them reside in cytoplasm. However, no direct or indirect evidence to date shows a relationship between Acyl-CoA-binding proteins (ACBPs) and cuticle lipid loading.

Unlike cuticular wax molecules, 2-MAGs have significant aqueous solubility (Yang et al., 2010), and this property may substantially facilitate the movement of 2-MAG in the cytosol or in an extracellular aqueous matrix. Here, it is speculated that the movement of cutin monomers (2-MAGs) is mediated by passive diffusion in an aqueous matrix, although the possibility that the traffic of cutin precursors is facilitated by a protein binding process cannot yet be rejected.

1.4.3 Assembly of cutin monomers

Cutin is a nonlinear, or cross-linked, polymer synthesized from cutin monomers. However, the mechanisms that mediate cutin polymerization have been undetermined until recently. *In-vitro* cutin polymerization by crude plant enzyme preparations was first reported in 1974: insoluble cutin biopolymer can be synthesized from 16-hydroxypalmitic acid, and 10, 16-dihydroxypalmitic acid (cutin monomers), using extracts from young *Vicia faba* leaf epidermal tissues with adenosine triphosphate and coenzyme A as the required cofactors (Croteau and Kolattukudy 1974). It was suggested that an unknown acyltransferase can then transfer the hydroxyacyl moieties of cutin monomers to the growing cutin polymer. Following this hypothesis, a 17 kDa protein was isolated by native PAGE electrophoresis from a crude leaf epidermis extract of *Agave americana*. The acyl-CoA:cutin transferase activity of this purified protein was tested *in vitro* using chemically synthesized oligohydroxy fatty esters as acceptors and labeled palmitoyl-CoA and oleoyl-CoA as acyl donors. The corresponding interesterified compounds were obtained from this experiment (Reina and Heredia, 2001). The 17 kDa protein was partially sequenced, but the sequence data presented in this paper were not informative; and the corresponding gene was not cloned. In another study by same research group, the gene *AgaSGNH,* encoding a SGNH-hydrolase, was isolated from the cDNA library of young leaf epidermis of *A. americana* using degenerated PCR primers designed according to the N-terminal

sequence of that purified 17 kDa protein (Reina and Heredia, 2001; Reina et al., 2007). It was demonstrated that the AgaSGNH protein was localized in the outer cell wall of the epidermal cells and had an acyltransferase activity, leading investigators to speculate that the protein is probably involved in plant cutin biosynthesis (Reina et al., 2007). In this paper, the authors mentioned that the amino terminal peptide sequence chosen to design the cloning primers was not present in the PCR fragment of the *AgaSGNH* cDNA; hence the function of AgaSGNH protein remains somewhat uncertain as there was no apparent association between the *AgaSGNH* gene and the purified 17 kDa protein.

The *bodyguard* (*bdg*) mutant of *Arabidopsis* exhibits a disorganized cuticle structure, but unexpectedly accumulates significantly more residual bound lipids (mainly cutin) and waxes per unit of leaf surface area. The BDG protein, which is located in the outermost cell wall of epidermal cells, belongs to a newly identified class of the α/β-hydrolase superfamily. The authors hypothesized that BDG may act directly as an extracellular synthase for cuticle formation (Kurdyukov et al., 2006). However, the function of this enzyme remains obscure, because no biochemical activity of BDG protein has been experimentally tested.

1.4.4 Proposed pathways of cutin monomer export and cutin synthesis

An overview of cutin biosynthesis, including the possible synthetic site, proposed transfer pathways and assembly site of cutin monomers is presented in Figure 1.9. In brief, *sn*-2 MAGs are presumably synthesized in the ER by the acyltransferases GPAT4 or GPAT6. Water soluble 2-MAG molecules likely move near the PM by passive diffusion, then are channeled through the PM by ABC-G family transporters, and finally move across the cell wall by passive diffusion or some other more coordinated mechanism.

Other possible transfer mechanisms of cuticle precursors, such as Golgi-mediated vesicular traffic through the secretion pathway and oleophilic droplet transport pathway have been proposed in several review papers (Kunst et al., 2006; Panikashvili and Aharoni 2008; Samuels et al., 2008). However, those proposed export pathways may exist for the transport of cuticular waxes but there is no solid evidence to substantiate that cutin monomers may be transferred via those pathways. The possible transport pathways for cuticular lipid are also illustrated in Figure 1.9 for reference (shown with dotted lines).

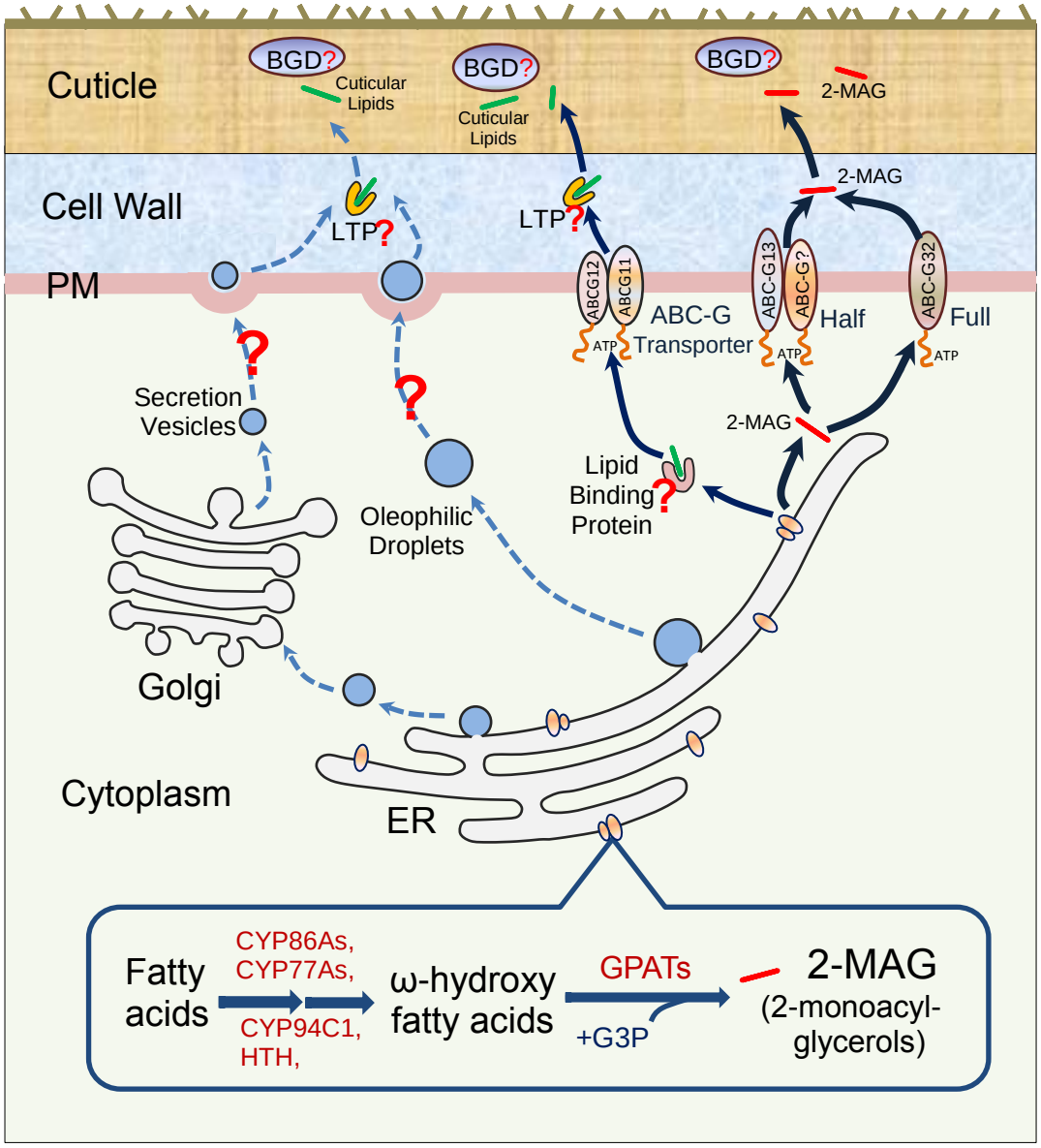

Figure 1.9 Biosynthesis and transport of cutin monomers.
In the ER, ω-hydroxy fatty acids are synthesized by several enzymatic oxidation reactions (CYP86A, CYP77A and HTH etc.), next are esterified to glycerol-3-phosphate by GPAT enzymes to synthesize 2-MAGs. The transport path of the cutin monomers (2-MAGs) in the cytoplasm and extracellular matrix remains unclear. Current evidence suggests that ABC transporters are likely involved in channeling cutin monomer across the PM. Several combinations of ABCG transporter pathways are illustrated in the diagram. Other proposed transport pathways of cuticular lipids such as oleophilic bodies and secretory vesicles, are still unresolved due to the lack of reliable evidence, and are drawn in dotted lines for reference.

1.5 Transcriptional Regulation of Cutin Biosynthesis

Knowledge of the transcriptional regulation of cutin-related metabolic pathways during plant development remains relatively sparse. The *WAX INDUCER 1* (*WIN1/SHN1*) gene, which encodes a member of the AP2/ERF (ethylene response factor) transcription factor family, can trigger wax production, thus enhancing plant drought tolerance (Aharoni et al., 2004; Broun et al., 2004). Further analysis has shown that *WIN1/SHN1* can also modulate cutin biosynthesis: overexpression of the *WIN1/SHN1* gene increased the cutin load on plant organs, while its down-regulation has the opposite effect (Kannangara et al., 2007). Regulatory network analysis has shown that the induction of *WIN1/SHN1* causes a rapid increase in the expression of some genes involved in cutin biosynthesis, including CYP86A7, CYP86A4, a GDSL-motif lipase/hydrolase, HTH-like and LACS2. In a chromatin immune-precipitation (ChIP) experiment, the LACS2 promoter was detected in WIN1/SHN1-binding genomic fragments, suggesting that LACS2 is likely to be directly targeted by this transcription factor (Kannangara et al., 2007). The result of co-silencing all three *SHN/WIN* clade members using an artificial microRNA approach demonstrated that the transcription factors act directly on downstream cutin and cell wall–modifying genes and broadly control floral organ development, specifically affecting cuticle assembly and cell wall remodeling (Shi et al., 2011). Nevertheless, current knowledge of the

modes of action of the SHN1/WIN1 transcription factor and involvement in particular pathways or processes is still limited.

The *serrate* (*se*) gene of *Arabidopsis* which encodes a protein of RNA–processing multi-protein complexes, can mediate the transcription of some genes associated with cutin and wax biosynthesis in a compensatory manner in several cuticle mutants, such as *lacerata* (*lcr*, CYP86A8), *fiddlehead* (*fdh*, *kcs10*) and *bodyguard* (*bdg*) (Voisin et al., 2009). Mutations in those genes cause a complex developmental syndrome that is characterized by ectopic organ fusions and leaf deformations. Unexpectedly, the mutants over-accumulate major cutin monomers in leaves. A genome-wide gene expression analysis by microarray showed that the range of genes involved in cuticle biosynthesis are coordinately up-regulated in all three cuticular mutants, suggesting that those mutants can alleviate the functional disorder of the cuticle by reinforcing their defense network. The *serrate*, gene was identified as a mediator (or enhancer) among putative enhancers and suppressors by meta-analysis of microarray data and its role as a mediator has been confirmed by the experimental result that the *se lcr* and *se bdg* double mutants can eradicate the typical phenotypes of *lcr* and *bdg*, such as organ fusions and severe leaf deformations (Voisin et al., 2009).

1.6 Tomato, an Attractive Model System for fruit Cuticle Studies

Arabidopsis thaliana has been widely used as a robust model for cutin biosynthesis studies for more than a decade, and many cuticle-associated mutants have been identified and cloned from this model plant (Nawrath, 2006; Pollard et al., 2008; Samuels et al., 2008; Javelle et al., 2011). However, high amounts of the C18:2 α, ω-dicarboxylic acid (DCA) cutin monomer (more than 50%) and glycerol are present in the cutin of *Arabidopsis*, suggesting that DCAs and glycerol molecules are presumably directly esterified together to produce atypical DCA–glycerol cutin polymers (Bonaventure et al., 2004; Franke et al., 2005; Pollard et al., 2008). Therefore, *Arabidopsis* is not a good representative model for cutin biology (Dominguez et al., 2010). In addition, the cuticle of *Arabidopsis* is thin and extremely delicate, increasing the difficulty of cuticle isolation and handling (Franke et al., 2005; Isaacson et al., 2009). Tomato fruit, on the other hand, offers an ideal alternative model system for cuticle studies. In tomato fruit cuticle, 9(10), 16-dihydroxy hexadecanoic acid is the most abundant cutin monomer (accounting for about 80% of total), which is also one of the typical cutin monomers (ω-hydroxy fatty acids) in many plants (Isaacson et al., 2009). Tomato fruit cuticles are relatively thick, easy to isolate and are astomatous, thereby providing intact cuticular membranes, which will help with functional characterizations of

cuticle permeability and pathogen infection (Vogg et al., 2004; Leide et al., 2011).

In the last decade, extensive tomato sequence data, such as numerous molecular markers and massive EST sequences, have been collected (http://solgenomics.net). This has culminated in a high-quality draft of the tomato genome sequence, and a gene annotation built by the International Tomato Genome Sequencing Project. Mutational approaches have been highly exploited in tomato genetic and molecular research. Several tomato mutant collections have been generated by fast neutron or EMS mutagenesis in different research labs (Menda et al., 2004; Minoia et al., 2010; Saito et al., 2011). In addition, tomato fruit cuticle have been studied in recent years, leading to the accumulation of a useful information regarding fruit cuticle biology (Leide et al., 2007; Mintz-Oron et al., 2008; Heredia et al., 2008; Buda et al., 2009; Yeats et al., 2010; Kosma et al., 2010; Leide et al., 2011; Matas et al., 2011).

Tomato is one of the world's most important vegetable crops and has emerged as the primary model system for studying climacteric fruit development, ripening and metabolism study. Studies to date have suggested that fruit cuticle is one of the key contributing factors influencing tomato fruit storability and shelf life (Saladie et al., 2007; Kosma et al., 2010). The elastic properties of plant cuticular membranes may play an important role in maintaining fruit integrity and reducing fruit cracking (Bargel et al., 2005;

Bargel and Neinhuis, 2005; Dominguez et al., 2011). Moreover, it has been suggested that the variation in fruit cuticle structure or composition may influence other important fruit traits, such as resistance to desiccation and microbial infection.

Considering the advantages such as typical cutin composition profile, the economic and scientific importance, and the abundant genetic information and materials, the tomato is an ideal model system for plant cuticle biology studies.

REFERENCES

Abe, M., Katsumata, H., Komeda, Y. and Takahashi, T. (2003) Regulation of shoot epidermal cell differentiation by a pair of homeodomain proteins in *Arabidopsis*. *Development,* **130**(4), 635-643.

Aharoni, A., Dixit, S., Jetter, R., Thoenes, E., van Arkel, G. and Pereira, A. (2004) The SHINE clade of AP2 domain transcription factors activates wax biosynthesis, alters cuticle properties, and confers drought tolerance when overexpressed in *Arabidopsis*. *Plant Cell,* **16**(9), 2463-2480.

Akoh, C.C., Lee, G. C., Liaw, Y. C., Huang, T. H. and Shaw, J. F. (2004) GDSL family of serine esterases/lipases. *Prog. Lipid Res.,* **43**(6), 534-552.

Bach, L. and Faure, J. D. (2010) Role of very-long-chain fatty acids in plant development, when chain length does matter. *C. R. Biol.,* **333**(4), 361-370.

Benitez, J.J., Garcia-Segura, R. and Heredia, A. (2004) Plant biopolyester cutin: A tough way to its chemical synthesis. *Biochim. Biophys. Acta,* **1674**(1), 1-3.

Bessire, M., Borel, S., Fabre, G., Carraca, L., Efremova, N., Yephremov, A., Cao, Y., Jetter, R., Jacquat, A. C., Metraux, J. P. and Nawrath, C. (2011) A member of the PLEIOTROPIC DRUG RESISTANCE family of ATP binding cassette transporters is required for the formation of a functional cuticle in *Arabidopsis*. *Plant Cell,* **23**(5), 1958-1970.

Bird, D., Beisson, F., Brigham, A., Shin, J., Greer, S., Jetter, R., Kunst, L., Wu, X., Yephremov, A. and Samuels, L. (2007) Characterization of *Arabidopsis* ABCG11/WBC11, an ATP binding cassette (ABC) transporter that is required for cuticular lipid secretion. *Plant J.,* **52**(3), 485-498.

Bonaventure, G., Beisson, F., Ohlrogge, J. and Pollard, M. (2004) Analysis of the aliphatic monomer composition of polyesters associated with *Arabidopsis* epidermis: Occurrence of octadeca-cis-6, cis-9-diene-1,18-dioate as the major component. *Plant J.,* **40**(6), 920-930.

Broun, P., Poindexter, P., Osborne, E., Jiang, C. Z. and Riechmann, J. L. (2004) WIN1, a transcriptional activator of epidermal wax accumulation in *Arabidopsis*. *Proc. Natl. Acad. Sci. U. S. A.,* **101**(13), 4706-4711.

Buda, G.J., Isaacson, T., Matas, A. J., Paolillo, D. J. and Rose, J. K. (2009) Three-dimensional imaging of plant cuticle architecture using confocal scanning laser microscopy. *Plant J.,* **60**(2), 378-385.

Buschhaus, C. and Jetter, R. (2011) Composition differences between epicuticular and intracuticular wax substructures: How do plants seal their epidermal surfaces? *J. Exp. Bot.,* **62**(3), 841-853.

Chassot, C., Nawrath, C. and Metraux, J. P. (2007) Cuticular defects lead to full immunity to a major plant pathogen. *Plant J.,* **49**(6), 972-980.

Chen, X., Goodwin, S. M., Boroff, V. L., Liu, X. and Jenks, M. A. (2003) Cloning and characterization of the WAX2 gene of *Arabidopsis* involved in cuticle membrane and wax production. *Plant Cell,* **15**(5), 1170-1185.

Chen, X., Truksa, M., Snyder, C. L., El-Mezawy, A., Shah, S. and Weselake, R. J. (2011) Three homologous genes encoding sn-glycerol-3-phosphate acyltransferase 4 exhibit different expression patterns and functional divergence in *Brassica napus*. *Plant Physiol.,* **155**(2), 851-865.

Croteau, R. and Kolattukudy, P. E. (1974) Biosynthesis of hydroxyfatty acid polymers. Enzymatic synthesis of cutin from monomer acids by cell-free preparations from the epidermis of *Vicia faba* leaves. *Biochemistry,* **13**(15), 3193-3202.

Dean, B.B. and Kolattukudy, P. E. (1976) Synthesis of suberin during wound-healing in jade leaves, tomato fruit, and bean pods. *Plant Physiol.,* **58**(3), 411-416.

Debono, A., Yeats, T. H., Rose, J. K., Bird, D., Jetter, R., Kunst, L. and Samuels, L. (2009) *Arabidopsis* LTPG is a glycosylphosphatidylinositol-anchored lipid transfer protein required for export of lipids to the plant surface. *Plant Cell,* **21**(4), 1230-1238.

Depege-Fargeix, N., Javelle, M., Chambrier, P., Frangne, N., Gerentes, D., Perez, P., Rogowsky, P. M. and Vernoud, V. (2011) Functional characterization of the HD-ZIP IV transcription factor OCL1 from maize. *J. Exp. Bot.,* **62**(1), 293-305.

Dobritsa, A.A., Shrestha, J., Morant, M., Pinot, F., Matsuno, M., Swanson, R., Moller, B. L. and Preuss, D. (2009) CYP704B1 is a long-chain fatty acid omega-hydroxylase essential for sporopollenin synthesis in pollen of *Arabidopsis*. *Plant Physiol.,* **151**(2), 574-589.

Dominguez, E., Heredia-Guerrero, J. A. and Heredia, A. (2011) The biophysical design of plant cuticles: An overview. *New Phytol.,* **189**(4), 938-949.

Dominguez, E., Heredia-Guerrero, J. A., Benitez, J. J. and Heredia, A. (2010) Self-assembly of supramolecular lipid nanoparticles in the formation of plant biopolyester cutin. *Mol. Biosyst,* **6**(6), 948-950.

Duan, H. and Schuler, M. A. (2005) Differential expression and evolution of the *Arabidopsis* CYP86A subfamily. *Plant Physiol.,* **137**(3), 1067-1081.

Elhiti, M. and Stasolla, C. (2009) Structure and function of homodomain-leucine zipper (HD-zip) proteins. *Plant. Signal. Behav.,* **4**(2), 86-88.

Franke, R., Briesen, I., Wojciechowski, T., Faust, A., Yephremov, A., Nawrath, C. and Schreiber, L. (2005) Apoplastic polyesters in *Arabidopsis* surface tissues--a typical suberin and a particular cutin. *Phytochemistry,* **66**(22), 2643-2658.

Gidda, S.K., Shockey, J. M., Rothstein, S. J., Dyer, J. M. and Mullen, R. T. (2009) *Arabidopsis thaliana* GPAT8 and GPAT9 are localized to the ER and possess distinct ER retrieval signals: Functional divergence of the dilysine ER retrieval motif in plant cells. *Plant Physiol. Biochem.,* **47**(10), 867-879.

Graca, J., Schreiber, L., Rodrigues, J. and Pereira, H. (2002) Glycerol and glyceryl esters of omega-hydroxyacids in cutins. *Phytochemistry,* **61**(2), 205-215.

Heredia, A. (2003) Biophysical and biochemical characteristics of cutin, a plant barrier biopolymer. *Biochim. Biophys. Acta,* **1620**(1-3), 1-7.

Heredia, A., Heredia-Guerrero, J. A., Dominguez, E. and Benitez, J. J. (2009) Cutin synthesis: A slippery paradigm. *Biointerphases,* **4**(1), P1-3.

Hovav, R., Chehanovsky, N., Moy, M., Jetter, R. and Schaffer, A. A. (2007) The identification of a gene (Cwp1), silenced during *Solanum* evolution, which causes cuticle microfissuring and dehydration when expressed in tomato fruit. *Plant J.,* **52**(4), 627-639.

Isaacson, T., Kosma, D. K., Matas, A. J., Buda, G. J., He, Y., Yu, B., Pravitasari, A., Batteas, J. D., Stark, R. E., Jenks, M. A. and Rose, J. K. (2009) Cutin deficiency in the tomato fruit cuticle consistently affects

resistance to microbial infection and biomechanical properties, but not transpirational water loss. *Plant J.,* **60**(2), 363-377.

Javelle, M., Vernoud, V., Depege-Fargeix, N., Arnould, C., Oursel, D., Domergue, F., Sarda, X. and Rogowsky, P. M. (2010) Overexpression of the epidermis-specific homeodomain-leucine zipper IV transcription factor outer cell Layer1 in maize identifies target genes involved in lipid metabolism and cuticle biosynthesis. *Plant Physiol.,* **154**(1), 273-286.

Javelle, M., Vernoud, V., Rogowsky, P. M. and Ingram, G. C. (2011) Epidermis: The formation and functions of a fundamental plant tissue. *New Phytol.,* **189**(1), 17-39.

Kandel, S., Sauveplane, V., Compagnon, V., Franke, R., Millet, Y., Schreiber, L., Werck-Reichhart, D. and Pinot, F. (2007) Characterization of a methyl jasmonate and wounding-responsive cytochrome P450 of *Arabidopsis thaliana* catalyzing dicarboxylic fatty acid formation in vitro. *FEBS J.,* **274**(19), 5116-5127.

Kannangara, R., Branigan, C., Liu, Y., Penfield, T., Rao, V., Mouille, G., Hofte, H., Pauly, M., Riechmann, J. L. and Broun, P. (2007) The transcription factor WIN1/SHN1 regulates cutin biosynthesis in *Arabidopsis thaliana*. *Plant Cell,* **19**(4), 1278-1294.

Kerstiens, G. (2006) Water transport in plant cuticles: An update. *J. Exp. Bot.,* **57**(11), 2493-2499.

Kolattukudy, P. E. (1977) Biosynthesis and degradation of lipid polymers. In *Advances in Phytochemistry*; Loewus, F. A., Runeckles, V. C., Eds.; Plenum Press: London. **11**,185-246.

Kolattukudy, P.E. (2001) Polyesters in higher plants. *Adv. Biochem. Eng. Biotechnol.,* **71**, 1-49.

Kosma, D.K., Bourdenx, B., Bernard, A., Parsons, E. P., Lu, S., Joubes, J. and Jenks, M. A. (2009) The impact of water deficiency on leaf cuticle lipids of *Arabidopsis*. *Plant Physiol.,* **151**(4), 1918-1929.

Kubo, H., Peeters, A. J., Aarts, M. G., Pereira, A. and Koornneef, M. (1999) ANTHOCYANINLESS2, a homeobox gene affecting anthocyanin distribution and root development in *Arabidopsis*. *Plant Cell,* **11**(7), 1217-1226.

Kunst, L. and Samuels, L. (2009) Plant cuticles shine: Advances in wax biosynthesis and export. *Curr. Opin. Plant Biol.,* **12**(6), 721-727.

Kurdyukov, S., Faust, A., Nawrath, C., Bar, S., Voisin, D., Efremova, N., Franke, R., Schreiber, L., Saedler, H., Metraux, J. P. and Yephremov, A. (2006) The epidermis-specific extracellular BODYGUARD controls cuticle development and morphogenesis in *Arabidopsis*. *Plant Cell,* **18**(2), 321-339.

Kurdyukov, S., Faust, A., Trenkamp, S., Bar, S., Franke, R., Efremova, N., Tietjen, K., Schreiber, L., Saedler, H. and Yephremov, A. (2006) Genetic and biochemical evidence for involvement of HOTHEAD in the biosynthesis of long-chain alpha-,omega-dicarboxylic fatty acids and formation of extracellular matrix. *Planta,* **224**(2), 315-329.

Le Bouquin, R., Skrabs, M., Kahn, R., Benveniste, I., Salaun, J. P., Schreiber, L., Durst, F. and Pinot, F. (2001) CYP94A5, a new cytochrome P450 from *Nicotiana tabacum* is able to catalyze the oxidation of fatty acids to the omega-alcohol and to the corresponding diacid. *Eur. J. Biochem.,* **268**(10), 3083-3090.

Lee, S.B., Go, Y. S., Bae, H. J., Park, J. H., Cho, S. H., Cho, H. J., Lee, D. S., Park, O. K., Hwang, I. and Suh, M. C. (2009) Disruption of glycosylphosphatidyl-inositol-anchored lipid transfer protein gene altered cuticular lipid composition, increased plastoglobules, and enhanced susceptibility to infection by the fungal pathogen *Alternaria brassicicola*. *Plant Physiol.,* **150**(1), 42-54.

Li, J., Liu, L., Chen, S., Du, G. and Chen, J. (2009) Advances in cutinase research. *Sheng Wu Gong Cheng Xue Bao,* **25**(12), 1829-1837.

Li, Y., Beisson, F., Koo, A. J., Molina, I., Pollard, M. and Ohlrogge, J. (2007) Identification of acyltransferases required for cutin biosynthesis and production of cutin with suberin-like monomers. *Proc. Natl. Acad. Sci. U. S. A.,* **104**(46), 18339-18344.

Li, Y., Beisson, F., Ohlrogge, J. and Pollard, M. (2007) Monoacylglycerols are components of root waxes and can be produced in the aerial cuticle by ectopic expression of a suberin-associated acyltransferase. *Plant Physiol.,* **144**(3), 1267-1277.

Li-Beisson, Y., Pollard, M., Sauveplane, V., Pinot, F., Ohlrogge, J. and Beisson, F. (2009) Nanoridges that characterize the surface morphology

of flowers require the synthesis of cutin polyester. *Proc. Natl. Acad. Sci. U. S. A.,* **106**(51), 22008-22013.

Lopez-Casado, G., Matas, A. J., Dominguez, E., Cuartero, J. and Heredia, A. (2007) Biomechanics of isolated tomato (*Solanum lycopersicum* L.) fruit cuticles: The role of the cutin matrix and polysaccharides. *J. Exp. Bot.,* **58**(14), 3875-3883.

Lopez-Casado, G., Salamanca, A. and Heredia, A. (2010) Viscoelastic nature of isolated tomato (*Solanum lycopersicum*) fruit cuticles: A mathematical model. *Physiol. Plant.,* **140**(1), 79-88.

Luo, B., Xue, X. Y., Hu, W. L., Wang, L. J. and Chen, X. Y. (2007) An ABC transporter gene of *Arabidopsis thaliana*, AtWBC11, is involved in cuticle development and prevention of organ fusion. *Plant Cell Physiol.,* **48**(12), 1790-1802.

Manas-Fernandez, A., Li-Beisson, Y., Alonso, D. L. and Garcia-Maroto, F. (2010) Cloning and molecular characterization of a glycerol-3-phosphate O-acyltransferase (GPAT) gene from *Echium* (Boraginaceae) involved in the biosynthesis of cutin polyesters. *Planta,* **232**(4), 987-997.

Matas, A.J., Yeats, T. H., Buda, G. J., Zheng, Y., Chatterjee, S., Tohge, T., Ponnala, L., Adato, A., Aharoni, A., Stark, R., Fernie, A. R., Fei, Z., Giovannoni, J. J. and Rose, J. K. (2011) Tissue- and cell-type specific transcriptome profiling of expanding tomato fruit provides insights into metabolic and regulatory specialization and cuticle formation. *Plant Cell,* .

McFarlane, H.E., Shin, J. J., Bird, D. A. and Samuels, A. L. (2010) *Arabidopsis* ABCG transporters, which are required for export of diverse cuticular lipids, dimerize in different combinations. *Plant Cell,* **22**(9), 3066-3075.

Miao, Y.C. and Liu, C. J. (2010) ATP-binding cassette-like transporters are involved in the transport of lignin precursors across plasma and vacuolar membranes. *Proc. Natl. Acad. Sci. U. S. A.,* **107**(52), 22728-22733.

Mintz-Oron, S., Mandel, T., Rogachev, I., Feldberg, L., Lotan, O., Yativ, M., Wang, Z., Jetter, R., Venger, I., Adato, A. and Aharoni, A. (2008) Gene expression and metabolism in tomato fruit surface tissues. *Plant Physiol.,* **147**(2), 823-851.

Molina, I., Ohlrogge, J. B. and Pollard, M. (2008) Deposition and localization of lipid polyester in developing seeds of *Brassica napus* and *Arabidopsis thaliana*. *Plant J.,* **53**(3), 437-449.

Muller, C. and Riederer, M. (2005) Plant surface properties in chemical ecology. *J. Chem. Ecol.,* **31**(11), 2621-2651.

Mustroph, A. and Bailey-Serres, J. (2010) The *Arabidopsis* translatome cell-specific mRNA atlas: Mining suberin and cutin lipid monomer biosynthesis genes as an example for data application. *Plant. Signal. Behav.,* **5**(3), 320-324.

Nawrath, C. (2006) Unraveling the complex network of cuticular structure and function. *Curr. Opin. Plant Biol.,* **9**(3), 281-287.

Osman, S.F., Gerard, H. C., Fett, W. F., Moreau, R. A. and Dudley, R. L. (1995) Method for the production and characterization of tomato cutin oligomers. *J. Agric. Food Chem.,* **43**(8), 2134-2137.

Otsuga, D., DeGuzman, B., Prigge, M. J., Drews, G. N. and Clark, S. E. (2001) REVOLUTA regulates meristem initiation at lateral positions. *Plant J.,* **25**(2), 223-236.

Panikashvili, D. and Aharoni, A. (2008) ABC-type transporters and cuticle assembly: Linking function to polarity in epidermis cells. *Plant. Signal. Behav.,* **3**(10), 806-809.

Panikashvili, D., Savaldi-Goldstein, S., Mandel, T., Yifhar, T., Franke, R. B., Hofer, R., Schreiber, L., Chory, J. and Aharoni, A. (2007) The *Arabidopsis* DESPERADO/AtWBC11 transporter is required for cutin and wax secretion. *Plant Physiol.,* **145**(4), 1345-1360.

Panikashvili, D., Shi, J. X., Bocobza, S., Franke, R. B., Schreiber, L. and Aharoni, A. (2010) The *Arabidopsis* DSO/ABCG11 transporter affects cutin metabolism in reproductive organs and suberin in roots. *Mol. Plant.,* **3**(3), 563-575.

Panikashvili, D., Shi, J. X., Schreiber, L. and Aharoni, A. (2009) The *Arabidopsis* DCR encoding a soluble BAHD acyltransferase is required for cutin polyester formation and seed hydration properties. *Plant Physiol.,* **151**(4), 1773-1789.

Panikashvili, D., Shi, J. X., Schreiber, L. and Aharoni, A. (2011) The *Arabidopsis* ABCG13 transporter is required for flower cuticle secretion and patterning of the petal epidermis. *New Phytol.,* .

Pighin, J.A., Zheng, H., Balakshin, L. J., Goodman, I. P., Western, T. L., Jetter, R., Kunst, L. and Samuels, A. L. (2004) Plant cuticular lipid export requires an ABC transporter. *Science,* **306**(5696), 702-704.

Pinot, F. and Beisson, F. (2011) Cytochrome P450 metabolizing fatty acids in plants: Characterization and physiological roles. *FEBS J.,* **278**(2), 195-205.

Pinot, F., Benveniste, I., Salaun, J. P., Loreau, O., Noel, J. P., Schreiber, L. and Durst, F. (1999) Production in vitro by the cytochrome P450 CYP94A1 of major C18 cutin monomers and potential messengers in plant-pathogen interactions: Enantioselectivity studies. *Biochem. J.,* **342**(1), 27-32.

Pinot, F., Salaun, J. P., Bosch, H., Lesot, A., Mioskowski, C. and Durst, F. (1992) Omega-hydroxylation of Z9-octadecenoic, Z9,10-epoxystearic and 9,10-dihydroxystearic acids by microsomal cytochrome P450 systems from *Vicia sativa*. *Biochem. Biophys. Res. Commun.,* **184**(1), 183-193.

Pinot, F., Skrabs, M., Compagnon, V., Salaun, J. P., Benveniste, I., Schreiber, L. and Durst, F. (2000) Omega-hydroxylation of epoxy- and hydroxy-fatty acids by CYP94A1: Possible involvement in plant defence. *Biochem. Soc. Trans.,* **28**(6), 867-870.

Pollard, M., Beisson, F., Li, Y. and Ohlrogge, J. B. (2008) Building lipid barriers: Biosynthesis of cutin and suberin. *Trends Plant Sci.,* **13**(5), 236-246.

Pruitt, R.E., Vielle-Calzada, J. P., Ploense, S. E., Grossniklaus, U. and Lolle, S. J. (2000) FIDDLEHEAD, a gene required to suppress epidermal cell interactions in arabidopsis, encodes a putative lipid biosynthetic enzyme. *Proc. Natl. Acad. Sci. U. S. A.,* **97**(3), 1311-1316.

Raffaele, S., Leger, A. and Roby, D. (2009) Very long chain fatty acid and lipid signaling in the response of plants to pathogens. *Plant. Signal. Behav.,* **4**(2), 94-99.

Raffaele, S., Vailleau, F., Leger, A., Joubes, J., Miersch, O., Huard, C., Blee, E., Mongrand, S., Domergue, F. and Roby, D. (2008) A MYB transcription factor regulates very-long-chain fatty acid biosynthesis for

activation of the hypersensitive cell death response in *Arabidopsis*. *Plant Cell,* **20**(3), 752-767.

Ramirez, F. J., Luque, P., Heredia, A., Bukovac, M. J. (1992) Fourier transform IR study of enzymatically isolated tomato fruit cuticular membrane. *Biopolymers*, **32**(11), 1425-1429.

Rani, S.H., Krishna, T. H., Saha, S., Negi, A. S. and Rajasekharan, R. (2010) Defective in cuticular ridges (DCR) of *Arabidopsis thaliana*, a gene associated with surface cutin formation, encodes a soluble diacylglycerol acyltransferase. *J. Biol. Chem.,* **285**(49), 38337-38347.

Rashotte, A.M., Jenks, M. A. and Feldmann, K. A. (2001) Cuticular waxes on eceriferum mutants of *Arabidopsis thaliana*. *Phytochemistry,* **57**(1), 115-123.

Reina, J.J. and Heredia, A. (2001) Plant cutin biosynthesis: The involvement of a new acyltransferase. *Trends Plant Sci.,* **6**(7), 296.

Reina-Pinto, J.J. and Yephremov, A. (2009) Surface lipids and plant defenses. *Plant Physiol. Biochem.,* **47**(6), 540-549.

Riederer, M. and Schreiber, L. (2001) Protecting against water loss: Analysis of the barrier properties of plant cuticles. *J. Exp. Bot.,* **52**(363), 2023-2032.

Rowland, O., Lee, R., Franke, R., Schreiber, L. and Kunst, L. (2007) The CER3 wax biosynthetic gene from *Arabidopsis thaliana* is allelic to WAX2/YRE/FLP1. *FEBS Lett.,* **581**(18), 3538-3544.

Rupasinghe, S.G., Duan, H. and Schuler, M. A. (2007) Molecular definitions of fatty acid hydroxylases in *Arabidopsis thaliana*. *Proteins,* **68**(1), 279-293.

Saladié, M., Matas, A.J., Isaacson, T. Jenks, M.A., Goodwin, S.M., Niklas, K.J., Xiaolin, R., Labavitch, J.M., Shackel, K.A., Fernie, A.R., Lytovchenko, A., O'Neill, M.A., Watkins, C.B. and Rose, J.K.C. (2007) A re-evaluation of the key factors that contribute to tomato fruit softening and integrity. *Plant Physiology*, **144**(2), 1012-1028.

Samuels, L., Kunst, L. and Jetter, R. (2008) Sealing plant surfaces: Cuticular wax formation by epidermal cells. *Annu. Rev. Plant. Biol.,* **59**, 683-707.

Sauveplane, V., Kandel, S., Kastner, P. E., Ehlting, J., Compagnon, V., Werck-Reichhart, D. and Pinot, F. (2009) *Arabidopsis thaliana*

CYP77A4 is the first cytochrome P450 able to catalyze the epoxidation of free fatty acids in plants. *FEBS J.,* **276**(3), 719-735.

Schnurr, J., Shockey, J. and Browse, J. (2004) The acyl-CoA synthetase encoded by LACS2 is essential for normal cuticle development in *Arabidopsis*. *Plant Cell,* **16**(3), 629-642.

Schreiber, L. (2010) Transport barriers made of cutin, suberin and associated waxes. *Trends Plant Sci.,* **15**(10), 546-553.

Seo, P.J., Lee, S. B., Suh, M. C., Park, M. J., Go, Y. S. and Park, C. M. (2011) The MYB96 transcription factor regulates cuticular wax biosynthesis under drought conditions in *Arabidopsis*. *Plant Cell,* **23**(3), 1138-1152.

Shechter, M. and Chefetz, B. (2008) Insights into the sorption properties of cutin and cutan biopolymers. *Environ. Sci. Technol.,* **42**(4), 1165-1171.

Shepherd, T. and Wynne Griffiths, D. (2006) The effects of stress on plant cuticular waxes. *New Phytol.,* **171**(3), 469-499.

Shi, J.X., Malitsky, S., De Oliveira, S., Branigan, C., Franke, R. B., Schreiber, L. and Aharoni, A. (2011) SHINE transcription factors act redundantly to pattern the archetypal surface of *Arabidopsis* flower organs. *PLoS Genet.,* **7**(5), e1001388.

Solovchenko, A. and Merzlyak, M. (2003) Optical properties and contribution of cuticle to UV protection in plants: Experiments with apple fruit. *Photochem. Photobiol. Sci.,* **2**(8), 861-866.

Tang, D., Simonich, M. T. and Innes, R. W. (2007) Mutations in LACS2, a long-chain acyl-coenzyme A synthetase, enhance susceptibility to avirulent pseudomonas syringae but confer resistance to botrytis cinerea in *Arabidopsis*. *Plant Physiol.,* **144**(2), 1093-1103.

Ukitsu, H., Kuromori, T., Toyooka, K., Goto, Y., Matsuoka, K., Sakuradani, E., Shimizu, S., Kamiya, A., Imura, Y., Yuguchi, M., Wada, T., Hirayama, T. and Shinozaki, K. (2007) Cytological and biochemical analysis of COF1, an *Arabidopsis* mutant of an ABC transporter gene. *Plant Cell Physiol.,* **48**(11), 1524-1533.

Verrier, P.J., Bird, D., Burla, B., Dassa, E., Forestier, C., Geisler, M., Klein, M., Kolukisaoglu, U., Lee, Y., Martinoia, E., Murphy, A., Rea, P. A., Samuels, L., Schulz, B., Spalding, E. J., Yazaki, K. and Theodoulou, F.

L. (2008) Plant ABC proteins--a unified nomenclature and updated inventory. *Trends Plant Sci.,* **13**(4), 151-159.

Voisin, D., Nawrath, C., Kurdyukov, S., Franke, R. B., Reina-Pinto, J. J., Efremova, N., Will, I., Schreiber, L. and Yephremov, A. (2009) Dissection of the complex phenotype in cuticular mutants of *Arabidopsis* reveals a role of SERRATE as a mediator. *PLoS Genet.,* **5**(10), e1000703.

Volokita, M., Rosilio-Brami, T., Rivkin, N. and Zik, M. (2011) Combining comparative sequence and genomic data to ascertain phylogenetic relationships and explore the evolution of the large GDSL-lipase family in land plants. *Mol. Biol. Evol.,* **28**(1), 551-565.

Wang, Z.Y., Xiong, L., Li, W., Zhu, J. K. and Zhu, J. (2011) The plant cuticle is required for osmotic stress regulation of abscisic acid biosynthesis and osmotic stress tolerance in *Arabidopsis*. *Plant Cell,* .

Wellesen, K., Durst, F., Pinot, F., Benveniste, I., Nettesheim, K., Wisman, E., Steiner-Lange, S., Saedler, H. and Yephremov, A. (2001) Functional analysis of the LACERATA gene of *Arabidopsis* provides evidence for different roles of fatty acid omega -hydroxylation in development. *Proc. Natl. Acad. Sci. U. S. A.,* **98**(17), 9694-9699.

Xiao, F., Goodwin, S. M., Xiao, Y., Sun, Z., Baker, D., Tang, X., Jenks, M. A. and Zhou, J. M. (2004) *Arabidopsis* CYP86A2 represses pseudomonas syringae type III genes and is required for cuticle development. *EMBO J.,* **23**(14), 2903-2913.

Xiao, S. and Chye, M. L. (2009) An *Arabidopsis* family of six acyl-CoA-binding proteins has three cytosolic members. *Plant Physiol. Biochem.,* **47**(6), 479-484.

Yang, W., Pollard, M., Li-Beisson, Y., Beisson, F., Feig, M. and Ohlrogge, J. (2010) A distinct type of glycerol-3-phosphate acyltransferase with *sn*-2 preference and phosphatase activity producing 2-monoacylglycerol. *Proc. Natl. Acad. Sci. U. S. A.,* **107**(26), 12040-12045.

Yeats, T.H. and Rose, J. K. (2008) The biochemistry and biology of extra-cellular plant lipid-transfer proteins (LTPs). *Protein Sci.,* **17**(2), 191-198.

Yeats, T.H., Howe, K. J., Matas, A. J., Buda, G. J., Thannhauser, T. W. and Rose, J. K. C.(2010) Mining the surface proteome of tomato (*Solanum lycopersicum*) fruit for proteins associated with cuticle biogenesis. *J. Exp. Bot.,* **61**(13), 3759-3771.

CHAPTER TWO

Map-Based Cloning of Three Fruit *Cutin-Deficient* Mutants of Tomato

2.1 Introduction

Biologically and commercially important features of plant fruit cuticles include their structure, composition and thickness, all of which may influence many important fruit traits, such as storability/shelf life, surface glossiness, and the capability of resistance to desiccation, microbial infection or cracking (Bargel et al., 2006; Bargel and Neinhuis, 2005; Kosma et al., 2010). Despite the fundamental importance of fruit cuticle, our knowledge of its synthesis and metabolism remains limited. A better understanding of the genetic and molecular mechanism underlying fruit cuticle formation in a model species is crucial for the genetic improvement of fruit crops. In this regard tomato, one of the most important vegetable and fruit crops, is an emerging model for fruit cuticle biology, as its fruit cuticle is compositionally typical of most plant cuticles, thick, astomatous and easily isolated compared to that of the experimental model plant *Arabidopsis thaliana*.

To date, most knowledge about cuticle biology has been obtained from the genetic and biochemical characterization of cuticle-related mutants and more than 50 genes involved in cuticle biosynthesis have been identified, mostly from *Arabidopsis,* maize or rice (Pollard et al., 2008; Samuels et al., 2008; Kunst and Samuels, 2009; Javelle et al., 2010).

Forward genetic approaches are valuable tool for identifying gene function or establishing a connection between the important phenotype and the genes. Screening genetic mutants from a mutagenesis population is the primary step for forward genetic analysis. Several tomato mutant collections using EMS or irradiation mutagenesis approaches have been released by different research labs (Menda et al., 2004; Minoia et al., 2010; Saito et al., 2011) (http://zamir.sgn.cornell.edu/mutants/; http://tgrc.ucdavis.edu/; http://tomatoma.nbrp.jp/index.jsp). In order to identify the genes involved in fruit cuticle biosynthesis, three fruit cuticle mutants obtained from the 'Genes that Make Tomatoes' collection (Menda et al., 2004) were chosen for gene function studies using map-based cloning strategy. The mapping results of these three genes are reported here.

Cloning of these three tomato genes was a substantial undertaking and took place at a time when there was no draft tomato genome sequence available. Therefore, this gene cloning was accomplished by a research group. Dr. Tal Isaacson initiated the mapping studies and did much of the phenotype analysis for the *cutin-deficient* mutants. Yonghua He did most genotyping

work for the cloning of *cd1* and *cd2*, as well as the part of *cd3* genotyping. Dr. Lingxia Zhao performed some genotyping for the fine-mapping of *cd3* gene and also the part of *cd1* genotyping.

2.2 Material and Methods

2.2.1 Tomato mutants, cultivars and growth conditions

Three tomato mutant lines e4247m1, e4393m2 and n3056m1 were derived from an EMS or fast neutron mutagenized population under the genetic background of tomato cultivar M82 (Menda et al., 2004; http://zamir.sgn.cornell.edu/ mutants/). These three cuticle mutants shared a similar phenotypic trait in the form of a dramatically reduced cuticular cutin load. As such, while they were named cuticle mutants 14, 15 and 20. They were later renamed *cutin-deficient 1* to *3* (*cd1*, *cd2, cd3*), respectively. The basic information about the mutants is listed in Table 2.1 and photographs of the mutant fruits from the 'Genes that Make Tomatoes' website are shown in Figure 2.1.

The fruits of three *cutin-deficient* mutants have a highly glossy appearance and a 'rubbery' surface texture with abnormal fruit color (Fig. 2.1 and Fig. 2.2), compared with those of wild-type M82, but no visible phenotype in other organs.

Table 2.1 Background information related to the three *cutin-deficient* mutants

Mutant lines	Mutagenesis	Phenotype description
e4247m1 (CM14, *cd1*)	EMS	Waxy epidermis
e4393m2 (CM15, *cd2*)	EMS	Colorless waxy epidermis; orange-tinge flesh; pink-tinge epidermis
n3056m1 (CM20, *cd3*)	Fast neutron	Gold cuticle

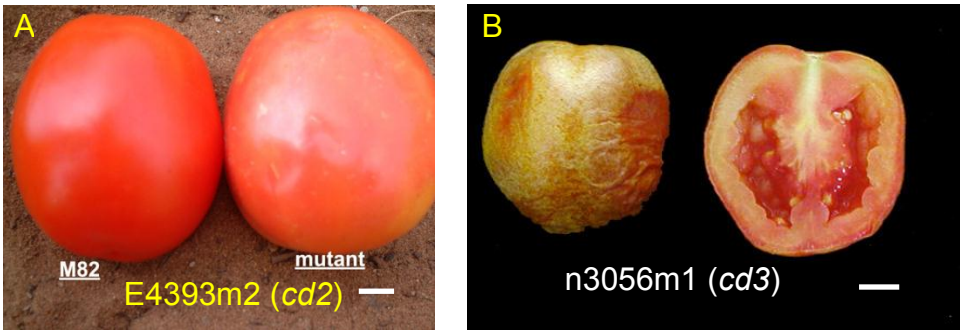

Figure 2.1 The original pictures of *cd2* and *cd3* fruits.
(A) *cd2* mutant, (B) *cd3* mutant . Scale bars = 1cm.
(From http://zamir.sgn.cornell.edu/mutants)

To assess whether the glossy fruit phenotypes of the three putative cuticle mutants were associated with quantitative or qualitative differences in wax or cutin content, the composition of isolated fruit cuticles from the three mutants and wild-type M82 at small green, mature green and red ripe stages were analyzed by GC-MS. The most striking result was that all three mutant

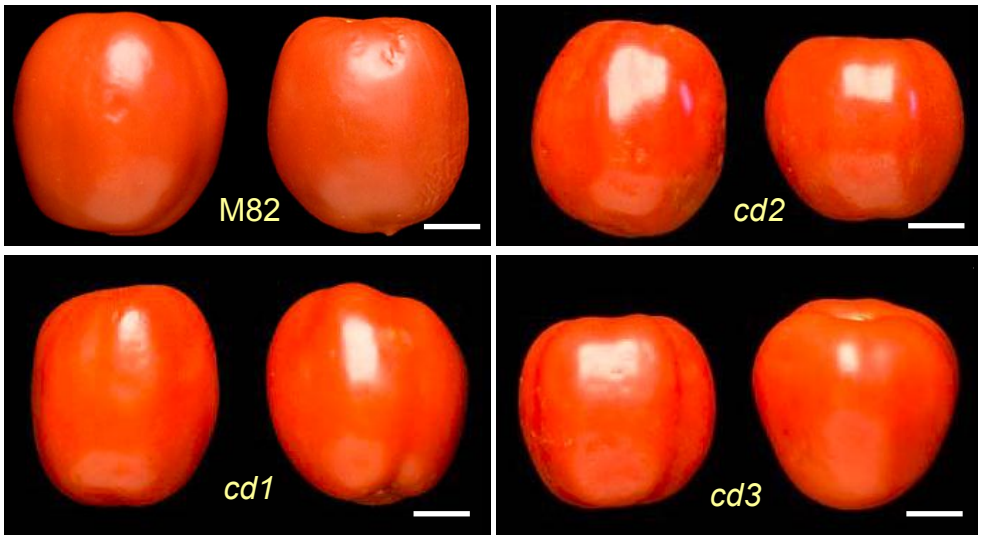

Figure 2.2 Appearance of *cutin-deficient* mutant fruit grown under greenhouse condition.
(From Isaacson et al., 2009. Scale bars = 1cm)

lines had a significantly lower level of total cutin per unit fruit surface area compared to M82, which indicated the severe cutin deficiency in these mutants. The fruits of the *cutin-deficient* mutants had normal levels of wax on a mass per area basis, but the wax compositions among mutant lines were somewhat different form wild type and from each other (Isaacson et al., 2009). Herein, the total cutin and wax load of fruit from the three mutants were depicted in Figure 2.3 for reference. The light microscope images of the fruit cutin layers of the three mutants and wild-type M82 stained by Sudan IV are shown in Figure 2.3A.

Three *cutin-deficient* mutants were back-crossed with M82 and crossed with each other for alleleism analyses. The segregation ratios of the glossy

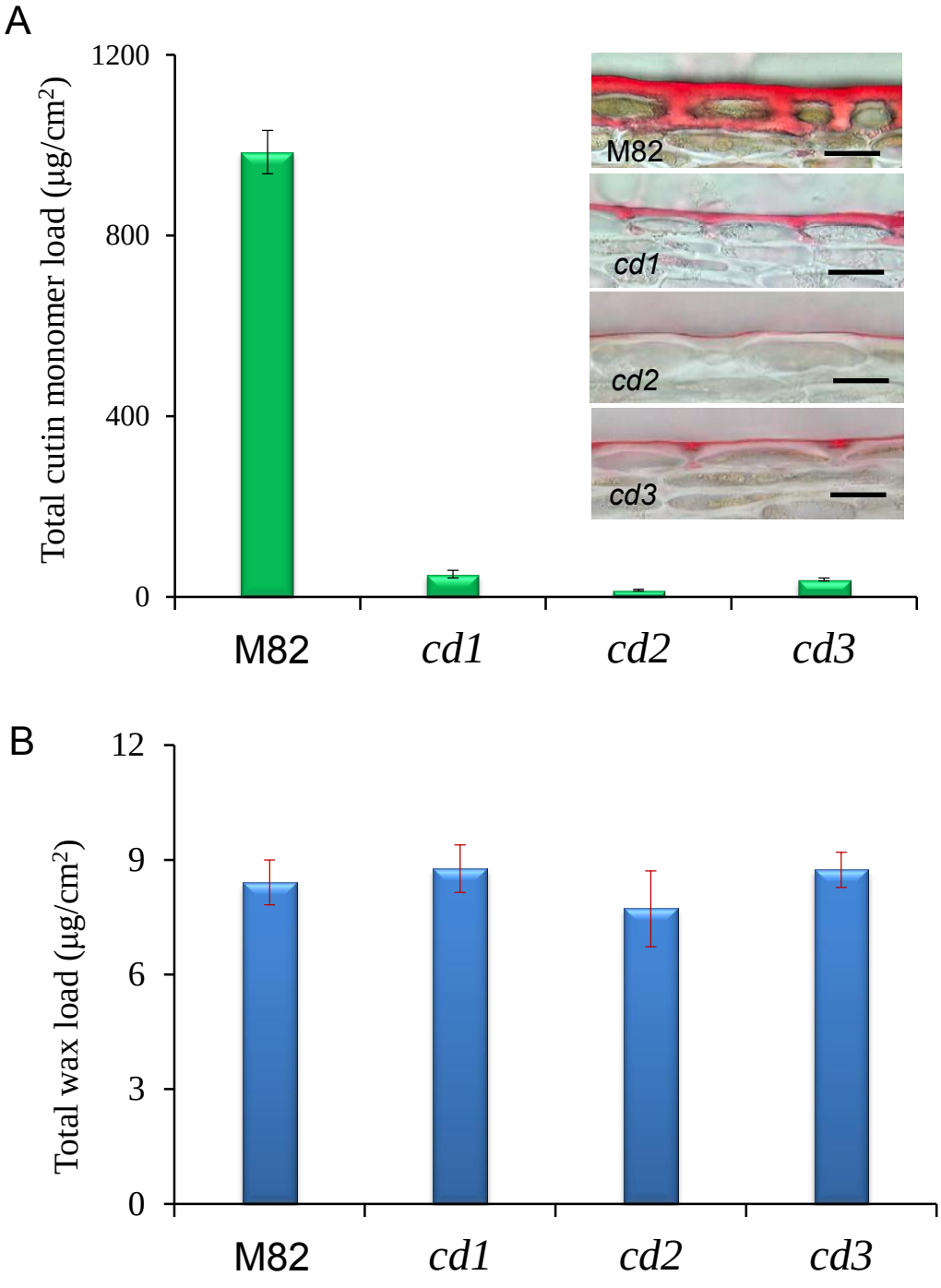

Figure 2.3 Total fruit cutin monomer (A) and wax (B) loads of *cd1, cd2* and *cd3* mutants and M82 in mature green stage.
(Adopted from Isaacson et al., 2009. Scale bars in panel A = 20 µm)

traits in the progeny indicated that the mutations occurred at three distinct gene loci. Moreover, the traits were inherited in a recessive mode in all three mutant lines.

Growth conditions: Plants were grown in a greenhouse in Ithaca, New York, with a photoperiod of 16h/8h (day/night), using standard practices.

2.2.2 Development of mapping population

Three *cutin deficient* mutants were crossed with the wild species *S. pimpinellifolium* (LA1589) to produce F_1 progenies. Seeds of the F_2 population were harvested from self-crossed F_1 plants of each population (Fig. 2.4).

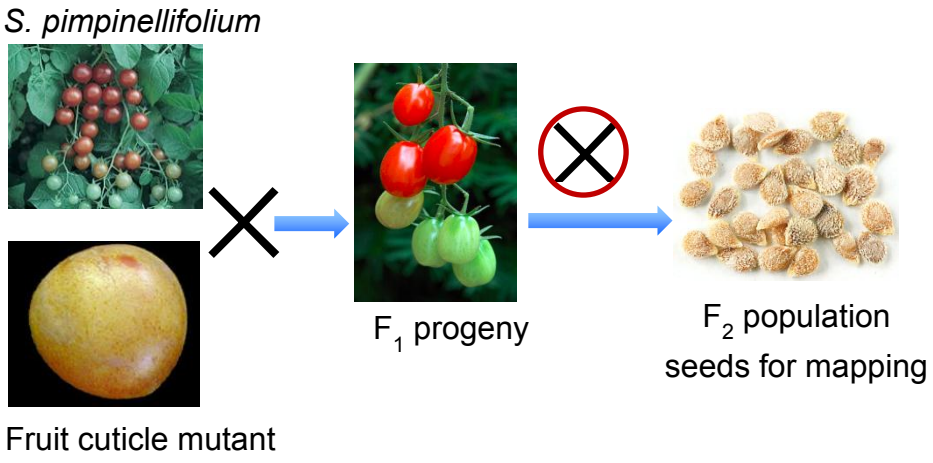

Figure 2.4 Development of F_2 mapping population of *cutin-deficient* mutants.

2.2.3 Marker design and DNA extraction

Marker development and design: Genetic markers designed for tomato TA209/*S. pimpinellifolium* mapping population in Dr. S. Tanksley's lab (Cornell University) were validated for the M82/*S. pimpinellifolium* population. For genome-wide genotyping, about 60 genetic markers were chosen that are distributed evenly across the 12 chromosomes with an interval about 20~30cM. The CAPs and dCAPs markers for gene fine mapping were designed according to the DNA sequence polymorphism by CAPS Designer (http://solgenomics.net/tools/caps_designer /caps_input.pl) and dCAPS Finder 2.0 (http://helix.wustl.edu/dcaps/dcaps.html). Descriptions of the genetic markers including marker name, location, restriction enzymes and marker quality are listed in Appendix I.

DNA extraction: For each mapping population, young leaf samples from the 94 F_2 plants plus 2 parents were collected. Genomic DNA was extracted according to the method described by Fulton et al. (1995).

2.2.4 Genotyping and phenotyping

Genotyping: PCR reactions were performed following standard protocols. PCR products were digested with appropriate restriction enzymes then fractionated on 4% agarose gels. For the first mapping population, 94

cd2 samples were genotyped with the 60 markers. Since it was determined that it was not necessary to screen with 94 samples for each population. To reduce the workload, 96 DNA samples from three mapping populations (*cd1*, *cd3* and *hcr1*, 32 samples each) were pipetted into a new plate, then genotyped with 48 markers.

Phenotyping: The phenotypes of three *cutin-deficient* mutants were scored by assessing fruit cuticle thickness using the enzymatic digestion method described in Isaacson et al. (2009).

2.2.5 Mapping data analysis

Genotype and phenotype data were analyzed using Qgene software 4.0 (http://coding.plantpath.ksu.edu/qgene/) (Joehanes and Nelson, 2008). The QTL analysis was performed with two regression models: Simple Interval Mapping (SIM) and Composite Interval Mapping (CIM-LS) with cofactor selection.

2.3 Results

2.3.1 mapping the *cd1* locus

30 plants of the F_2 population were phenotyped for cuticle thickness and then genotyped with 48 markers. The QTL map of *cd1* population is

shown in Figure 2.5. A substantial QTL (LOD =12) was located near the north end of chromosome 11 and the *CD1* gene was located between marker TG497 (11.001) and T1657 (11.009).

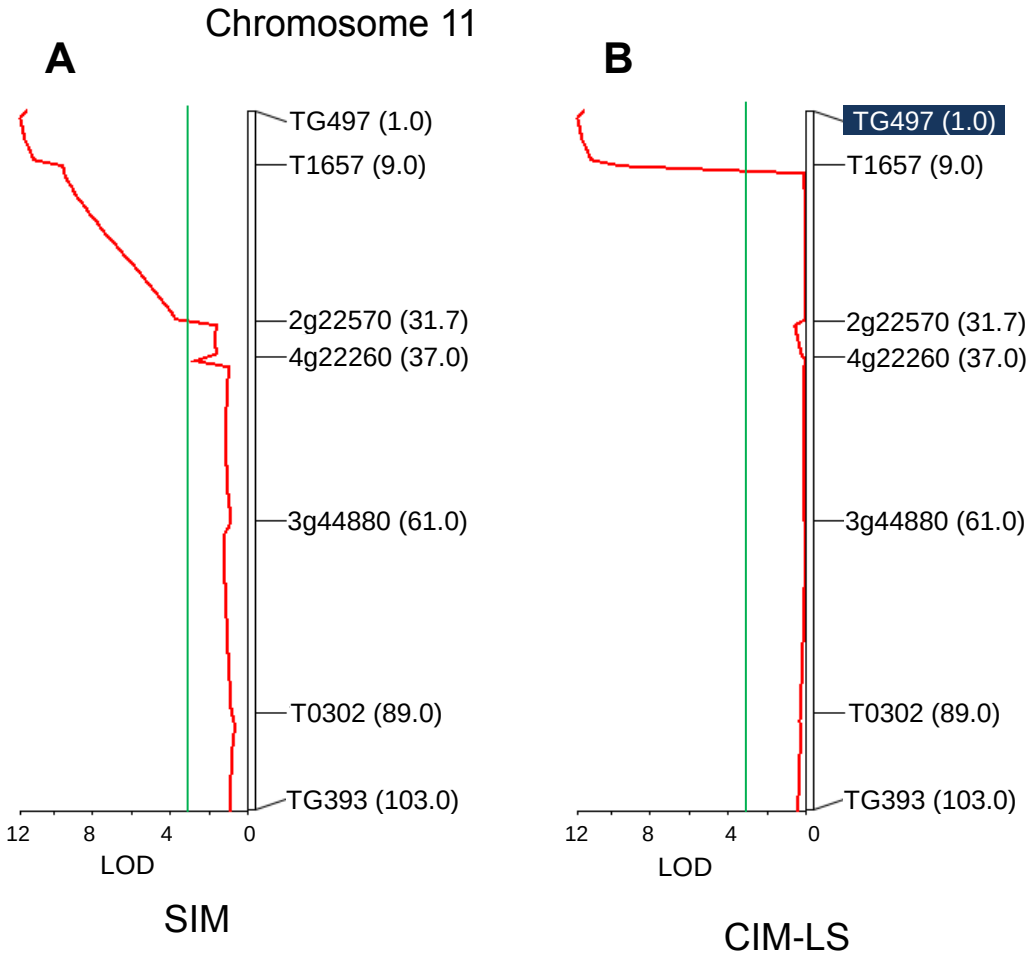

Figure 2.5 QTL map in the *cd1* mapping population

(A) QTL analysis by Simple Interval Mapping (SIM) model.
(B) QTL analysis by Composite Interval Mapping (CIM-LS) with cofactor maker (with blue background) selection.
Red line – the value of log-likelihood ratio (LOD) score
Green line – LOD threshold)
(The number in parentheses indicates the marker location in cM.)

For fine mapping, 880 F_2 plants from the *cd1* population were screened for recombinants with markers TG497 (11.001) and At5g04420 (11.015). A total of 105 recombinants were identified and their cuticle thickness phenotypes were scored. The recombinants were genotyped using newly designed CAPS (or dCAPS) markers. The phenotypic and genotypic data of important recombinants are shown in Table 2.2 and 2.3 in Appendix II.

The location of the *cd1* gene was first narrowed down to a 3.22 Mbp tomato WGS scaffold SL1.03sc01386, (corresponding to SL2.40sc03748 in version 2.3 of the ITAG tomato genome annotation, http://solgenomics.net) and subsequently to a 61 kb region between markers P120 and P140 (Fig. 2.6A). The *cd1* gene showed perfect co-segregation with marker T1968 (11.005) in all recombinants. Six putative genes were annotated in this 61 kb region and a GDSL-motif lipase/hydrolase gene (SGN-U585129) was chosen as the most promising candidate because it showed very high predicted amino acid sequence similarity (71%) to AgaSGNH, a protein that has been associated with cutin load in the leaves of *Agave americana* (Reina et al., 2007). A genomic sequence comparison of the candidate gene was performed between M82 and *cd1* mutant and a DNA polymorphism was found in the last exon of the gene. Specifically this comprised a ‘G to A’ nucleotide substitution that is predicted to introduce a stop codon (TAG) in the last exon of the *cd1* gene, the consequence of which is a predicted truncation of the last 41 amino acids, including 2 residues of the catalytic triad (Fig. 2.6B).

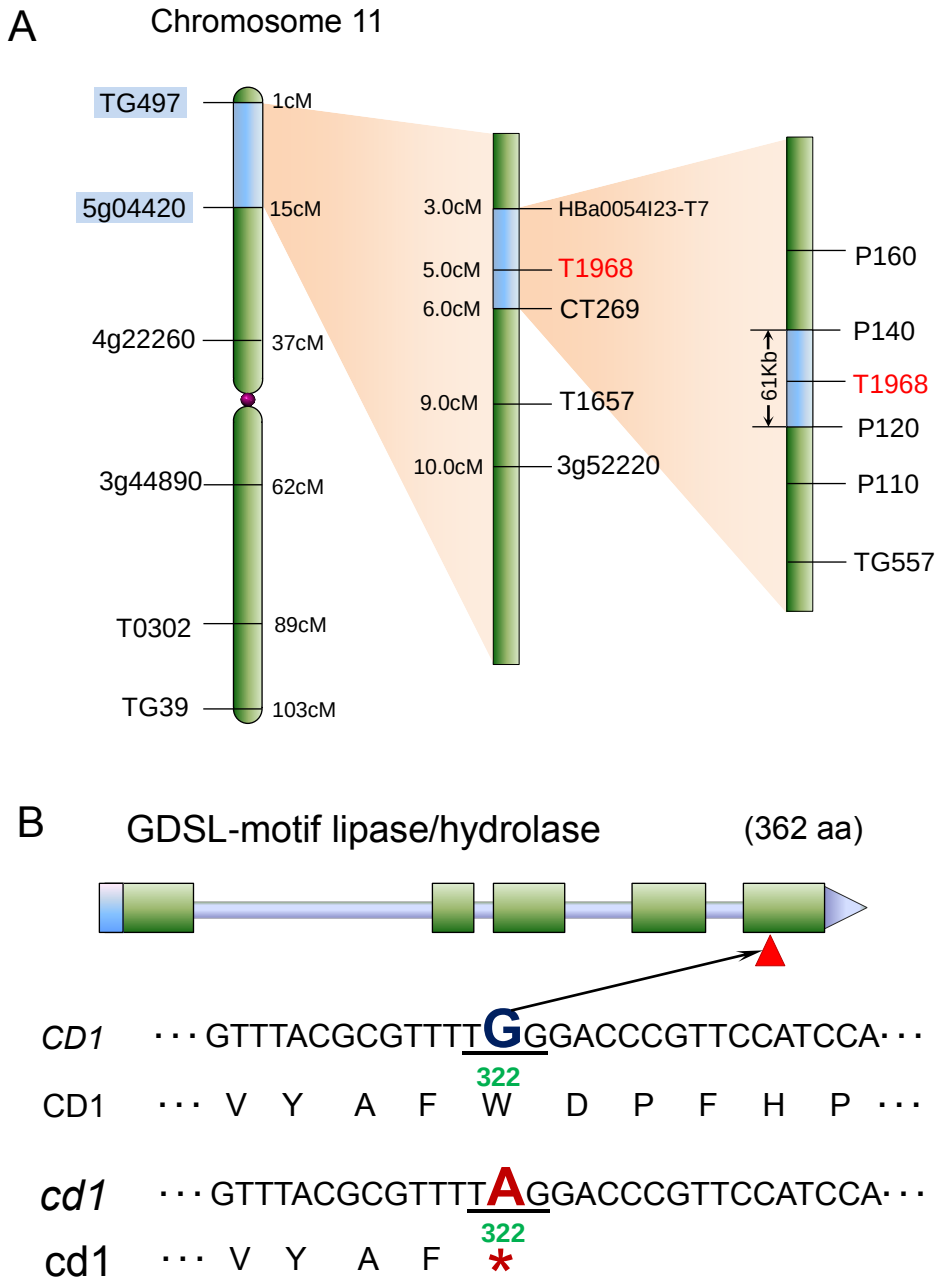

Figure 2.6 Mapping of the *cd1* locus. (A) Schematic diagram showing the mapping of *CD1* to chromosome 11 between the markers P120 and P140. (B) *CD1* gene model. The nucleotide substitution G to A introduces a stop codon (TAG) in the last exon, leading to the truncation of the last 41 amino acids including 2 residues of the catalytic triad.

Thus, a likely functional mutation associated with the *cd1* phenotype was identified. The chromosomal position of *CD1* is SL2.40 ch11:1004362… 1007293. The Genbank accession number for *CD1*: JF968592

The *CD1* gene is predicted to encode a 362 amino acid protein (Solyc11g006250.1.1). The BLAST search showed that CD1 contains a SGNH plant lipase like domain (with an E-value = 2.73e-101), and corresponds to a hydrolases in plant specific subfamily of the SGNH-family. It has been suggested that this class of protein is involved in a lipid metabolic process with a hydrolase activity.

2.3.2 mapping *cd2* locus

94 plants from the *cd2* F_2 population were genotyped using 60 markers across whole tomato genome and their fruits were phenotyped for cuticle thickness. QTL analysis of the *cd2* population showed a sharp peak (LOD >300) on chromosome 1 between the two CAPS markers T1162 (1.059) and At4g01210 (1.081) (Fig. 2.7). More than 1,200 plants of the *cd2* F_2 population were screened for recombinant events using the two above-mentioned markers. A total of 105 recombinants were identified and their cuticle phenotypes were scored. The phenotypic and the genotypic data of the recombinants are shown in Table 2.4 and 2.5 in Appendix II.

The *cd2* gene co-segregated with marker 14A17sp6 in this mapping population. At the time of the screen, no BAC or other DNA sequence

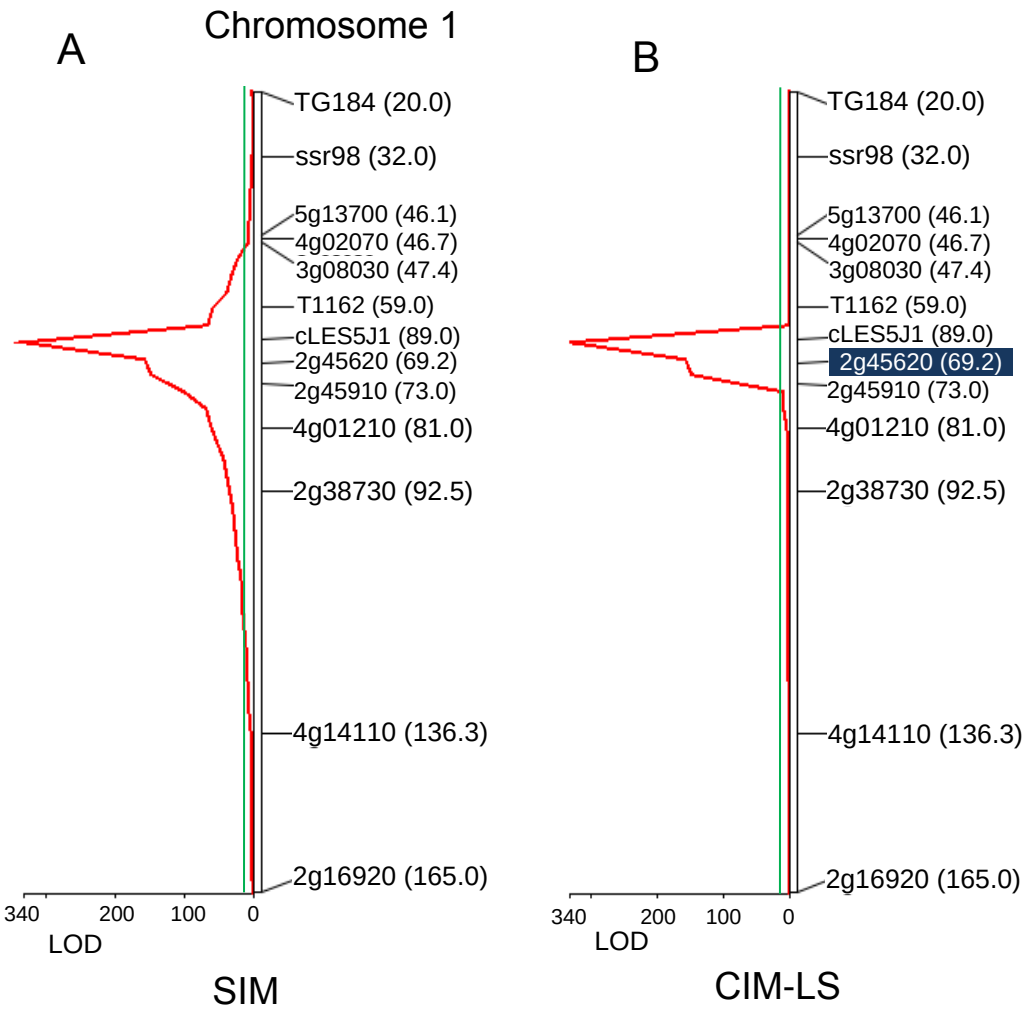

Figure 2.7 QTL map in the *cd2* mapping population.

(A) QTL analysis by Simple Interval Mapping (SIM) model.

(B) QTL analysis by Composite Interval Mapping (CIM-LS) with cofactor maker (with blue background) selection.

Red line – the value of log-likelihood ratio (LOD).

Green line – LOD threshold (>3).

(The number in parentheses indicates the marker location in cM.)

information was available around the region, other than several markers and BAC end sequences. A BAC hybridization screen was therefore carried out

using the DNA markers 14A17sp6 and TG59 as hybridization probes. Nine BACs were identified using the probes and BAC C01SLm0026F20 (130 Kb) was sequenced.

New markers were designed according to the BAC sequence and the genomic region containing the *cd2* gene was further narrowed down to a region of approximately 8 kb around marker 14A17sp6 (Fig. 2.8A), which contained only one putative gene. A DNA polymorphism was found by genomic sequence comparison between *cd2* and M82, corresponding to a 'G to A' mutation in the last exon of the *cd2* gene (Solyc01g091630.2.1:31… 3021). This is predicted to result in an amino acid change from a glycine to an arginine at position 736 of the protein (Fig. 2.8B), which likely represents the functional mutation associated with *cd2* phenotype. The chromosomal position of *CD2* is: SL2.40ch01: 76982077…76988233 and the Genbank accession number for *CD2* is GQ222185.

The BLAST search result indicated that the *CD2* gene has high similarity (Identities = 68%, E-value = 3.1e-273) to *HDG1* gene of *Arabidopsis* (AT4G00730, *HOMEODOMAIN GLABROUS 1*). The *CD2* encodes a predicted homeobox-leucine zipper family protein, with 821 amino acids (Solyc01g091630.2.1). The protein contains START_ ArGLABRA2_like domain (E-value: 2.34e-96) and has sequence-specific DNA binding transcription factor activity.

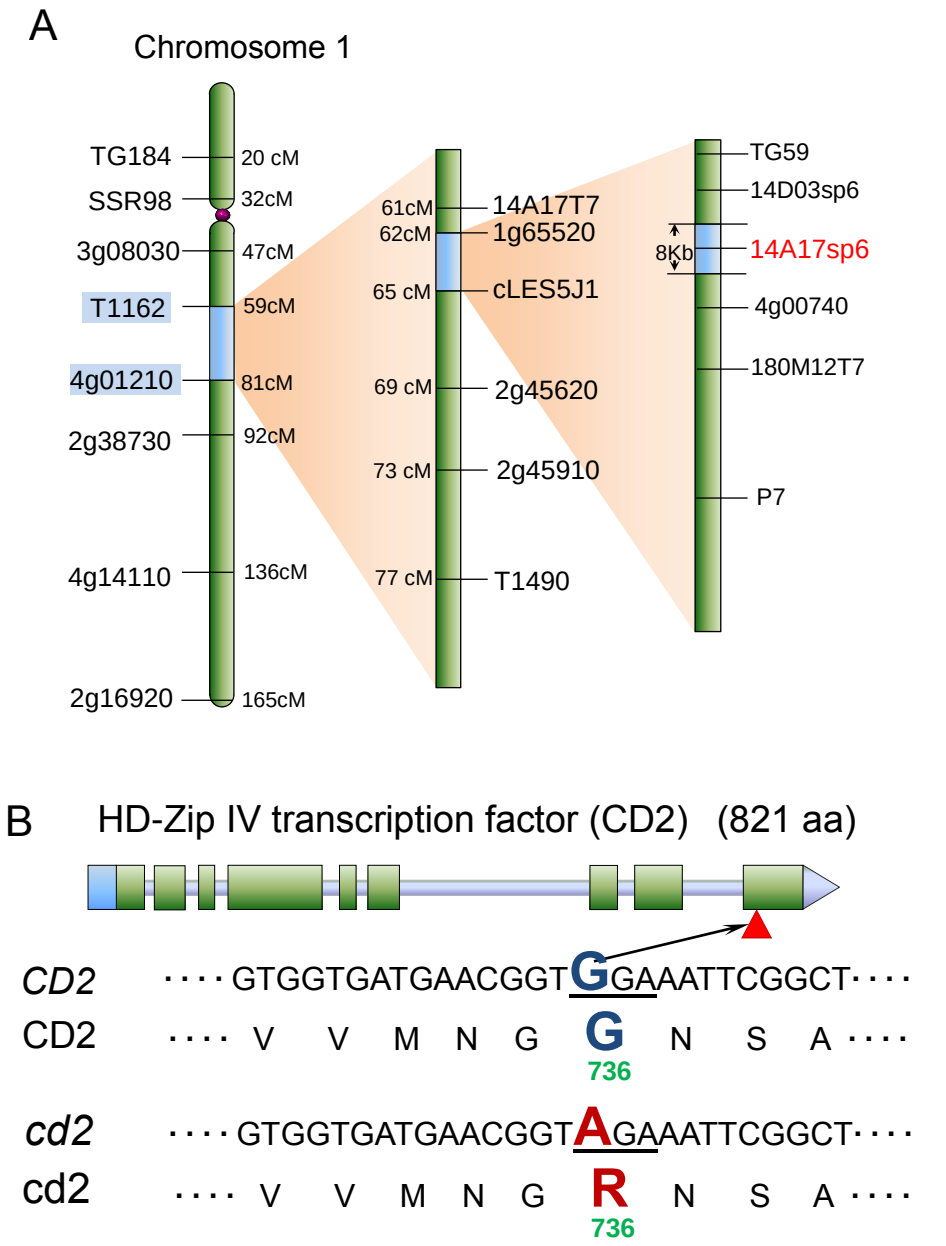

Figure 2.8 Mapping of the *cd2* locus. (A) Schematic diagram showing the mapping of *cd2* to an 8 kb region around marker 14A17sp6 on chromosome 1. (B) *CD2* gene model. A 'G to A' mutation in the last exon of the HD-Zip IV gene results in an amino acid substitution from glycine to arginine at position 736.

2.3.3 *cd3* locus mapping

A total of 47 F_2 plants in the *cd3* population were phenotyped for their fruit cuticle thickness. Out of the 47 F2 plants, a total of 30 (13 with a thin cuticle and 17 with normal cuticles) were genotyped using 48 markers across the genome. The QTL analysis showed that the *cd3* gene was located near the south end of chromosome 8, with a QTL peak (LOD =9) between the markers TG 294 (8.087) and U233990 (8.0685) (Fig. 2.9).

Recombinants were screened using two markers C2_At4g11560 (72cM) and TG294 (87cM). The genomic region containing *cd3* gene was first narrowed down to a BAC contig (C08.18_contig45) and further fine mapping localized it within a region of approximately 90 kb (Fig. 2.10A). A predicted CYP86A gene in the region was chosen as the most promising candidate as a homolog in Arabidopsis has been shown to be involved in ω-hydroxylation of fatty acids (Wellesen et al., 2001; Rupasinghe et al., 2007). Genomic sequence comparison of this candidate gene between M82 and *cd3* showed that a small DNA fragment (1.1 kb, from chromosome 7) is inserted into the exon of this CYP86A gene, leading to the truncation of the last 153 amino acids from its protein (Fig. 2.10B), which likely explains the functional mutation associated with *cd2* phenotype. The chromosomal position of *CD3* is: SL2.40ch08:61445543…61448207.

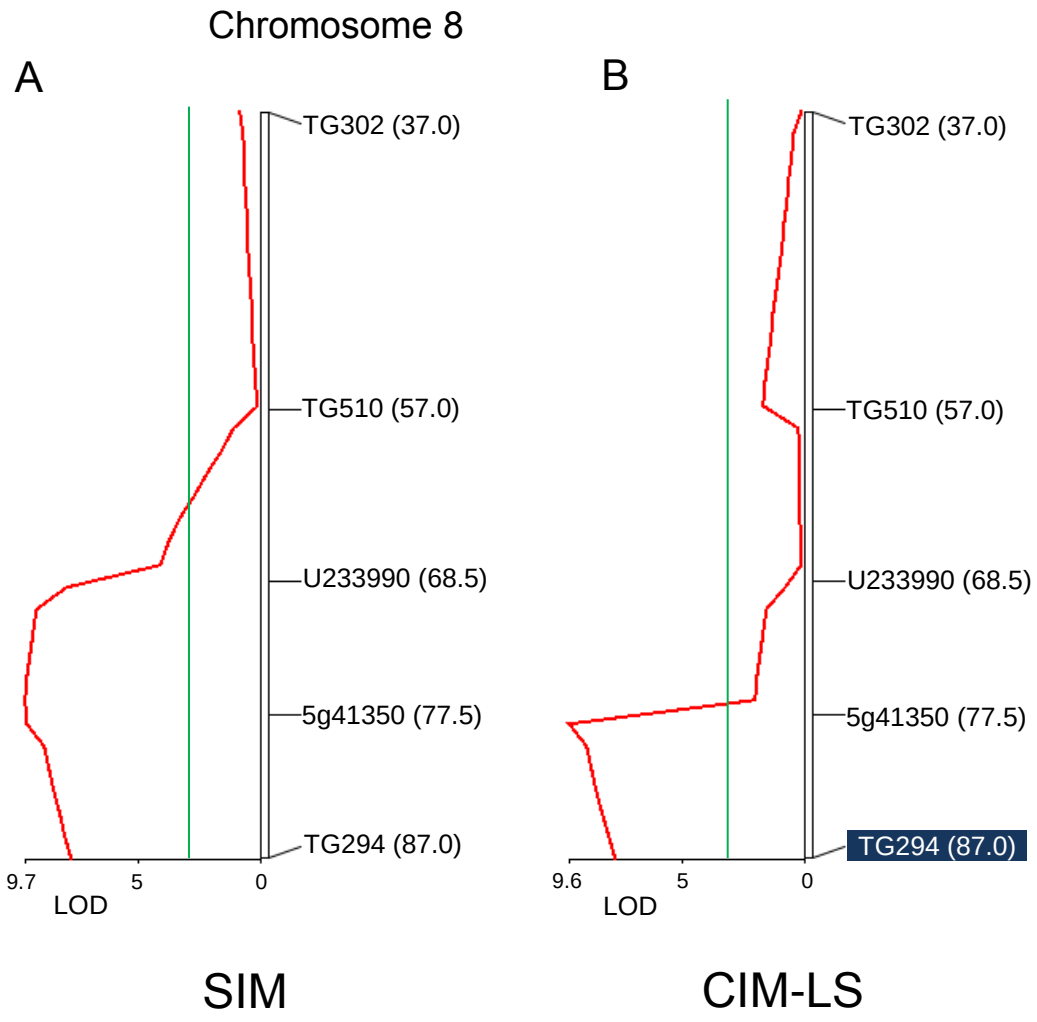

Figure 2.9 QTL map in the *cd3* mapping population

(A) QTL analysis by Simple Interval Mapping (SIM) model.
(B) QTL analysis by Composite Interval Mapping (CIM-LS) with cofactor maker (with blue background) selection.
Red line – the value of log-likelihood ratio (LOD) score
Green line – LOD threshold (>3)
(The number in parentheses indicates the marker location in cM.)

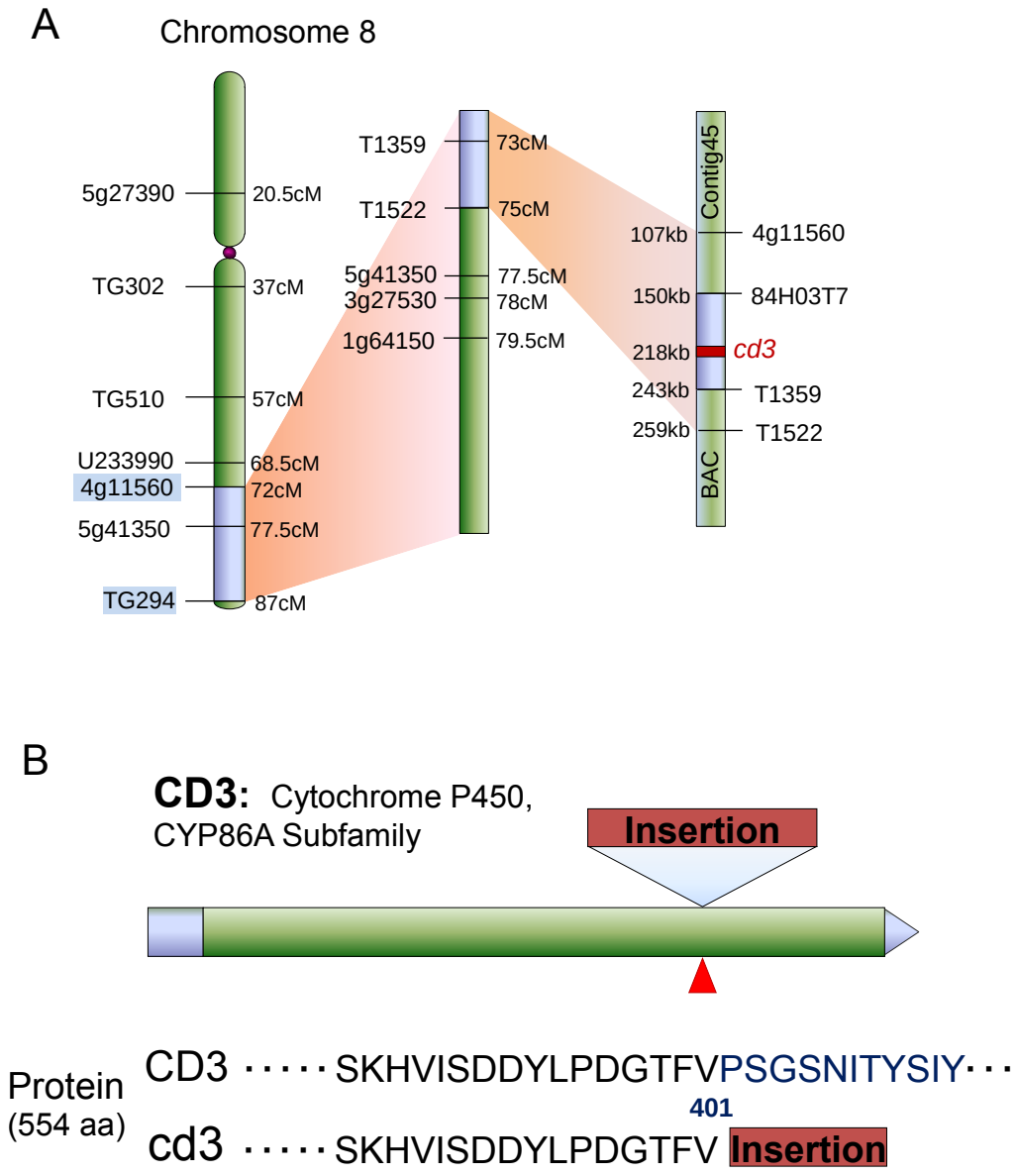

Figure 2.10 Mapping of the *cd3* locus. (A) Schematic diagram showing the mapping of *cd3* to BAC contig_45. (B) Gene model of *CD3*. A small DNA fragment (from Chr. 7) was inserted into the exon of a CYP86A subfamily gene at Chr. 8, leading to the truncation of the last 153 amino acids from the protein.

The *CD3* gene contains only one exon and encodes a 554 amino acids protein (Solyc08g081220.1.1) in the CYP86A subfamily of the cytochrome P450 family. The CD3 protein displays high amino acid sequence similarity with *Arabidopsis* CYP86A8 (70% identity ,P= 8.6e-213) and CYP86A2 (68% identity, P= 2.3e-212), suggesting that CD3 has alkane 1-monooxygenase activity and functions as an enzyme for ω-hydroxylation of fatty acids in the cutin biosynthesis pathway.

2.4 Discussion

The possible functions of three *cutin deficient* genes in cutin biosynthesis pathway the will be discussed here.

The *CD1* gene: The *cutin deficient 1* (*CD1*) gene has been intensively studied by our research group, and its function clarified. It was predicted that the CD1 protein belongs to the GDSL-motif lipase/hydrolase family (Fig. 2.11), with an acyltransferase activity, acting on ester bonds. Immunolocalization analysis indicated that the CD1 protein is almost exclusively localized in the tomato fruit cuticle. Biochemical studies showed that the recombinant CD1 protein has acyltransferase activity, with a preference for 2-MAG as an acyl donor. These results suggested that CD1 catalyzes cutin biosynthesis by successively esterifying the hydroxyacyl group of 2-MAG to the hydroxyl group of growing cutin polymer at the site of cutin formation (unpublished).

```
CD1         MATPTIILSFL-----LIFGVAICQSEARAFFVFGDSLVDSGNNNYLATTARADSPPYGI 55
AT5G33370   MTNSVAKLALLGFCILQVTSLLVPQANARAFLVFGDSLVDNGNNDFLATTARADNYPYGI 60
            *:...  *::*      : .: : *::****:********.***::********. ****

CD1         DYPTRRATGRFSNGYNIPDIISQQIGSSESPLPYLDPALTGQRLLVGANFASAGIGILND 115
AT5G33370   DFPTHRPTGRFSNGLNIPDLISEHLGQ-ESPMPYLSPMLKKDKLLRGANFASAGIGILND 119
            *:**:*.******* ****:**:::*. ***:***.* *. ::** **************

CD1         TGIQFINIIRMPQQLAYFRQYQSRVSGLIGEANTQRLVNQALVLMTLGGNDFVNNYYLVP 175
AT5G33370   TGIQFLNIIRITKQLEYFEQYKVRVSGLVGEEEMNRLVNGALVLITLGGNDFVNNYYLVP 179
            *****:****:.:** **.**: *****:** : :**** ****:***************

CD1         NSARSRQFSIQDYVPYLIREYRKILMNVYNLGARRVIVTGTGPLGCVPAELAQRSRNGEC 235
AT5G33370   FSARSRQFSLPDYVVFVISEYRKVLRKMYDLGARRVLVTGTGPMGCVPAELAQRSRNGEC 239
             ********: *** ::* ****:* ::*:******:******:****************

CD1         SPELQRAAGLFNPQLTQMLQGLNSELGSDVFIAANTQQMHTNFITNPQAYGFITSKVACC 295
AT5G33370   ATELQRAASLFNPQLIQMITDLNNEVGSSAFIAANTQQMHMDFISDPQAYGFVTSKVACC 299
            :.******.****** **: .**.*:**..********** :**::******:*******

CD1         GQGPYNGLGLCTPLSNLCPNRDVYAFWDPFHPSERANKIIVQQIMSGTTELMNPMNLSTI 355
AT5G33370   GQGPYNGIGLCTPLSNLCPNRDLFAFWDPFHPSEKASRIIAQQILNGSPEYMHPMNLSTI 359
            *******:**************::**********:*.:**.***:.*:.* *:********

CD1         LAMDSHA 362
AT5G33370   LTVDSMT 366
            *::** :
```

Figure 2.11 The alignment of CD1 sequence with the homolog in *Arabidopsis*. Score = 546 bits (1406), Expect = 5e-160, Method: Compositional matrix adjust. Identities = 256/350 (73%), Positives = 303/350 (87%). AT5G33370 = GDSL-like Lipase/ Acylhydrolase superfamily protein.

In addition, free 2-mono (10, 16-dihydroxyhexadecanoyl) glycerol (2-MHG), a 2-MAG species converted from the predominant cutin monomer of tomato (10, 16-diOH hexeadecanoic > 80%), accumulates in *cd1* fruit cuticle (unpublished). This result reinforces the notion that 2-MAG is a putative monomeric cutin precursor, as well as a transport substrate for cutin monomer movement.

The *CD2* gene: The CD2 protein possibly resides in nuclear lamina, as predicted by Subnuclear Compartments Prediction System (Version 2.0) (Lei and Dai, 2005; http://array.bioengr.uic.edu/subnuclear.htm), ESLpred (Bhasin and Raghava, 2004; http://www.imtech.res.in/raghava/eslpred/submit.html) and NucPred (Brameier et al., 2007; http://www.sbc.su.se/~maccallr/nucpred/). A BLAST search showed that the CD2 protein belongs to the IV group of the homeodomain-leucine zipper family (HD-Zip IV) (Fig. 2.12), with two predicted functional domains: a 'homeodomain' DNA binding domain and a 'StAR (steroidogenic acute regulatory protein) related lipid transfer (START)' domain.

HD-Zip proteins, being transcription factors unique to plants, are encoded by more than 25 genes in *Arabidopsis,* of which 16 members are classified in the HD-Zip IV group (Elhiti and Stasolla, 2009). Several members of the HD-Zip IV group are often expressed in outer cells of plant organs and are considered to regulate epidermis-related biological processes, such as epidermal fate, trichome formation, anthocyanin accumulation and cuticle biosynthesis (Kubo et al., 1999; Otsuga et al., 2001; Abe et al., 2003; Javelle et al., 2010). The phenotype characterization and the gene cloning of the *cd2* mutant in our lab made the first direct link between HD-ZIP IV transcription factors and cutin biosynthesis (Isaacson et al., 2009; Javelle et al., 2010).

```
CD2       MNFGGFLDNNSGGG--GARIVADIPFNHNNSSSNNDNKNNMPTGAISQPRLLPQSLAKNM 58
ANL2      MNFGSLFDNTPGGGSTGARLLSGLSYGNHTAATNVLPGGAMAQAAAAAS-LFSPPLTKSV 59
          ****.::**..***  ***:::.:.:.::.:::*    . *. .* : . *:. .*:*.:

CD2       FNSPGLSLALQTGMEGQS--EVTRMAENYEG------NNSVGRRSREEEPDSRSGSDNLE 110
ANL2      YASSGLSLALEQPERGTNRGEASMRNNNNVGGGGDTFDGSVNRRSREEEHESRSGSDNVE 119
          : *.******:   .* .  *.:   :*  *      :.**.******* :*******:*

CD2       GASGDEQDATDKPPRKKRYHRHTPQQIQELESLFKECPHPDEKQRLELSKRLSLETRQVK 170
ANL2      GISGEDQDAADKPPRKKRYHRHTPQQIQELESMFKECPHPDEKQRLELSKRLCLETRQVK 179
          * **::***:**********************:******************.*******

CD2       FWFQNRRTQMKTQLERHENSILRQENDKLRAENMSIREAMRNPICTNCGGPAMIGEISLE 230
ANL2      FWFQNRRTQMKTQLERHENALLRQENDKLRAENMSIREAMRNPICTNCGGPAMLGDVSLE 239
          ******************::**********************************:*::***

CD2       EQHLRIENARLKDELDRVCALAGKFLGRPISSLVTSMPPPMPNSSLELGVGSNGFGGMSN 290
ANL2      EHHLRIENARLKDELDRVCNLTGKFLGHHHN--------HHYNSSLELAVGTNNNGGHFA 291
          *:**************** *:*****:  .           ******.**:*. **

CD2       VPTTLPLAPPDFGVGISNSLPVVPSTRQSTGIERSLERSMYLELALAAMEELVKMAQTDE 350
ANL2      FP-------PDFGGGGG-CLP--PQQQQSTVINGIDQKSVLLELALTAMDELVKLAQSEE 341
          .*       **** * . .**  *. :*** *:   ::*: *****:**:****:**::*

CD2       PLWFRSIEGGREILNHEEYIRTFTPCIGMRPNSFISEASRETGMVIINSLALVETLMDSN 410
ANL2      PLWVKSLDGERDELNQDEYMRTFS---STKPTGLATEASRTSGMVIINSLALVETLMDSN 398
          ***.:*::* *: **::**:***:   . :*..: :**** :******************

CD2       KWAEMFPCLIARTSTTDVISSGMGGTRNGALQLMHAELQVLSPLVPIREVNFLRFCKQHA 470
ANL2      RWTEMFPCNVARATTTDVISGGMAGTINGALQLMNAELQVLSPLVPVRNVNFLRFCKQHA 458
          :*:***** :**::******.**.** *******:***********:*:***********

CD2       EGVWAVVDVSIDTIRETSGAPTFPNSRRLPSGCVVQDMPNGYSKVTWVEHAEYEEGANHH 530
ANL2      EGVWAVVDVSIDPVRENSGG--APVIRRLPSGCVVQDVSNGYSKVTWVEHAEYDENQIHQ 516
          ************.:**.**.   *  ***********:.**************:*.  *:

CD2       LYRQLISAGMGFGAQRWVATLQRQCECLAILMSSTVSARDHTAITPSGRRSMLKLAQRMT 590
ANL2      LYRPLLRSGLGFGSQRWLATLQRQCECLAILISSSVTSHDNTSITPGGRKSMLKLAQRMT 576
          *** *: :*:***:***:*************:**:*:::*:*:***.**:**********

CD2       NNFCAGVCASTVHKWNKLCAGNVDEDVRVMTRKSVDDPGEPAGIVLSAATSVWLPVSPQR 650
ANL2      FNFCSGISAPSVHNWSKLTVGNVDPDVRVMTRKSVDDPGEPPGIVLSAATSVWLPAAPQR 636
           ***:*:.*.:**:*.** .**** ***************.*************.:***

CD2       LFDFLRDERLRSEWDILSNGGPMQEMAHIAKGQDHGNCVSLLRASAMNANQSSMLILHET 710
ANL2      LYDFLRNERMRCEWDILSNGGPMQEMAHITKGQDQG--VSLLRSNAMNANQSSMLILQET 694
          *:****:**:*.*****************:****:*  *****:.************:**

CD2       CIDAAGALVVYAPVDIPAMHVVMNGGNSAYVALLPSGFSIVPDGPGSRGSNGPSCNGGPD 770
ANL2      CIDASGALVVYAPVDIPAMHVVMNGGDSSYVALLPSGFAVLPDG-GIDG--GGSGDGDQR 751
          ****:**********************:*:*********:::*** *  *  * * :*.

CD2       QRISGSLLTVAFQILVNSLPTAKLTVESVETVNNLISCTVQKIKAALQCES 821
ANL2      PVGGGSLLTVAFQILVNNLPTAKLTVESVETVNNLISCTVQKIRAALQCES 802
             .*************.************************:*******
```

Figure 2.12 The alignment of CD2 sequence with an *Arabidopsis* homolog. Score = 1100 bits (2845), Expect = 0.0, Method: Compositional matrix adjust. Identities = 572/840 (68%), Positives = 662/840 (79%). ANL2 = AT4G00730, a homeodomain protein in the HD-GLABRA2 group.

Recently, more evidence about the involvement the t HD-ZIP IV gene in the regulation of cutin biosynthesis was obtained from overexpression study of the maize *OCL1* gene. Phylogenetic analysis revealed that the maize OCL1 protein and tomato CD2 protein are clustered in the same clade of the HD-ZIP IV family, suggesting a possible function of OCL1 in the regulation of cutin or wax biosynthesis in maize (Javelle et al., 2010). Fourteen genes that are up- or down-regulated in transgenic maize plants over-expressing *OCL1* were identified by a microarray analysis. These target genes are involved in several physiological processes, such as lipid transfer, cuticle biosynthesis, envelope-related functions and plant defense (Javelle et al., 2010). Interestingly, five of the up-regulated genes shared similar annotation related to lipid transport, including type-2 lipid transfer protein (MZ00031783), SEC14/ phosphatidylinositol transfer protein (MZ00031955) and three of the ABC transporters in the WBC11/ABCG11 clade. This finding provided useful clue for the future study of the CD2 transcription factor in tomato fruits.

The *cd2* mutants were phenotypically normal except for their highly glossy fruit surface. The fruit cuticle of *cd1* mutant had a striking reduction (98%) in cutin content, but no significant difference could be detected in wax content, suggesting that this transcription factor might specifically regulate the expression of the genes involved in cutin biosynthesis. Therefore, the genetic manipulation of *CD2* gene is promising for the improvement of tomato fruit quality.

The *CD3* gene: The CD3 contains the conserved domains of fatty acid omega-hydroxylase and exhibits 70% amino acid sequence identity to CYP86A8 (LCR) and 68% to CYP86A4 of *Arabidopsis* (Fig. 2.13). This

```
CD3        MDISTGMMIVAIVVAYLLWFKSITKSMKGPKGPKIWPIVGSLPGLLENGNRMHEWIAENL 60
CYP86A8    MEISTALMILSAITAYFLWLTFISRCLKGPR---VWPILGSLPGLIENCERMHDWISDNL 57
           *:***.:**:: :.**:**:. *:::.:***:   :***:******:** :***:**::**

CD3        RVCTGTYQTCICAIPFLARKQGLVTVTCDPKNLEHILKVRFDNYPKGPTWQAVFHDLLGE 120
CYP86A8    RACSGTYQTCICAIPFLAKKQGLVTVTCDPRNLEHILKNRFDNYPKGPTWQAVFHDLLGQ 117
           *.*:**************:***********:******* ********************:

CD3        GIFNSDGDTWLFQRKTAALEFTTRTLRQAMGRWVNRAIKNRFCPILEMAQVQGKPVELQD 180
CYP86A8    GIFNSDGDTWLFQRKTAALEFTTRTLRQAMARWVNRAIKLRFLPILENARLGSEPIDLQD 177
           ******************************.******** ** **** *:: .:*::****

CD3        LLLRLTFDNICGLTFGKDPETLSPGLPENIFATSFDRATEATLHRFIIPEFVWKLKKMLG 240
CYP86A8    LLLRLTFDNICGLTFGKDPRTCAPGLPVNTFAVAFDRATEASLQRFILPEILWKFKRWLR 237
           ******************.* :**** * **.:*******:*:***:**::**:*: *

CD3        LGVEVSLSRSLKQLDNYMTDIINTRKLELMNHHNGGPQHDDLLSRFMKKKESYSDKFLQH 300
CYP86A8    LGLEVSLTRSLVQVDNYLSEIITTRKEEMMTQHNNGKHHDDLLSRFIKKKESYSDETLQR 297
           **:****:*** *:***:::**.*** *:*.:**.* :********:********: **:

CD3        VALNFILAGRDTSSVALSWFFWLVSLNPRVEEKILIELCTVLVETRGNDTSKWLEEPLVF 360
CYP86A8    VALNFILAGRDTSSVALSWFFWLITQHPAIEDKILREICTVLVETRGDDVALWTDEPLSC 357
           **********************:: :* :*:*** *:*********:*.: * :***

CD3        EEVDQLTYLKAALSETLRLYPSVPEDSKHVISDDYLPDGTFVPSGSNITYSIYSTGRMKF 420
CYP86A8    EELDRLVFLKAALSETLRLYPSVPEDSKRAVKDDVLPDGTFVPAGSSITYSIYSAGRMKS 417
           **:*:*.:********************:.:.** ********:**.*******:****

CD3        IWGEDCLEFKPERWMSK-DGNKYQVQDAFRFVAFNAGPRICLGKDLAYLQMKSIAAAVLL 479
CYP86A8    TWGEDCLEFKPERWISQSDGGRFINHDPFKFVAFNAGPRICLGKDLAYLQMKSIASAVLL 477
           *************:*: **.::  :*.*:**************************:****

CD3        RHRLAVAPGHKVEQKMSLTLFMKYGLVMNVNPRDLTPILAKIENFCKIDHSCGGEHMINN 539
CYP86A8    RHRLTVVTGHKVEQKMSLTLFMKYGLLVNVHERDLTAIAADLR-ECKSN-------VVND 529
           ****:*..******************::**: ****.* *.::  ** :       ::*:

CD3        GINQPGATAVNGIAA 554
CYP86A8    GVG-------NGVSS 537
           *:.       **:::
```

Figure 2.13 The alignment of CD3 sequence with an *Arabidopsis* homolog. Score = 830 bits (2143), Expect = 0.0, Method: Compositional matrix adjust. Identities = 392/542 (72%), Positives = 461/542 (85%). CYP86A8 has alkane 1-monooxygenase activity, involved in ω-hydroxylation of fatty acids.

suggests that the CD3 protein probably has alkane 1-monooxygenase activity and catalyzes the ω-hydroxylation of fatty acids. The CD3 is likely an ER protein, as predicted by Predotar v. 1.03 (http://urgi.versailles.inra.fr/predotar/predotar.html) and P2SL (Atalay and Cetin-Atalay 2005; http://www.i-cancer.org/p2sl/).

A schematic diagram summarizing and integrating the predicted functions and subcellular localizations of three *cutin deficient* proteins in the cutin biosynthesis pathway is shown in Figure 2.14.

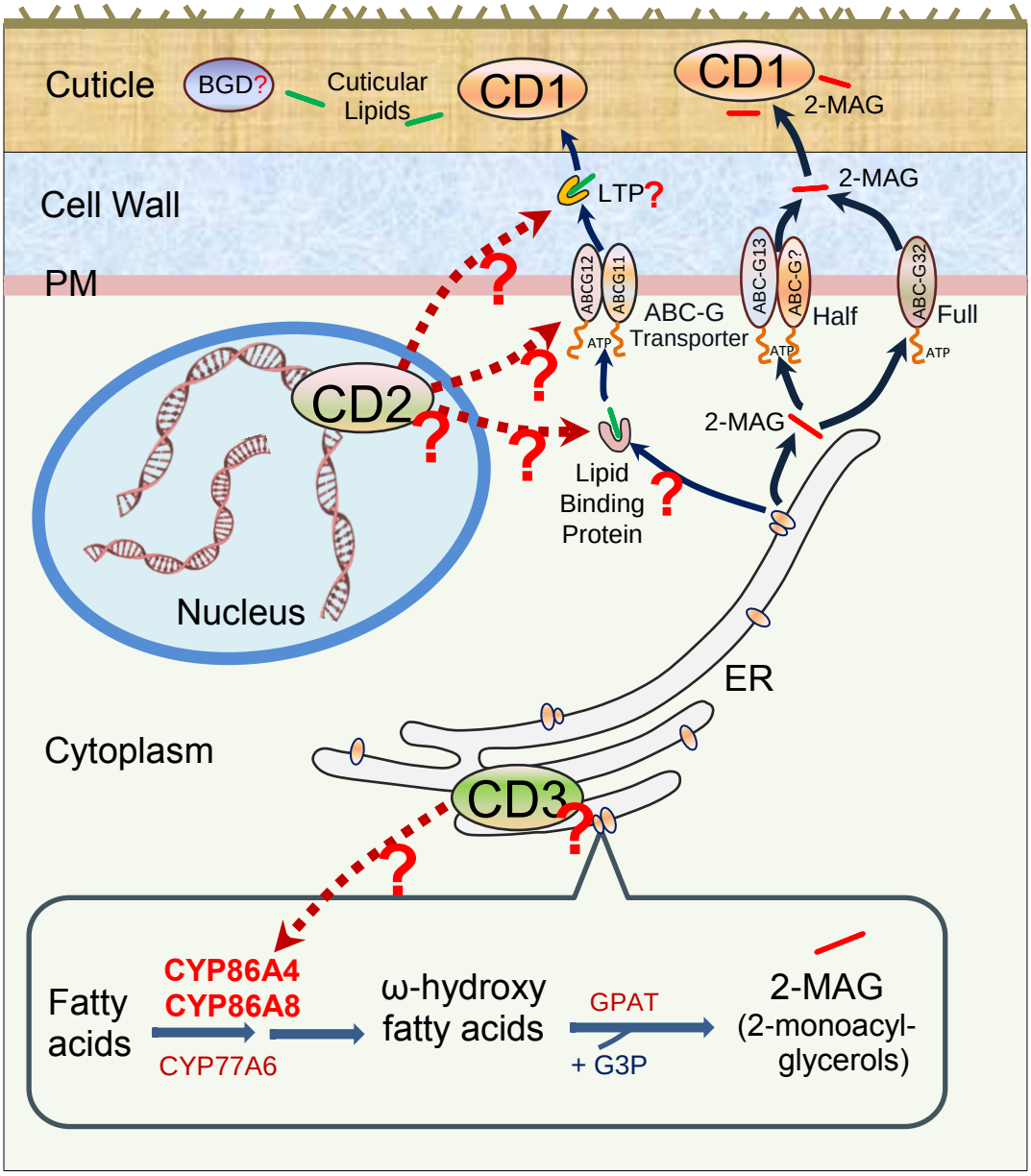

Figure 2.14 Model of the putative functions of three *cutin deficient* genes in the cutin biosynthesis pathway. Predictions: CD1 catalyzes cutin polymerization via successive transesterification of 2-MAG to the growing cutin polymer at the cutin synthesis site. CD2 is a transcription factor in the HD-Zip IV subfamily, possibly regulating the expression of the genes that encode lipid transfer proteins or ABC transporters. CD3 has alkane 1-monooxygenase activity and can catalyze ω-hydroxylation of fatty acids, probably in ER.

REFERENCES

Atalay, V. and Cetin-Atalay, R. (2005) Implicit motif distribution based hybrid computational kernel for sequence classification. *Bioinformatics,* **21**(8), 1429-1436.

Bargel, H. and Neinhuis, C. (2005) Tomato (*Lycopersicon esculentum* mill.) fruit growth and ripening as related to the biomechanical properties of fruit skin and isolated cuticle. *J. Exp. Bot.,* **56**(413), 1049-1060.

Bargel, H. and Neinhuis, C. (2004) Altered tomato (*Lycopersicon esculentum* mill.) fruit cuticle biomechanics of a pleiotropic non ripening mutant. *J. Plant Growth Regul.,* **23**(2), 61-75.

Bonaventure, G., Beisson, F., Ohlrogge, J. and Pollard, M. (2004) Analysis of the aliphatic monomer composition of polyesters associated with *Arabidopsis* epidermis: Occurrence of octadeca-cis-6, cis-9-diene-1,18-dioate as the major component. *Plant J.,* **40**(6), 920-930.

Brameier, M., Krings, A. and MacCallum, R. M. (2007) NucPred--predicting nuclear localization of proteins. *Bioinformatics,* **23**(9), 1159-1160.

Buda, G.J., Isaacson, T., Matas, A. J., Paolillo, D. J. and Rose, J. K. (2009) Three-dimensional imaging of plant cuticle architecture using confocal scanning laser microscopy. *Plant J.,* **60**(2), 378-385.

Dominguez, E., Heredia-Guerrero, J. A. and Heredia, A. (2011) The biophysical design of plant cuticles: An overview. *New Phytol.,* **189**(4), 938-949.

Dominguez, E., Cuartero, J. and Heredia, A. (2011) An overview on plant cuticle biomechanics. *Plant Sci.,* **181**(2), 77-84.

Franke, R., Briesen, I., Wojciechowski, T., Faust, A., Yephremov, A., Nawrath, C. and Schreiber, L. (2005) Apoplastic polyesters in *Arabidopsis* surface tissues--a typical suberin and a particular cutin. *Phytochemistry,* **66**(22), 2643-2658.

Fulton, M.T., Chunwongse, J., Tanskley, S. D. (1995) Microprep protocol for extraction of DNA from tomato and other herbaceous plants. *Plant Mol. Biol. Rep.*, **13**(3), 207-209.

Heredia, A., Heredia-Guerrero, J. A., Dominguez, E. and Benitez, J. J. (2009) Cutin synthesis: A slippery paradigm. *Biointerphases,* **4**(1), 1-3.

Higuchi, M., Kondou, Y., Ichikawa, T. and Matsui, M. (2011) Full-length cDNA overexpressor gene hunting system (FOX hunting system). *Methods Mol. Biol.,* **678**, 77-89.

Isaacson, T., Kosma, D. K., Matas, A. J., Buda, G. J., He, Y., Yu, B., Pravitasari, A., Batteas, J. D., Stark, R. E., Jenks, M. A. and Rose, J. K. (2009) Cutin deficiency in the tomato fruit cuticle consistently affects resistance to microbial infection and biomechanical properties, but not transpirational water loss. *Plant J.,* **60**(2), 363-377.

Javelle, M., Vernoud, V., Rogowsky, P. M. and Ingram, G. C. (2011) Epidermis: The formation and functions of a fundamental plant tissue. *New Phytol.,* **189**(1), 17-39.

Javelle, M., Vernoud, V., Depege-Fargeix, N., Arnould, C., Oursel, D., Domergue, F., Sarda, X. and Rogowsky, P. M. (2010) Overexpression of the epidermis-specific homeodomain-leucine zipper IV transcription factor outer cell Layer1 in maize identifies target genes involved in lipid metabolism and cuticle biosynthesis. *Plant Physiol.,* **154**(1), 273-286.

Joehanes, R. and Nelson, J. C. (2008) QGene 4.0, an extensible java QTL-analysis platform. *Bioinformatics,* **24**(23), 2788-2789.

Kondou, Y., Higuchi, M., Takahashi, S., Sakurai, T., Ichikawa, T., et al. (2009) Systematic approaches to using the FOX hunting system to identify useful rice genes. *Plant J.,* **57**(5), 883-894.

Kosma, D.K., Parsons, E. P., Isaacson, T., Lu, S., Rose, J. K. and Jenks, M. A. (2010) Fruit cuticle lipid composition during development in tomato ripening mutants. *Physiol. Plant.,* **139**(1), 107-117.

Kunst, L. and Samuels, L. (2009) Plant cuticles shine: Advances in wax biosynthesis and export. *Curr. Opin. Plant Biol.,* **12**(6), 721-727.

Lei, Z. and Dai, Y. (2006) Assessing protein similarity with gene ontology and its use in subnuclear localization prediction. *BMC Bioinformatics,* **7**, 491.

Lei, Z. and Dai, Y. (2005) An SVM-based system for predicting protein subnuclear localizations. *BMC Bioinformatics,* **6**, 291.

Leide, J., Hildebrandt, U., Vogg, G. and Riederer, M. (2011) The positional sterile (ps) mutation affects cuticular transpiration and wax biosynthesis of tomato fruits. *J. Plant Physiol.,* **168**(9), 871-877.

Leide, J., Hildebrandt, U., Reussing, K., Riederer, M. and Vogg, G. (2007) The developmental pattern of tomato fruit wax accumulation and its impact on cuticular transpiration barrier properties: Effects of a deficiency in a beta-ketoacyl-coenzyme A synthase (LeCER6). *Plant Physiol,* **144**(3), 1667-79.

Menda, N., Semel, Y., Peled, D., Eshed, Y. and Zamir, D. (2004) In silico screening of a saturated mutation library of tomato. *Plant J.,* **38**(5), 861-872.

Minoia, S., Petrozza, A., D'Onofrio, O., Piron, F., Mosca, G., Sozio, G., Cellini, F., Bendahmane, A. and Carriero, F. (2010) A new mutant genetic resource for tomato crop improvement by TILLING technology. *BMC Res. Notes,* **3**, 69.

Mintz-Oron, S., Mandel, T., Rogachev, I., Feldberg, L., Lotan, O., Yativ, M., Wang, Z., Jetter, R., Venger, I., Adato, A. and Aharoni, A. (2008) Gene expression and metabolism in tomato fruit surface tissues. *Plant Physiol.,* **147**(2), 823-851.

Nakamura, H., Hakata, M., Amano, K., Miyao, A., Toki, N., Kajikawa, M., Pang, J., Higashi, N., Ando, S., Toki, S., Fujita, M., Enju, A., Seki, M., Nakazawa, M., Ichikawa, T., Shinozaki, K., Matsui, M., Nagamura, Y., Hirochika, H. and Ichikawa, H. (2007) A genome-wide gain-of function analysis of rice genes using the FOX-hunting system. *Plant Mol. Biol.,* **65**(4), 357-371.

Pollard, M., Beisson, F., Li, Y. and Ohlrogge, J. B. (2008) Building lipid barriers: Biosynthesis of cutin and suberin. *Trends Plant Sci.,* **13**(5), 236-246.

Reina, J.J., Guerrero, C. and Heredia, A. (2007) Isolation, characterization, and localization of AgaSGNH cDNA: A new SGNH-motif plant hydrolase specific to *Agave americana* L. leaf epidermis. *J. Exp. Bot.,* **58**(11), 2717-2731.

Rigola, D., van Oeveren, J., Janssen, A., Bonne, A., Schneiders, H., van der Poel, H. J., van Orsouw, N. J., Hogers, R. C., de Both, M. T. and van Eijk, M. J. (2009) High-throughput detection of induced mutations and natural variation using KeyPoint technology. *PLoS One,* **4**(3), e4761.

Rupasinghe, S.G., Duan, H. and Schuler, M. A. (2007) Molecular definitions of fatty acid hydroxylases in *Arabidopsis thaliana*. *Proteins,* **68**(1), 279-293.

Saito, T., Ariizumi, T., Okabe, Y., Asamizu, E., Hiwasa-Tanase, K., Fukuda, N., Mizoguchi, T., Yamazaki, Y., Aoki, K. and Ezura, H. (2011)

TOMATOMA: A novel tomato mutant database distributing micro-tom mutant collections. *Plant Cell Physiol.,* **52**(2), 283-296.

Samuels, L., Kunst, L. and Jetter, R. (2008) Sealing plant surfaces: Cuticular wax formation by epidermal cells. *Annu. Rev. Plant. Biol.,* **59**, 683-707.

Tsai, H., Howell, T., Nitcher, R., Missirian, V., Watson, B., Ngo, K. J., Lieberman, M., Fass, J., Uauy, C., Tran, R. K., Khan, A. A., Filkov, V., Tai, T. H., Dubcovsky, J. and Comai, L. (2011) Discovery of rare mutations in populations: TILLING by sequencing. *Plant Physiol.,* **156**(3), 1257-1268.

Vogg, G., Fischer, S., Leide, J., Emmanuel, E., Jetter, R., Levy, A. A. and Riederer, M. (2004) Tomato fruit cuticular waxes and their effects on transpiration barrier properties: Functional characterization of a mutant deficient in a very-long-chain fatty acid beta-ketoacyl-CoA synthase. *J Exp Bot,* **55**(401), 1401-10.

Wellesen, K., Durst, F., Pinot, F., Benveniste, I., Nettesheim, K., Wisman, E., Steiner-Lange, S., Saedler, H. and Yephremov, A. (2001) Functional analysis of the LACERATA gene of *Arabidopsis* provides evidence for different roles of fatty acid omega -hydroxylation in development. *Proc. Natl. Acad. Sci. U. S. A.,* **98**(17), 9694-9699.

Yeats, T.H., Howe, K. J., Matas, A. J., Buda, G. J., Thannhauser, T. W. and Rose, J. K.C. (2010) Mining the surface proteome of tomato (*Solanum lycopersicum*) fruit for proteins associated with cuticle biogenesis. *J. Exp. Bot.,* **61**(13), 3759-3771.

CHAPTER THREE

Physiological and Developmental Characterization of the *hcr1* Mutant

3.1 Introduction

Fruit cuticle cracking, also called ‘swell cracking’, ‘shrink cracking’, ‘crazing’ and ‘cuticle blotch’, is a common problem encountered by commercial tomato growers (Dorais 2004). Cuticle cracking downgrades fruit quality as it causes poor appearance such as roughened skin or corky tissues and also reduces fruit shelf life. In the case of severe cracking, such as concentric and radial fruit cracking where large, deep cracks occur on the cuticle, the cracked fruits become essentially unmarketable for fresh consumption, resulting in reduced commercial yield.

A number of physiological and biophysical studies have demonstrated that the development of cuticle cracking is associated with fruit characteristics such as fruit anatomy, shape and growth rate, water status and sugar content (Emmons and Scott, 1998; Dorais 2004). Cracking is also intimately associated with features of the fruit epidermis, such as cuticle thickness, ultrastructure and mechanical properties (Matas et al., 2004, 2005; Lopez-

Casado et al., 2007; Dominguez et al., 2011; Hetzroni et al., 2011). The cuticle biomechanical parameters change during plant growth and are affected by components of fruit cuticular membrane, such as cutin, wax and polysaccharides. In addition, tomato fruit cuticle cracking is considerably influenced by cultivation practices such as growth season and irrigation management, and environmental factors such as air temperature, humidity and illumination (Dorais 2004; Matas et al., 2005; Hahn, 2011). Cuticular cracking initiation typically occurs after fruit absolute growth rates reach maximum values and so growth rate, at the moment the cracks are first observed, is usually unrelated to the actual incidence of cracking (Ehret et al., 1993).

Susceptibility to fruit cuticle cracking has been intensely studied among various tomato cultivars (Emmons and Scott, 1998; Dorais 2004; Matas et al., 2004), leading to the conclusion that many genes may be involved in the development of fruit cracking, and each type of cracking may be influenced by specific genes (Cuartero et al., 1981). However, studies targeting the genetic or molecular mechanisms underlying fruit cracking are extremely limited compared with equivalent morphological and physiological studies, in which has limited the breeding and development of cracking-resistant cultivars (Moctezuma et al., 2003).

To shed new light on the cracking phenomenon and particularly to investigate the underlying molecular bases, a search was performed online of

the ‘Genes that Make Tomatoes’ collection (http://zamir.sgn.cornell.edu/mutants/; Menda et al., 2004) for mutants that were annotated as exhibiting a fruit cracking phenotype. One mutant (# e4702m1) was identified as having substantial fruit cuticle cracking and was named *hypercracking 1* (*hcr1*). In this chapter, the characterization of the physiological and developmental phenotypes of the *hcr1* mutant is described and the possible underlying mechanisms are discussed.

3.2 Material and Methods

3.2.1 Plant materials

Seeds of *hcr1* mutant were obtained from the ‘Genes that Make Tomatoes’ EMS mutagenesis collection (Menda et al., 2004). Tomato plants were grown in the Guterman greenhouse at Cornell University, Ithaca, New York, under 16 hour of light and 8 hour of dark, using standard practices. Due to the low self-pollination rate of *hcr1* under greenhouse condition, the flowers of *hcr1* and M82 were hand-pollinated and tagged. Fruits from mutant and wild-type plants were harvested at the appropriate number of days after pollination (DAP). For the mature green (MG) stage, fruits were collected when they reached full size, but were still green and the red ripe (RR) stage corresponded to fruits 4-5 days after the color break.

3.2.2 Microscopy

For structural analyses of the fruit pericarp, fruit tissue was fixed and embedded in paraffin as described by Jackson (1992) and 6 µm paraffin sections of fruit pericarp were prepared. Sudan IV, Toluidine Blue and Neutral Red staining were conducted as described in Buda et al. (2009). For estimating cell size and the number of pericarp cell layers, paraffin sections were stained with Toluidine Blue and 10 or more sections were counted, as described in Vrebalov et al. (2009). The size of the parenchyma cells was estimated by counting cell numbers within a certain area using ImageJ software (http://rsbweb.nih.gov/ij/) and 8 or more sections were measured each sample.

3.2.3 Scanning electron microscopy (SEM)

Scanning electron microscopy (SEM) was performed as described previously by Isaacson et al. (2009) with minor modifications. Briefly, whole fruits at young stages (3-9 DAP) were frozen in liquid nitrogen, freeze dried, mounted on aluminum stubs and sputter coated with gold: palladium 60:40 using a Denton Desk II coater. Microscopic observations of fruit surface were made with a Leica 440 scanning electron microscope using an accelerating voltage of 5 kV (Leica, http://www.leica.com).

3.2.4 Statistics

The measurement results of some phenotypes in the chapter 3 and 4 were represented as means ± S.D. (Standard Deviation). The significant differences were determined by the Student's t-test.

3.3 Results

3.3.1 The phenotypes of the *hcr1* mutant

Greenhouse grown *hcr1* plants are phenotypically normal during vegetative growth. After emergence of the first inflorescence, necrotic spots gradually developed on some of the newly emerging leaves (Fig. 3.1A) and some necrosis was apparent on the surface of some of the anthers (Fig. 3.1B).

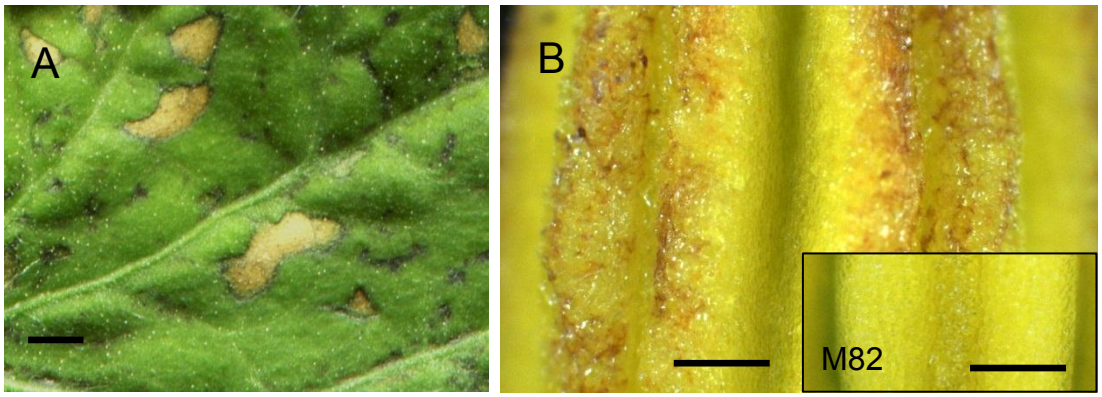

Figure 3.1 Necrosis on leaves and anthers of *hcr1* mutant
(A) Necrotic spots on a leaf of the *hcr1* mutant. Scale bar = 2 mm.
(B) Enzymatic discoloration on anther surface of *hcr1* mutant. The picture in the bottom right corner shows the normal anther surface of M82. Scale bars = 500 μm.

However, the major phenotypes were apparent on the *hcr1* fruits during their rapid expansion phase, including fruit discoloration (Fig. 3.2), reduced fruit expansion (Fig. 3.3), fruit cracking (Fig. 3.4) and suberization (Fig. 3.5).

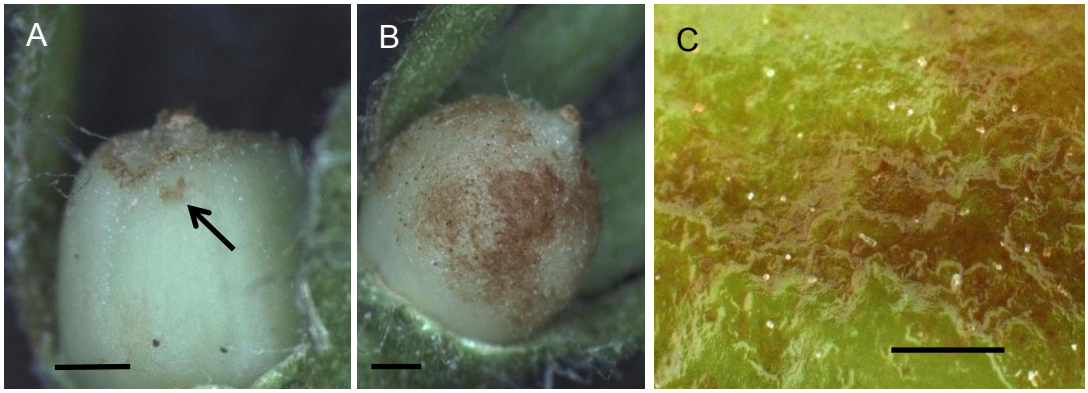

Figure 3.2 Discoloration phenotype of young *hcr1* fruits. Necrotic phenotypes of *hcr1* fruits at (A) 3 DAP (highlighted with an arrowhead). Scale bar = 1 mm. (B) 5 DAP. Scale bar = 1 mm. (C) 9 DAP. Scale bar = 500 µm

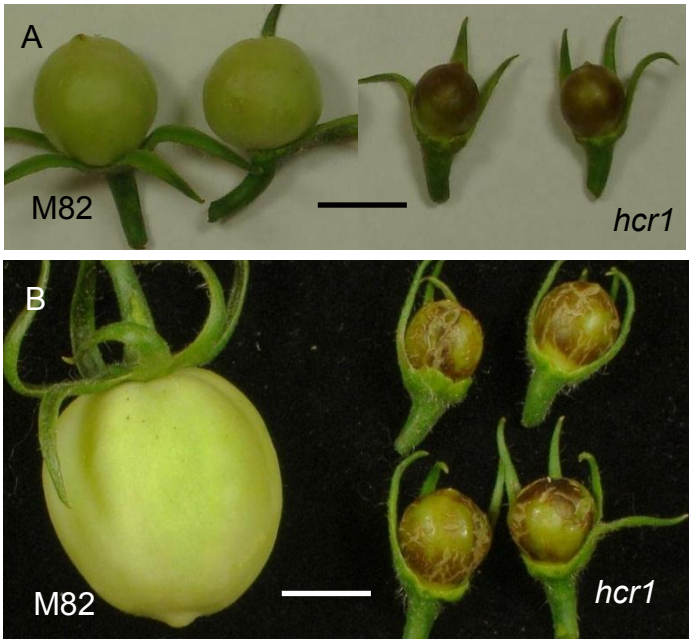

Figure 3.3 The fruit size phenotype of *hcr1*. Comparison of fruit sizes between *hcr1* and M82 at (A) 7 DAP and (B) 14 DAP. Scale bars = 1 cm

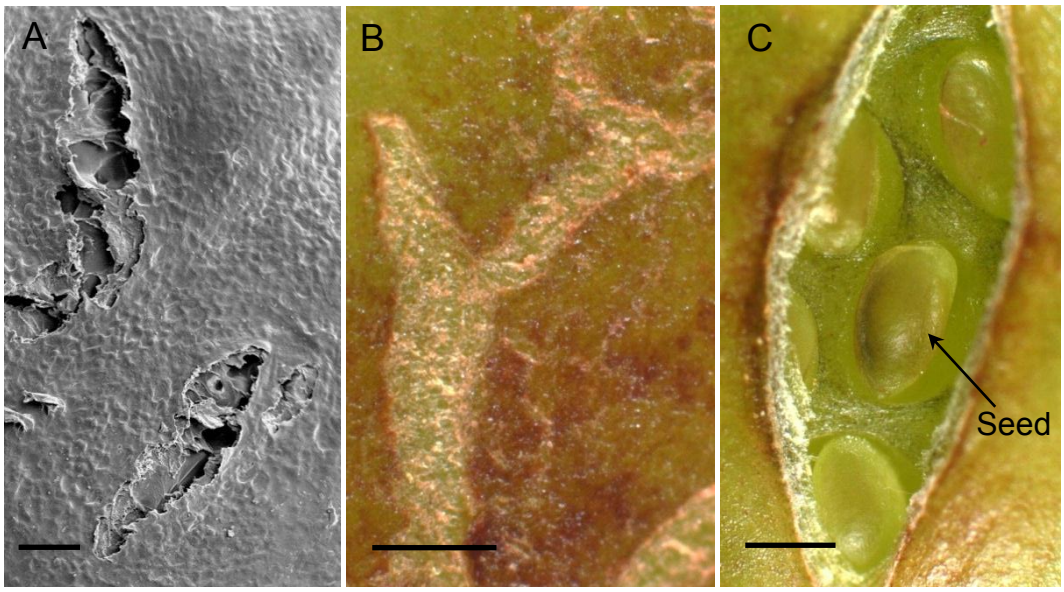

Figure 3.4 Fruit cracking in *hcr1* fruits. (A) Scanning Electron Micrograph (SEM) of *hcr1* fruit surface at 6 DAP showing the small cracks. Scale bar = 50 µm. (B) and (C) cracks on *hcr1* fruit at 9 DAP. Scale bars = 500 µm

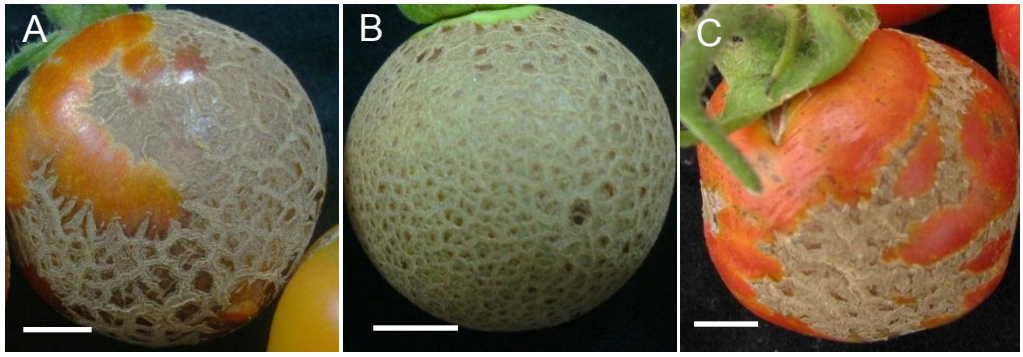

Figure 3.5 The suberization phenotype of *hcr1* fruits, showing different patterns of suberin scars. Scale bars = 1 cm

Fruit discoloration occurred as early as 3 DAP, and all fruits exhibited some discoloration at 6 DAP (Fig. 3.6). The first visible cracks were generally

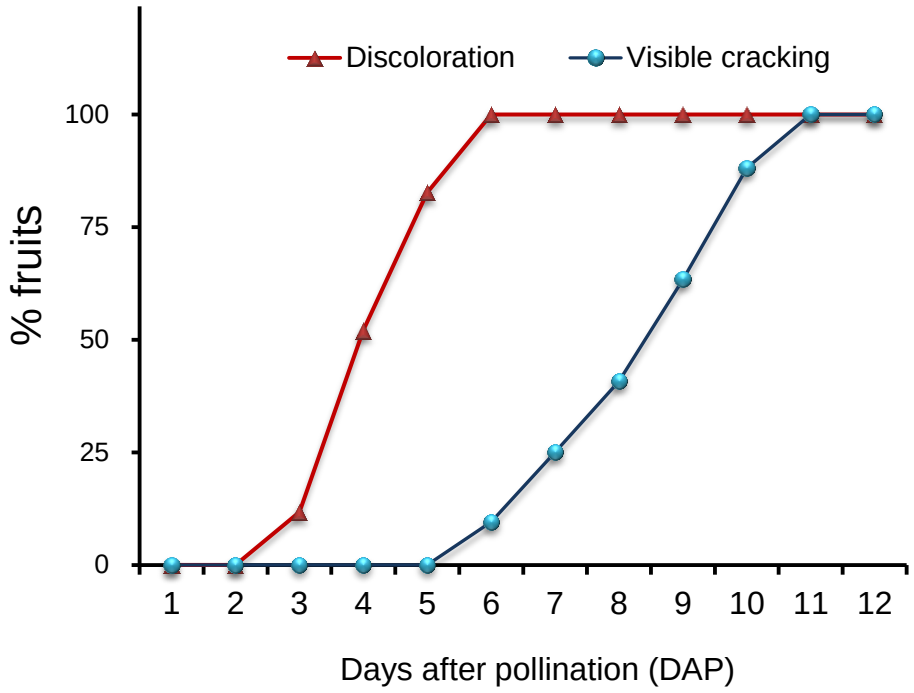

Figure 3.6 Time course of the occurrence of discoloration or visible cracks on the *hcr1* fruit surface.

seen 3-5 days after the appearance of discoloration. However, the most striking phenotype of*hcr1* fruit was the deposition of large suberized scars (Fig. 3.5) which typically occurred coincident with the cracks indicating that the suberization is a wounding response to the cracking. Interestingly, parthenocarpic fruits, which typically occur at a low frequency in tomato, showed no surface suberin scars or cracking in the case of *hcr1* (Fig. 3.7). From the cross sections of fruits at 14 DAP (Fig. 3.8), it was apparent that the pericarp of *hcr1* fruit is far thinner and there are very small locular cavities, or sometimes no apparent cavity compared to that of the M82 wild type fruit.

Figure 3.7 Parthenocarpic fruits of the *hcr1* showing the absence of suberization on the surface. Scale bars = 1 cm

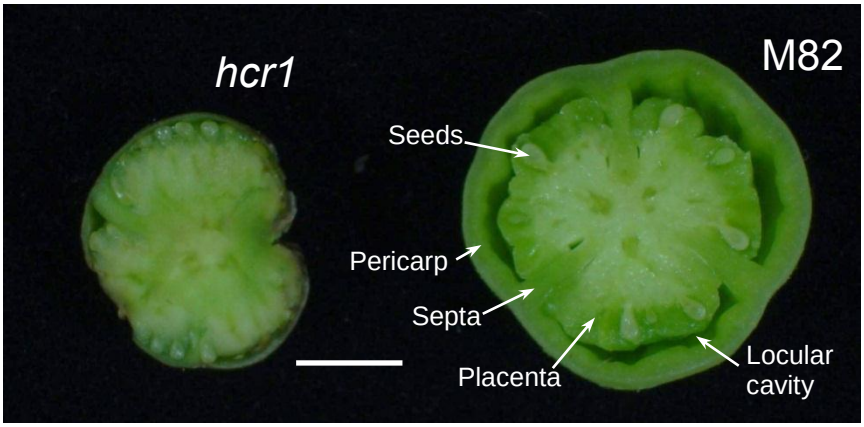

Figure 3.8 Comparisons of fruit cross sections of *hcr1* and M82 fruit. Fruit cross sections of *hcr1* and M82 at 14 DAP. Scale bars = 1 cm.

The morphology of the *hcr1* fruit pericarp cells was obviously altered by the mutation, in comparison with that of the wild-type. At 7 DAP, several layers of misshapen cells with aberrant cell wall thickening were observed near the epidermis in *hcr1* (Fig. 3.9B), in contrast to well-organized epidermal

cells of M82 (Fig 3.9A). At 14 DAP, the cutin layer of *hcr1* fruit (Fig. 3.9D) was significantly thinner than that of M82 (Fig. 3.9C), suggesting a defect in cuticle development. Substantial suberization was apparent associated with the cracked areas of *hcr1* fruit (Fig. 3.9F).

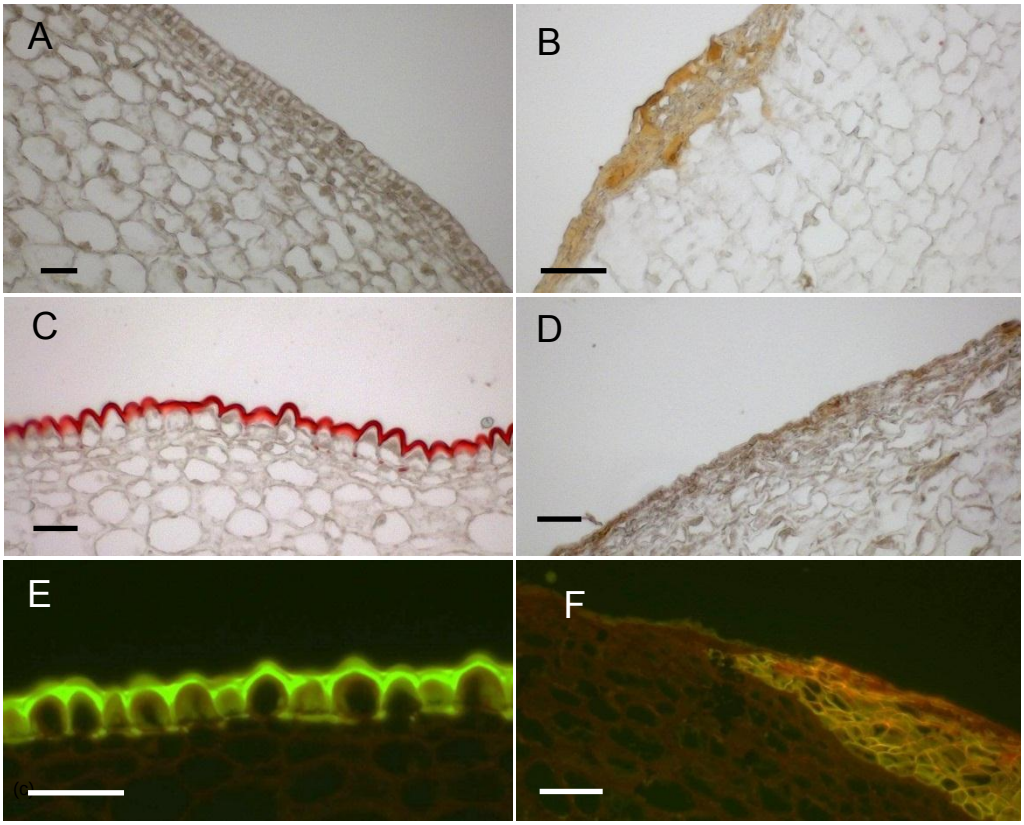

Figure 3.9 Light microscopy images of *hcr1* fruit surface tissues using a range of stains to highlight different polymer matrices
(A-B) Fruit pericarp cross sections of M82 (A) and *hcr1* (B) at 7 DAP, stained with Sudan IV, showing disordered epidermal cells with thickened cell walls in *hcr1*. (C-D) Fruit pericarp cross sections of M82 (C) and *hcr1* (D) at 14 DAP, stained with Sudan IV, showing the developing cutin layer in M82 (C), but almost no cutin layer in *hcr1* (D). (E-F) Fluorescence images of fruit pericarp cross sections at 21DAP, stained with neutral red, showing a well-developed cutin layer in M82 (E) and the suberized tissues in *hcr1*(F). (Scale bars = 50 μm)

The average size of *hcr1* pericarp parenchyma cells in cross section was substantially less than that of wild-type (Fig. 3.10), indicating an inhibition of the cell expansion in *hcr1* fruits.

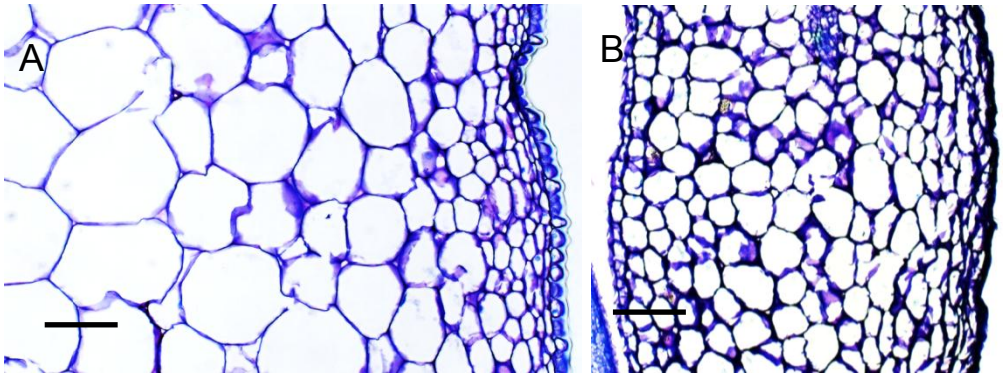

Figure 3.10 Cell size comparison of the pericarp of *hcr1* and M82 fruit. Light microscopy images of pericarp cross section from M82 (A) and *hcr1* (B) fruit at 14 DAP in the same magnification, showing inhibition of cell expansion in *hcr1*(B). Scale bars = 100 μm

3.3.2 Abnormal cell, tissue and organ development of *hcr1* fruit is associated with aberrant cell expansion and division

To quantify some of the clear anatomical abnormalities of the *hcr1* fruit, measurements were made of the pericarp thickness and the ratios of the fresh weights of pericarp versus those of the inner tissues at an early fruit developmental stage, compared with M82 (Fig. 3.11). No differences were detected in pericarp (ovary wall) thickness at 0 DAP (Fig. 3.11A) but significant differences (P-value = 2.8E-06) were present by 3 DAP. The pericarp

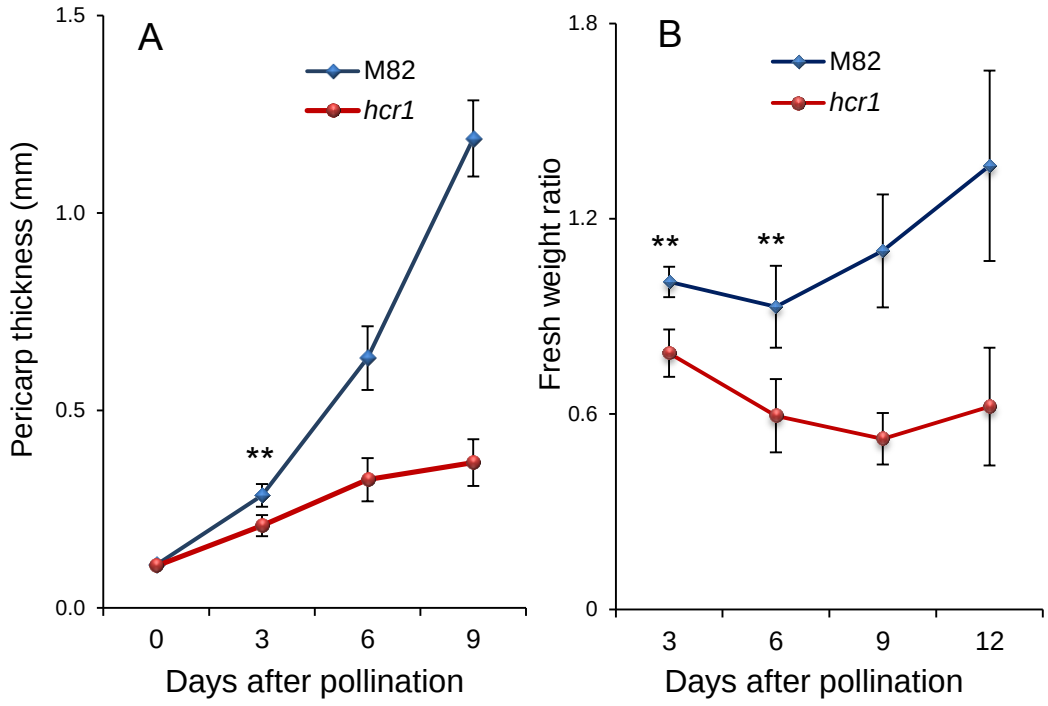

Figure 3.11 Pericarp and inner tissue development of *hcr1* fruit.
(A) A comparison of fruit pericarp thickness in *hcr1* and M82.
(B) Fresh weight ratio of pericarp to inner tissue of fruit in *hcr1* and M82.
(Mean ± SD of N ≥ 8; ** P < 0.01 by two-tailed t-test.)

thickness of *hcr1* fruits was less than 30% of that of the wild-type pericarp by 9 DAP. The lack of normal pericarp development was also reflected in measurements of the fresh weight ratio of pericarp versus inner tissue in *hcr1* fruit, which was substantially smaller than that of M82 at 3 DAP (Fig. 3.11B). The ratio in *hcr1* fruits continued to decline until 9 DAP in contrast to that in M82, which continued to increase throughout the time course. These results confirmed that the growth of pericarp of *hcr1* fruits was significantly inhibited compared with wild-type fruits.

To determine whether this was a consequence of defective cell expansion or division, the number of pericarp cell layers was counted and the parenchyma cell sizes were measured by light microscopy analysis of pericarp sections (Fig. 3.12). No differences were seen in the number of cell layers in the ovary wall between the *hcr1* mutant and M82 at 0 DAP, but a significant (p-value = 1.4E-05) reduction was present in *hcr1* by 3 DAP. A substantial difference (approximately 30% reduction) from 6 DAP onwards (Fig. 3.12A), indicating that the cell *hcr1* mutation caused a disruption of cell division. For the average areas of pericarp parenchyma cells, no difference was observed between mutant and wild type at 0 and 3 DAP, but by 12 DAP, the average

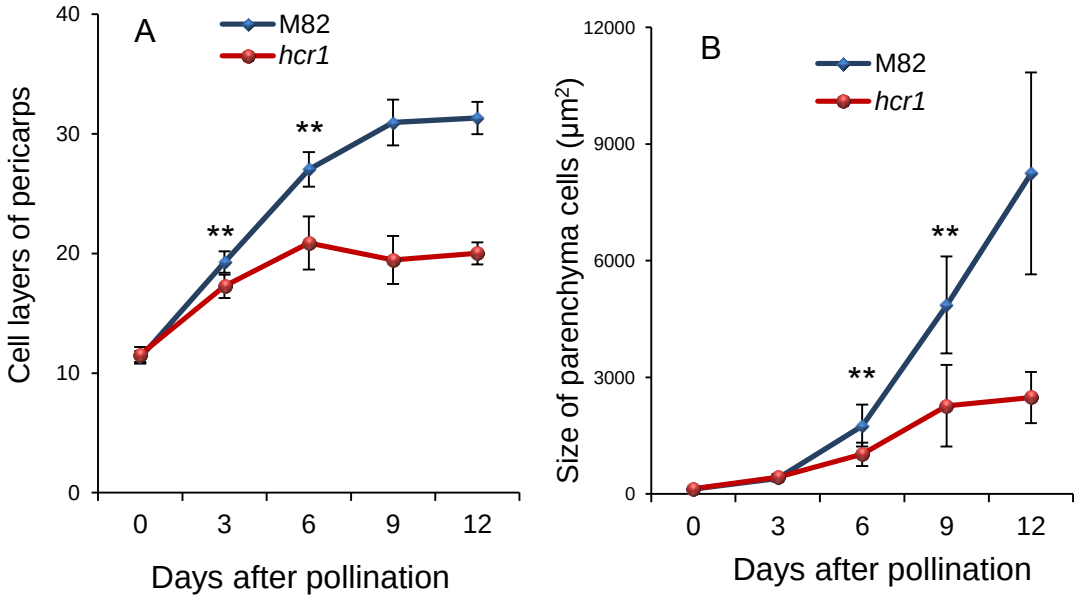

Figure 3.12 Inhibition of cell division and expansion in the *hcr1* fruit pericarp. (A) Comparison of the number of fruit pericarp cell layers of *hcr1* and M82. (B) The average areas of pericarp parenchyma cells in *hcr1* and M82 fruit.

area of an *hcr1* parenchyma cell was less than 30% that of M82 at 12 DAP (Fig. 3.12B), indicating a severe inhibition of cell expansion.

3.4 Discussion

The *hcr1* mutant exhibits an array of phenotypes that are most evident in fruits. These traits emerge in a distinct chronological order, suggesting that some have causal relationships with others. Essentially no differences were apparent, based on visual inspection and light microscopy between ovaries of *hcr1* and wild-type prior to pollination at 0 DAP. However, by 3 DAP, several traits, including pericarp thickness (Fig. 3.11A), weight ratio of pericarp to inner tissue (Fig. 3.11B) and the number of pericarp cell layers (Fig. 3.12A) showed significant differences between the mutant and wild type. In addition, brown discoloration of the surface of some fruits, indicative of necrosis, was noticeable by 3 DAP (Fig. 3.2A). By 6 DAP, the average size of the parenchyma cells of the *hcr1* pericarp was significantly smaller than that of the control (Fig. 3.12B) and discoloration was prevalent in most fruits, together with visible cracking on the surface of some fruits (Fig. 3.6). By this developmental time point, disordered epidermal cells with thickened wall cells were observed in pericarp cross sections (Fig. 3.9B). Suberization of the areas around the cracks was also commonly observed (Fig. 3.5), presumably representing a wound healing response to fruit cracking.

Other than the severe cracking, the most striking phenotype of the *hcr1* fruit is the absence of a fully developed pericarp, which reflects a major impairment in both pericarp cell expansion and cell division. Interestingly, no major phenotypes were observed in other parts of the plant in this regard and the only other plant phenotype was the appearance of mild necrosis on some leaves. A reasonable hypothesis is that the *hcr1* mutation impairs cell division and expansion specifically in the pericarp and so as the fruits expand, the biomechanical stresses imposed on the outer pericarp tissues result in rupture and cracking. The cracking is first apparent as microfissures, detectable here only with SEM, which are associated with the early discoloration and necrosis, and these later develop into the major cracks, triggering tissue suberization.

In the next chapter the cloning of the *hcr1* gene is described and a model is presented linking *hcr1* function with the phenotypes described above.

REFERENCES

Buda, G.J., Isaacson, T., Matas, A. J., Paolillo, D. J. and Rose, J. K. (2009) Three-dimensional imaging of plant cuticle architecture using confocal scanning laser microscopy. *Plant J.,* **60**(2), 378-385.

Dominguez, E., Cuartero, J. and Heredia, A. (2011) An overview on plant cuticle biomechanics. *Plant Sci.,* **181**(2), 77-84.

Ehret, D.L. and Helmer, T. (1995) Factors contributing to cuticle cracking in greenhouse tomato fruit. *HortScience,* **30**(4), 846.

Ehret, D.L., Helmer, T. and Hall, J. W. (1993) Cuticle cracking in tomato fruit. *J. Hortic. Sci.,* **68**(2), 195-201.

Emmons, C.L.W. and Scott, J. W. (1998) Ultrastructural and anatomical factors associated with resistance to cuticle cracking in tomato (*Lycopersicon esculentum* mill.). *Int. J. Plant Sci.,* **159**(1), 14-22.

Hetzroni, A., Vana, A. and Mizrach, A. (2011) Biomechanical characteristics of tomato fruit peels. *Postharvest Biol. Technol.,* **59**(1), 80-84.

Isaacson, T., Kosma, D. K., Matas, A. J., Buda, G. J., He, Y., Yu, B., Pravitasari, A., Batteas, J. D., Stark, R. E., Jenks, M. A. and Rose, J. K. (2009) Cutin deficiency in the tomato fruit cuticle consistently affects resistance to microbial infection and biomechanical properties, but not transpirational water loss. *Plant J.,* **60**(2), 363-377.

Jackson, D.P. (1992) In-situ hybridization in plants. In Molecular Plant Pathology: A Practical Approach. Edited by Gurr, S.J., McPhereson, M. and Bowles, D.J. pp. 163–174. Oxford University Press, Oxford.

Matas, A.J., Cobb, E. D., Paolillo, D. J. J. and Niklas, K. J. (2004) Crack resistance in cherry tomato fruit correlates with correlates with cuticular membrane thickness. *HortScience,* **39**(6), 1354-1358.

Matas, A.J., Lopez-Casado, G., Cuartero, J. and Heredia, A. (2005) Relative humidity and temperature modify the mechanical properties of isolated tomato fruit cuticles. *Am. J. Bot.,* **92**(3), 462-468.

Menda, N., Semel, Y., Peled, D., Eshed, Y. and Zamir, D. (2004) In silico screening of a saturated mutation library of tomato. *Plant J.,* **38**(5), 861-872.

Moctezuma, E., Smith, D. L. and Gross, K. C. (2003) Antisense suppression of a beta-galactosidase gene (TB G6) in tomato increases fruit cracking. *J. Exp. Bot.,* **54**(390), 2025-2033.

Vrebalov, J., Pan, I. L., Arroyo, A. J., McQuinn, R., Chung, M., Poole, M., Rose, J., Seymour, G., Grandillo, S., Giovannoni, J. and Irish, V. F. (2009) Fleshy fruit expansion and ripening are regulated by the tomato SHATTERPROOF gene TAGL1. *Plant Cell,* **21**(10), 3041-62.

CHAPTER FOUR

Cloning and Molecular Characterization of the *hcr1* Mutant

4.1 Introduction

The development of fruit epidermis has significant impacts on the horticultural quality of fruits, because fruit epidermis performs vital protection functions, which include minimizing water loss, protecting against pathogen, maintaining fruit integrity and preventing fruit from other physical damages. Fruit cracking and catfacing (corky scars on fruit surface) are common physiological disorder related with fruits epidermis damage. Those disorders are persistent and widespread problem, degrading fruit appearance and quality and subsequently causing serious economic loss. *Hypercracking 1* (*hcr1*), a mutant derived from a tomato line M82 by EMS mutagenesis, show fruit cracking at an early stage and consequent excessive suberization throughout the fruit development. In Chapter Three, we have characterized the phenotypic features and discussed the possible causal relations of some phenotypes. In this chapter, the molecular characterization of the *hcr1* gene is described, together with the possible mechanisms underlying the inhibition of

cell expansion/division in *hcr1* fruit and a model about *hcr1* fruit cracking is presented.

4.2 Material and Methods

4.2.1 Genetic mapping of *HCR1*

An F_2 mapping population was generated by crossing *hcr1* mutant with the wild tomato species *S. pimpinellifolium* (accession LA1589), and then harvesting F_2 self-pollinated seeds from F_1 progenies. Genomic DNA was extracted from young leaves of seedlings according to the method described by Fulton *et al*. (1995). Ninety-four plants of the *hcr1* F_2 population were phenotyped (using fruit cracking as the identifying trait), and then genotyped with 51 genetic markers that are distributed across the 12 chromosomes with an interval about 10~30cM. Genotype and phenotype data were analyzed by Qgene 4.0.

4.2.2 Plasmid constructions and plant transformation

A binary vector pCAMBIA1305.1 was used as the basis of the β-glucuronidase (GUS) reporter (Jefferson et al., 1987) and complementation constructs. All PCRs were performed by Bio-Rad iProof^{tm} High-Fidelity PCR kit. For the native promoter complementation construction, a 3.1kb DNA

fragment located upstream of *HCR1* gene was amplified from M82 genomic DNA using gene specific primers (Forward: 5'-CCTTTAGTCTCAGGGCACA TGAA-3' and Reverse: 5'-TTCGTAGCGG ATGAGCATTTCGAC-3'). The native promoter was cloned into the *Pst I* and *BstE II* sites of pCAMBIA1305.1 vector. The coding region of *HCR1* was amplified from cDNA of M82 using gene specific primers (Forward: 5'-CAGTCGTCTTAAGCCAATGAGTGAATGA TGCTGCACG-3' and Reverse: 5'- CAGTCGTggttaccCCAATGAGTGAATGAT GCTGCACG-3'); and then was subcloned into the vector described above at *BstE II* site. For the 35S promoter construct, the coding DNA of *HCR1* gene was amplified using gene specific primers (Forward: 5'-ACTGCagatctCATG GGTGAAGAAAAATGGTGTGTGGTGAC-3' and Reverse: 5'-ACCTCAcacgtg GGATG TTCTCCCATCAATGCTAGACCA-3'); and then was cloned into the pCAMBIA 1305.1 vector at *Bgl II* and *Pml I* site. For the GUS reporter expression construct, the native promoter was amplified using the gene specific primers (Forward: 5'-CCTTTAGTCTCAGGGCACATGAA-3' and Reverse: 5'-ACGCCAGccatggTGCCAAGAGATTGAGATTCTTCAAGG-3'), then was cloned into the pCAMBIA 1305.1 vector by replacing CaMV35S promoter fragment using *Pst I* and *Nco I* for the enzyme digestion. The two complementation constructs were transformed into *hcr1* mutant plants by *Agrobacterium*-mediated transformation (Van Eck et al., 2006) using plant transformation facility in UC Davis. The GUS construct was transformed into M82 plants by the *Agrobacterium*-mediated method (Van Eck et al., 2006;

http://irc.igd.cornell.edu/Protocols/Tomatotransform.html) in the plant transformation facility at the Boyce Thompson Institute or Plant Research, Cornell University.

4.2.3 Sterol profiling

Tomato leaf tissue (without petioles) was harvested from the leaves at the third node counting from top of each plant when flower buds in the first inflorescence were still small. Fruit pericarp samples were collected from 3 different stages: 15 DAP, MG and RR. Samples were flash frozen in liquid nitrogen and lyophilized in FreeZone Freeze Dry System (Labconco, Model: 77520) for 24 hours and then stored in plastic screw-cap tubes at -80°C until being subjected to lipid extraction.

Extraction was performed as described by Wewer et al. (2011) with minor modifications. A total of 1g of material was used for lipid extraction with 15 ml of chloroform/methanol (2:1). For each extract, a phase separation was effected by addition of 5 ml of 0.145 M NaCl solution. The sample was vortexed and centrifuged for 2 min at 5000 g. The non-polar fraction containing free sterols was removed with a pipette. Two additional extraction of chloroform/methanol (2:1) were performed and the organic phases combined, and the solvent was evaporated under N_2 gas. The polar fraction containing non-free sterols were separated by TLC in acetone:toluene:water

(91:30:8) and the lipids isolated from the silica plates with chloroform:methanol (2:1). This fraction was hydrolyzed in 1 ml 1 N methanolic HCl at 90°C for 30 min. After the addition of 1 ml of 0.154 M NaCl solution, the hydrolyzed sterols were extracted with 1 ml of hexane. Sterols were derivatized with 100 µl N-methyl-N-(trimethylsilyl)-trifluoroacetamide (MSTFA) and analyzed by comparison with authentic standards using GC-MS (GC: 6890 series, HP and Mass Selective detector: Agilent, Model: 5973).

4.2.4 RNA isolation, cDNA synthesis and Quantitative PCR analysis

Pericarp tissue from three biological replicates for each stage were harvested, flash frozen in liquid nitrogen then stored at –80°C. For un-pollinated ovaries/fruits (at 0 DAP), whole fruits were sampled as it was difficult to separate ovary wall/pericarp from adjacent tissues. Total RNA was isolated from frozen tissue (10~80 mg) using an RNeasy mini kit (Qiagen) and on-column DNase digestion was performed with the RNase-free DNase set (Qiagen), following the manufacturer's instructions. A total of 3 µg of total RNA was used for cDNA synthesis with SuperScript III reverse transcriptase and oligo (dT) primers (Invitrogen), according to the manufacturer's instructions.

Quantitative PCR experiments were performed using 7900HT Real-Time PCR System (Applied Biosystems) with 384-well block module. Twenty microliter qPCR mixtures, prepared with 10 µl 2× HotStart-IT SYBR Green

qPCR Master Mix (Affymetrix, Santa Clara, CA, USA), 6 µl 30-fold diluted cDNA and 4 µl other reaction components (Primers: 0.5 µl each, ROX passive reference dye: 0.4 µl and water: 2.6 µl) were loaded into each well of a 384-well plate. To estimate PCR amplification efficiency, calibration dilution experiments were performed in the same plate using a dilution series (10-fold dilution from10× to 10^5× as well as a blank and a 30×dilution) from the cDNA mixture which was mixed with the same volume of cDNA from each sample. The default thermal cycling condition for standard 384-well plate was applied for all qPCR runs (95°C for 10 min, 40 circles: 95°C for 15 seconds, 60°C for 60 seconds), and a dsDNA high-resolution melt curve analysis was followed.

The sequences of oligonucleotide primers are listed in Table 4.1. Specificity of the products was determined by product sequencing, gel electrophoresis and dissociation/melting analysis. qPCR data were analyzed using SDS2.1 software (Applied Biosystems). A mean normalized expression of genes was calculated using Q-Gene software (http://www.gene-quantification.de/download.html) in Microsoft Excel. The *RPL2* gene (Yeats et al., 2010) was served as a constitutive control in all gene expression experiments.

4.2.5 Protein sequence alignment

ClustalW2 program (http://www.ebi.ac.uk/Tools/msa/clustalw2/) was used for protein sequence alignment.

Table 4.1 PCR primers used for gene expression analysis

Target	Forward Primer Sequence	Reverse Primer Sequence	PCR length(bp)
RPL2 (SGN-U581377)	CAGCGGATGTCGTGCTATGAT	GGGATGCTCCACTGGATTCA	154
3β-HSD/D1 (*HCR1-1*) (SGN-U582999)	AGCGTACTTGGGATCATTTCACC	TCCCATCAATGCTAGACCA	140
3β-HSD/D1 (*HCR1-2*) (SGN-U582999)	GCAAGTGACCAACTAGGATACGCACCT	ATCCTTTCCCGACCCGTGTTC	108
3β-HSD/D2 (*HCR2*) (SGN-U583000)	GGAATCCCAGGTGCCTTTAC	CCCAGAAATATCAGACTTCAACTTCC	117
Polyphenol Oxidase F (SGN-U577900)	AGCCTTCATGAGTTGGTGGCT	AGGCAGTAACGAGCTATCCAGC	124
Polyphenol Oxidase E (SGN-U579941)	GTCTGCATGAGTTGGTGGCT	AGCATTAACACAACTAGCAATCAGC	130
GDSL-motif lipase/hydrolase (SGN-U585129)	GTAGCATGTTGTGGACAAGGACCA	TTTGCCCTCTCAGATGGATGGAAC	122
SlCER6 (SGN-U566767)	CCAGTGTTCATCCCAGAGATTGTC	GTCTGAGAGCTCACACACGTT	171
Feruloyl-Coenzyme A Transferase (SGN-U562949)	ACGGATTTCGGGTGGGGAGA	CTTCATAGCTGAAGCTGGCAGTCC	138
SlCESA1 (SGN-U585892)	AGAGGTATGTGGCTTGGACTGTG	CCCCTTGTTCCTTCTCCCTGAGT	99
SlCESA6-like (SGN-U569487)	CTGGGCTGTTCTCCTTGCATCC	ACCACATTGACCTCTTGCAGCA	99
SlCESA3 (SGN-U585891)	GGACCAGATGTTCAGGCTTGTGG	TCACATGGATGACCTTCACGCT	95

4.2.6 GUS histochemical staining

Pericarp sections were cut by hand from fresh tissues, and fixed in cooled 80% acetone for about 30 minutes. GUS histochemical staining was performed according to Jefferson et al. (1987).

4.2.7 Subcellular localization of HCR1–tdTOMATO

The protocol used for subcellular localization of *HCR1* gene was performed as described in Kelley et al. (2010). The cytoplasmic GFP and ER-GFP markers (which were kindly provided by J.Y. Lee, Delaware Biotechnology Institute, University of Delaware, Newark, DE) and pART-27 vector (Gleave, 1992) are also same as those described in the paper. Briefly, the coding region of *HCR1* was amplified from cDNA of M82 using gene specific primers (Forward: 5'-CCGATGctcgagATGGGTGAAGAAAAATGGTGTG TGGTG-3' and Reverse: 5'-CGGATCggtaccATTCTTCTTGCTTTTGTCAAATATC AAG-3'); and then was subcloned into the pART-27 vector with tdTOMATO (red fluorescence) (Shu et al., 2006) reporter sequence at *Xho I* and *Kpn I* site to generate the protein expression structure: 35S::HCR1: tdTOMATO: OCS-term. Confocal microscopy imaging of the co-expression of HCR1-tdTOM and cytoplasmic GFP or ER-GFP marker was observed by transient protein expression in onion epidermal cells.

4.2.8 Cellulose analysis

The procedure for crude cell wall isolation and acid hydrolysis of cell wall was performed as described by Foster et al. (2010). The amount of glucose hydrolyzed from crystalline cellulose was measured using the colorimetric PAHBAH (p-hydroxybenzoic acid hydrazide) assay (Blakeney and

Mutton, 1980), in which the absorbance values were measured by Multiskan EX Microplate Photometer (Thermo Electron Corporation) with 405nm filter.

4.3 Results

4.3.1 The mapping result of HCR1 gene

The *HCR1* gene was first mapped to the middle portion of tomato chromosome two with a substantial QTL (LOD=32) between the markers 1g11430 (2.070) and 2g18030 (2.083) (Fig. 4.1). Following a screen of approximately 6,000 F2 individuals for recombination events by the two markers, the gene was further narrowed down to a 42 kb interval between two flanking CAPS markers: Seq19600 and UDP4F within a BAC contig (corresponding to C02.40_contig20 in version 2.4 of tomato BAC contigs database, http://solgenomics.net) (Fig. 4.2A). A point mutation was found by comparing the genomic DNA sequences of *hcr1* and M82 in this region (Fig. 4.2B). This nucleotide substitution (G→A) is located in the predicted 3' splicing site of the seventh exon of the *HCR1* gene, which results in the removal of the seventh exon from the mRNA (Fig 4.2B), as confirmed subsequently by the RT-PCR (Fig 4.3). The chromosomal position of *HCR1* is: SL2.40ch02:40139750…40146827.

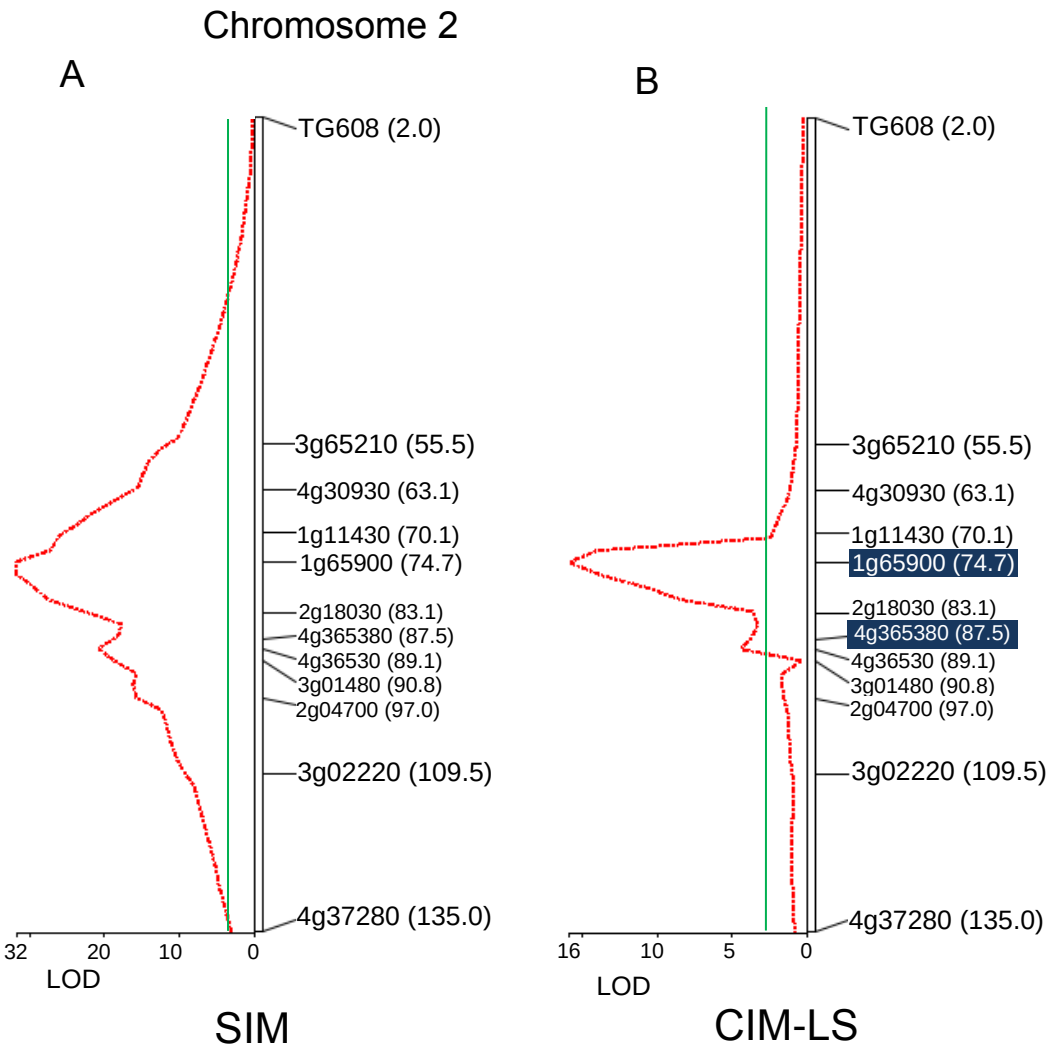

Figure 4.1 QTL map in the *hcr1* mapping population
(A) QTL analysis using a Simple Interval Mapping (SIM) (B) QTL analysis using Composite Interval Mapping (CIM-LS) with cofactor maker (with blue background) selection. The red line indicates the value of log-likelihood ratio (LOD) and the green line indicates the LOD threshold (>3). The number in parentheses indicates the marker location in cM.

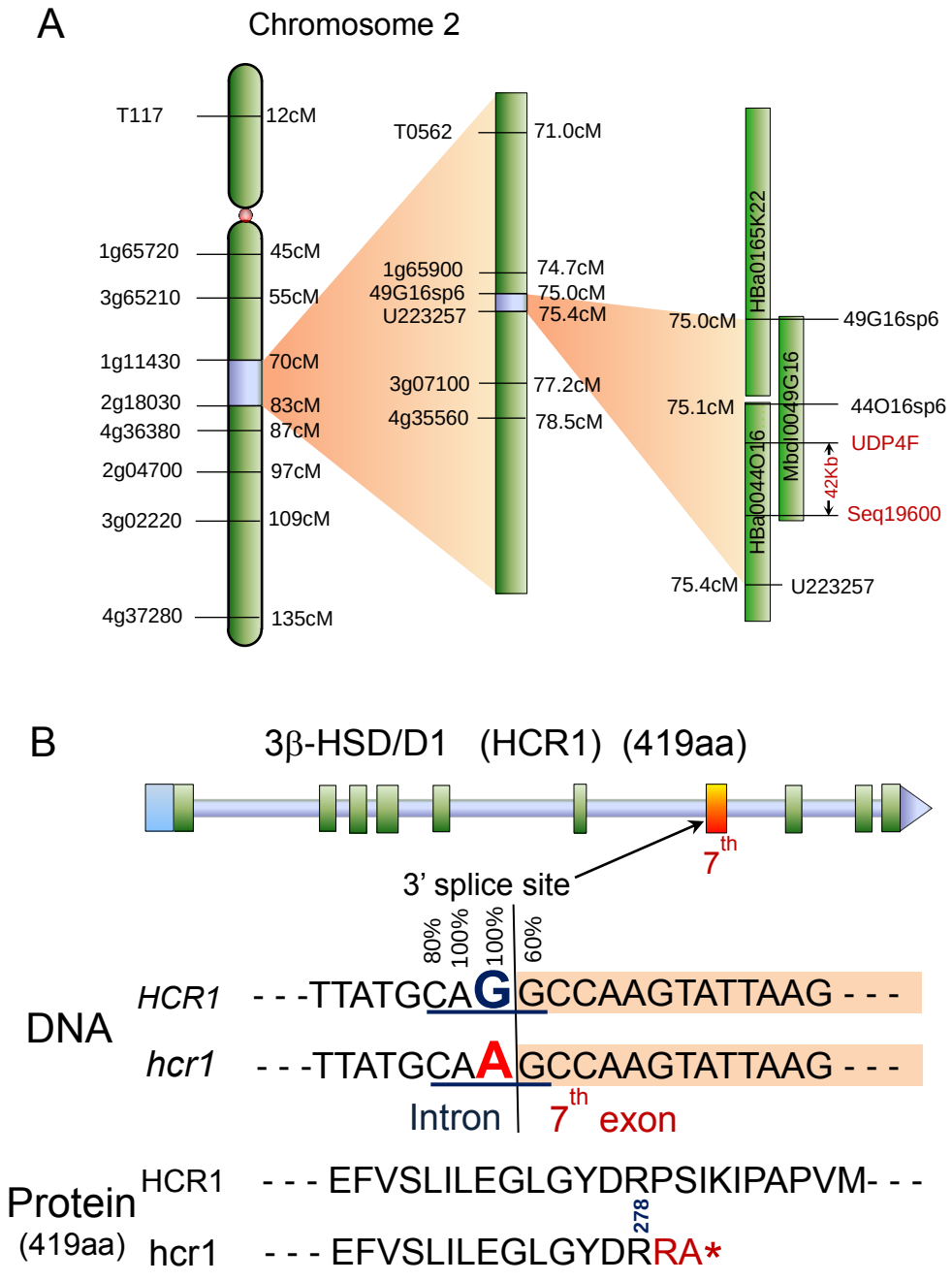

Figure 4.2 Mapping of the *hcr1* locus. Schematic diagram showing the mapping of *hcr1* to chromosome 2 between the marker Seq19600 and UDP4F. (B) *HCR1* gene model. The nucleotide substitution G to A at the 3' splice site results in the removal of the seventh exon from the mRNA of the *3β-HSD/D1* gene, leading to the truncation of the last 142 amino acids from the protein.

Figure 4.3 RT-PCR of the *HCR1* gene

4.3.2 Complementation test of the *HCR1* gene

To validate the identity of the *HCR1* gene, complementation tests were performed using two plasmid constructs: (i) CaMV35S:: *HCR1* cDNA and (ii) Native Promoter:: *HCR1* cDNA. All defective phenotypes of *hcr1*, including fruit discoloration, early cracking and cuticle suberization were entirely absent in the transgenic plants (T_0) with either of the complementation constructs (Fig. 4.4). Segregation analysis in the subsequent generation (T_1) revealed that the progenies of selected transgenic (T_0) lines showed approximately 3:1 segregation ratios. Thus it was confirmed that the single nucleotide mutation in the splicing site of the seventh exon of the *HCR1* gene was responsible for the *hcr1* phenotypes.

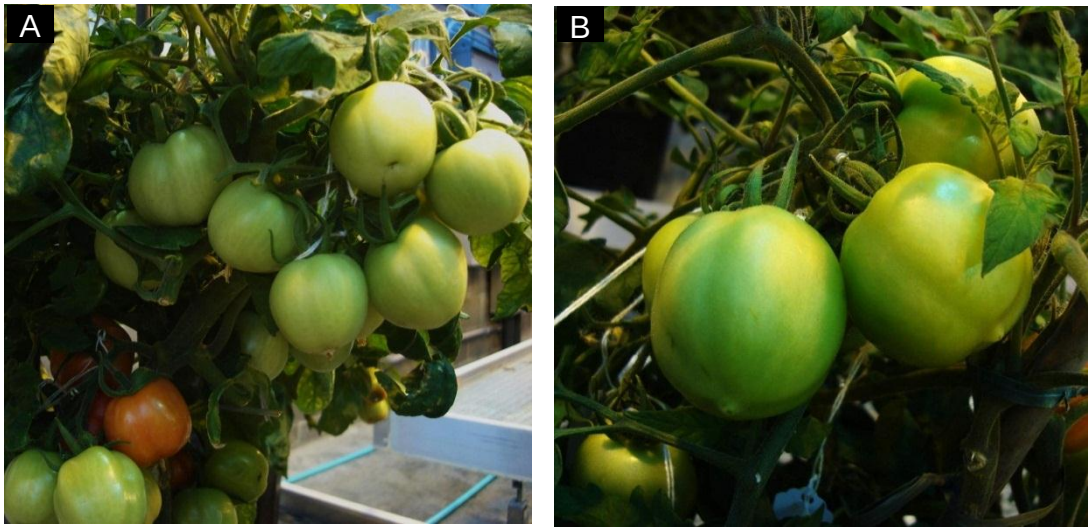

Figure 4.4 Complementation of *hcr1*. T_0 transgenic lines transformed with (A) CaMV35S:: *HCR1* cDNA and (B) Native Promoter :: *HCR1* cDNA.

4.3.3 HCR1 and HCR2 proteins

The *HCR1* gene is predicted to encode a 419 amino acid polypeptide that bears a conserved 3β-HSD multi-domain pfam01073 (3-283aa, $1.27e^{-74}$). A BLAST search against the *Arabidopsis* protein database showed that the tomato HCR1 protein exhibits a sequence identity of 78% and a similarity of 88% with 3β-Hydroxysteroid Dehydrogenases/C-4 Decarboxylases (At3β-HSD/D1) (Fig. 4.5). The HCR1 contains a conserved glycine and aspartic residues, $TGGXGXXAX_{18}D$ near the N terminus, which is required to form the coenzyme-binding site (Rahier et al., 2006). The highly conserved YX_3K segment [156~160aa], assigned to the catalytic center, is also present in HCR1 (Jornvall et al., 1995, Rahier, 2011). A transmembrane helix

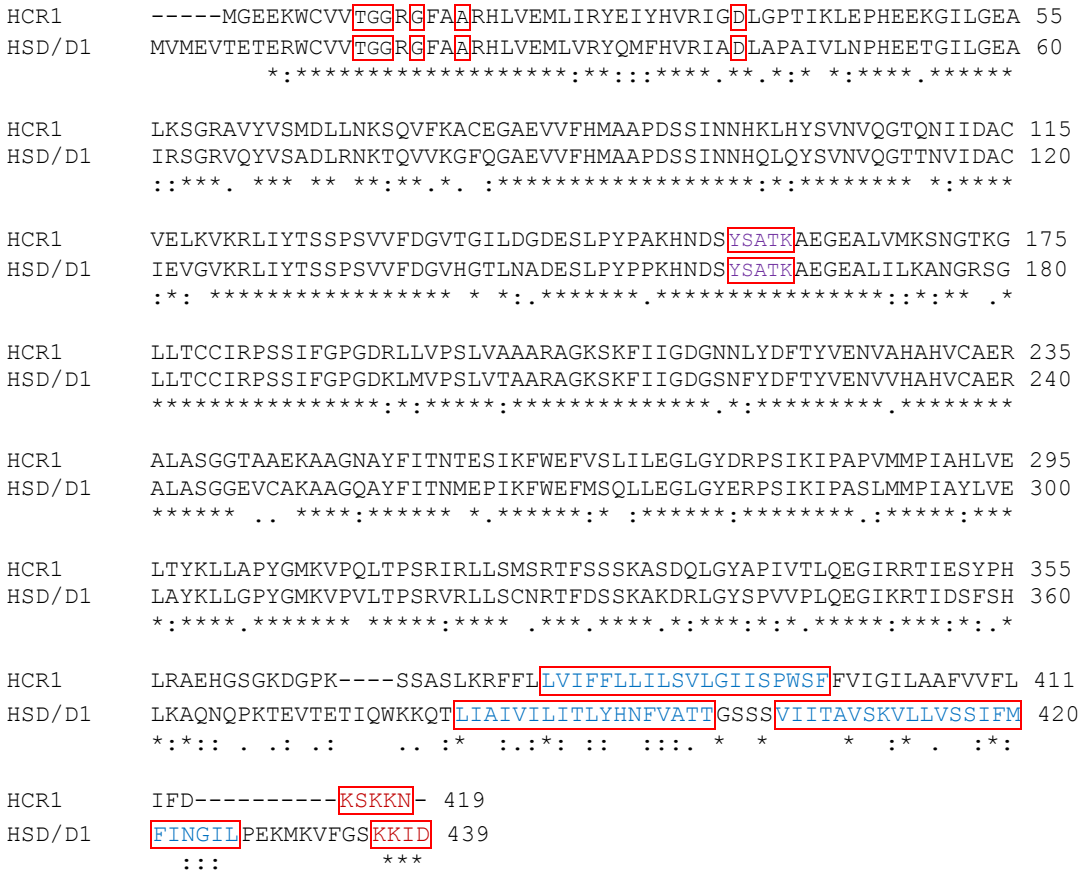

Figure 4.5 Sequence alignment of HCR1 and At3β-HSD/D1.
CLUSTAL 2.1 multiple sequence alignment, Score = 67.0
Identities = 285/384 (74%), Positives=325/384 (85%)

[379~413aa] close to the C-terminal was predicted by TMHMM 2.0 (http://www.dtu.dk/services/ TMHMM/) and a putative ER retention and retrieving signal KSKKN motif of type-I ER membrane protein was found at the C-terminus (http://elm.eu.org/). In the *hcr1* mutant, the removal of the seventh exon from the *HCR1* mRNA leads to the truncation of the last 142 amino acids (from 278aa to 419aa) from the protein (Fig. 4.2B), which would almost certainly result in the loss of activity and correct subcellular localization.

A homolog of the *HCR1* gene, named here *HCR2* (SGN-U583000), was identified in the tomato genome sequence by a BLAST search. Both *HCR1* and *HCR2* are located on the chromosome 2, but with a distance of about 21 Mbp. The predicted HCR2 protein has 562 amino acids and shows and a sequence identity to the HCR1 protein of 84% (Fig. 4.6).

```
HCR1    MG--EEKWCVVTGGRGFAARHLVEMLIRYEIYHVRIGDLGPTIKLEPHEEKGILGEALKS 58
HCR2    MADVQERWCVVTGGRGFAARHLVEMLIRYEMFQVRIADLGTAIKLEPDEEEGTVGKAMRS 60
        *.  :*:************************:::***.***.:*****.**:* :*:*::*

HCR1    GRAVYVSMDLLNKSQVFKACEGAEVVFHMAAPDSSINNHKLHYSVNVQGTQNIIDACVEL 118
HCR2    GRAKYVSMDLRDKSQVLKACEGAEVVFHMAAPDSSVNNHQLHHSVNVLGTKNIIDACVEL 120
        *** ****** :****:******************:***:**:**** **:*********

HCR1    KVKRLIYTSSPSVVFDGVTGILDGDESLPYPAKHNDSYSATKAEGEALVMKSNGTKGLLT 178
HCR2    KVKRLIYTSSPSVVFDGVHGITNGDESLPYPSKHNDFYSATKAEGEALVIKSNDTKGLLT 180
        ****************** ** :********:**** ************:***.******

HCR1    CCIRPSSIFGPGDRLLVPSLVAAARAGKSKFIIGDGNNLYDFTYVENVAHAHVCAERALA 238
HCR2    CCIRPSSIFGPGDRLLVPSLVAAARAGKSKFIIGDGNNMYDFTYVENVAHAHVCAERALA 240
        ************************************:********************

HCR1    SGGTAAEKAAGNAYFITNTESIKFWEFVSLILEGLGYDRPSIKIPAPVMMPIAHLVELTY 298
HCR2    SGGAVAEKASGQAYFVTNMEPIKFWDFVALILEGLGYGRPRIKIPASVMMPIAYLVELTY 300
        ***:.****:*:***:** *.****:**:********.** *****.******:******

HCR1    KLLAPYGMKVPQLTPSRIRLLSMSRTFSSSKASDQLGYAPIVTLQEGIRRTIESYPHLRA 358
HCR2    KLLAAYGMKVPQLTPSRIRLLSRSRTFSCSKANDRLGYTPIIPLQEGLRRTIESYPHLRA 360
        ****.***************** *****.***.*:***:**:.****:************

HCR1    EHGSGKDGP---------------------------------------------------- 367
HCR2    EQRLKKEGPSKASLFLGSGRVADTLLWRNKKQTLMAALVLAAIYFNFIASGSTIITSIST 420
        *:   *:**

HCR1    ----------------------------------------------------KSSASL 373
HCR2    ILLVASVFLFIHGRLPQRIMGYKFAKVPVSSFHVSEETSHQFALSVVSGWNSAVKGLKSL 480
                                                              *.  **

HCR1    KR-----FFLLVIFFLLILSVLGIISPWSFFVIGILAAFVVFLIFDK------------- 415
HCR2    CKGADCMFFLKVALSLLILSILGTISLQSLFAIGIPGAFTLFYIYEKKEEEIDHVLQDIV 540
         :     *** * : *****:** **  *:*.*** .**.:* *::*

HCR1    -----------------SKKN- 419
HCR2    LFTWKLKSDISGKIFSSTKKDR 562
                        :**:
```

Figure 4.6 Sequence alignment of HCR1 and HCR2
CLUSTAL 2.1 multiple sequence alignment Score = 78.0
Identities = 310/371 (84%), Positives = 338/371 (91%)

The enzymatic characteristics of two 3β-HSD/D isoenzymes in *Arabidopsis* have been characterized (Rahier et al., 2006; 2009; Rahier, 2011). At3β-HSD/Ds are bifunctional short-chain proteins with 3β-hydroxysteroid-dehydrogenase/C4-decarboxylase activities, acting as a key enzyme for C-4 demethylation in the sterol biosynthesis pathway. HCR1, HCR2 and the two *Arabidopsis* At3β-HSD/Ds show high amino acid sequence identity (more than 65%) and structural similarity to each other, suggesting that HCR1 and HCR2 most likely have 3β-hydroxysteroid-dehydrogenase /C4-decarboxylase activities.

4.3.4 *hcr1* mutation causes a mild reduction of sterol contents in *hcr1* fruits

Since the *HCR1* gene encodes a key enzyme in sterol pathway, the contents of bulk sterols in leaves and fruit pericarp at three developmental stages were measured by GC-MS (Fig. 4.7 and Table 4.1). Despite the loss of HCR1 enzymatic activity, the sterol profiles of *hcr1* leaves were similar to those of M82 during vegetative growth of plants. Strikingly, the conjugated sterols such as sterol glucoside (SG) and acylated sterol glucoside (ASG) were dominant in tomato leaves, accounting for more than 98% of total sterols (Table 4.1), which contrasts with the content of conjugated sterols in *Arabidopsis*: only account for about 20% of total leaf sterols (Wewer, 2011).

The total sterol content of the *hcr1* pericarp was reduced to 84~89% of wild-type levels at 15 DAP, mature green and red ripe stages, which while relatively small, was statistically significant in all three stages (Fig. 4.7, Table

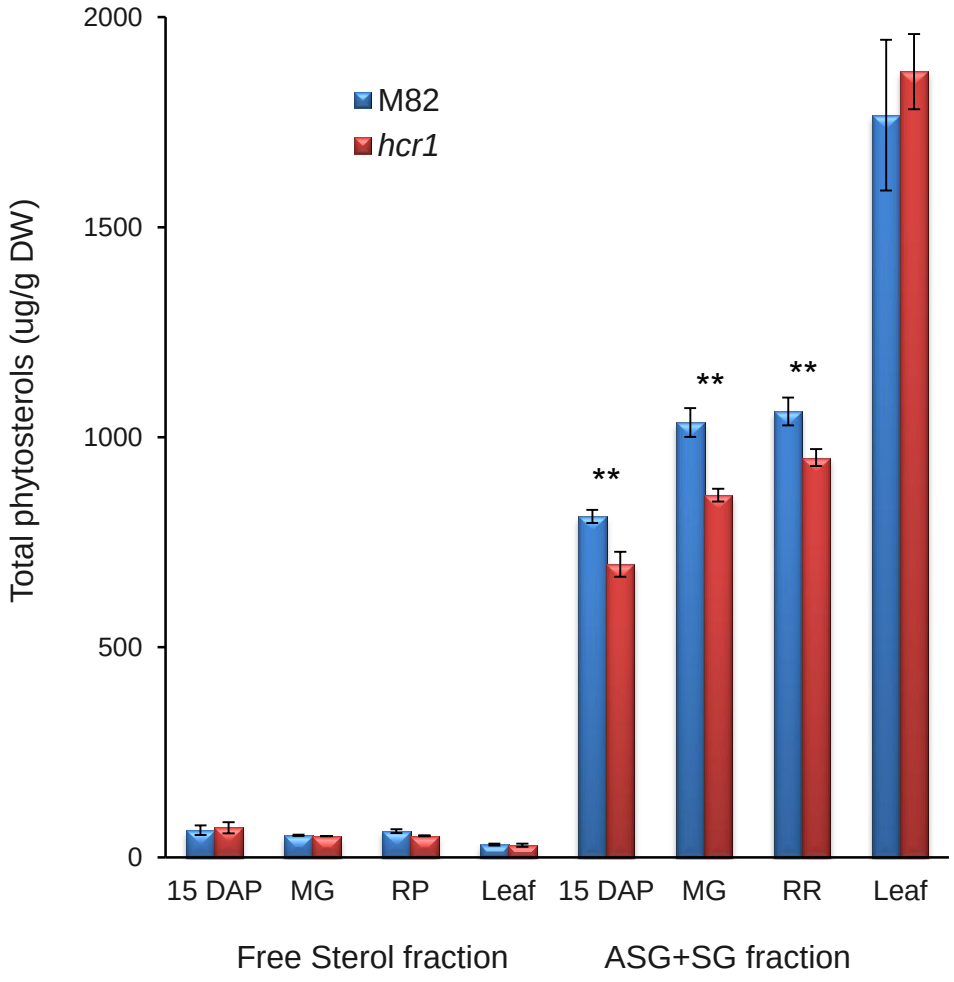

Figure 4.7 The sterol profile of fruit pericarps and leaves in M82 and *hcr1*. Total free sterols and total steryl glucosides are shown on the left and the right, respectively. (Mean ± SD of N = 3. ** P < 0.01 by two-tailed t-test.)

4.1). Similarly, the conjugated sterols (particularly sitosterol and stigmasterol) were dominant in tomato fruit pericarp in all three stages and accounted for more than 90% of total sterols (Table 4.1), which was consistent with previous findings (Whitaker et al., 1988, 1991 and 2008).

4.3.5 Spatial and developmental expression patterns of HCR1 gene

The spatial and developmental expression pattern of the *HCR1* gene was determined using the GUS reporter driven by the *HCR1* gene promoter. The results indicated that *HCR1* gene is ubiquitously expressed in all tomato tissues (Fig. 4.8, 4.9 and 4.10). GUS accumulation was relatively low in fruits at 1 DAP (Fig. 4.8 A), but quickly peaked by 3~5 DAP (Fig. 4.8B). Expression was more sparse in older fruits, first showing absence in some parenchyma cells at 12 DAP (Fig. 4.8C) and then in mature green (Fig. 4.8D) and red ripe (Fig. 4.8E) fruits, only appearing in the epidermis, sporadically in some cells near the epidermis and in vascular tissues.

In stems, GUS staining was detected in all cells and was particularly abundant in young tissues (Fig. 4.9A), then gradually declined as the tissues aged (Fig. 4.9B, C), until staining was no longer detectable in well-developed stem tissues (Fig. 4.9D). The *HCR1* gene expression in petioles showed a similar developmental pattern to that in stems (Fig. 4.9E-H). Interestingly, GUS staining of rings of endodermal cells and xylem rays (Fig. 4.9C) was observed in the stem. From the results of the GUS reporter experiments, it

Table 4.1 Sterol composition of steryl lipids from leaves and pericarp tissues at three stages in M82 and *hcr1* mutant (µg/g DW)

Sterols	15 DAP Pericarp		Mature Green Pericarp	
	M82	*hcr1*	M82	*hcr1*
Free sterols				
Campesterol	3.3 ± 0.5	3.0 ± 1.4	1.9 ± 0.3	2.0 ± 0.1
Stigmasterol	12.2 ± 3.8	13.4 ± 3.6	10.1 ± 2.0	13.3 ± 3.0
Sitosterol	42.7 ± 7.1	46.5 ± 8.0	37.6 ± 1.2	32.3 ± 2.4
Cycloartenol	1.3 ± 0.3	1.6 ± 0.7	0.7 ± 0.3	0.7 ± 0.3
Cholesterol	5.1 ± 0.8	6.0 ± 0.7	2.2 ± 0.4	2.0 ± 0.3
Total	64.7 ± 11.3	70.5 ± 13.4	52.5 ± 1.7	50.3 ± 0.5
SG+ASG *				
Campesterol	17.9 ± 5.3	17.3 ± 2.6	13.8 ± 1.5	15.2 ± 1.2
Stigmasterol	**119.0 ± 3.0**	**97.8 ± 6.6**	**255.5 ± 12.7**	**142.8 ± 19.5**
Sitosterol	**637.7 ± 24.5**	**543.3 ± 26.4**	**736.9 ± 27.8**	**677.6 ± 7.6**
Cycloartenol	10.3 ± 0.8	9.7 ± 0.8	11.2 ± 0.1	10.8 ± 0.3
Cholesterol	26.6 ± *3.7*	29.4 ± 5.5	17.8 ± 0.8	15.8 ± 0.7
Total	**811.6 ± 15.9**	**697.4 ± 29.8**	**1035 ± 34.3**	**862.1 ± 14.9**
Sterols	Red Ripe Pericarp		Leaf	
	M82	*hcr1*	M82	*hcr1*
Free sterols				
Campesterol	6.0 ± 1.6	5.7 ± 0.8	2.7 ± 0.7	2.8 ± 0.5
Stigmasterol	**27.4 ± 2.5**	**21.7 ± 1.3**	10.0 ± 0.6	12.0 ± 1.6
Sitosterol	**26.6 ± 2.0**	**20.6 ± 0.5**	**15.0 ± 1.7**	**10.7 ± 2.9**
Cycloartenol	1.0 ± 0.5	1.3 ± 0.6	0.6 ± 0.2	0.5 ± 0.1
Cholesterol	1.3 ± 0.1	1.5 ± 0.8	1.8 ± 0.2	2.8 ± 0.6
Total	**62.3 ± 4.7**	**50.9 ± 1.1**	30.0 ± 2.3	28.8 ± 3.8
SG+ASG *				
Campesterol	28.7 ± 2.3	24.5 ± 0.9	27.6 ± 4.4	29.0 ± 5.6
Stigmasterol	**294.5 ± 14.7**	**227.0 ± 5.1**	519.2 ± 68.5	575.6 ± 24.4
Sitosterol	**714.5 ± 20.8**	**671.6 ± 24.2**	1041 ± 111.1	1070.3 ± 61.3
Cycloartenol	**12.8 ± 0.9**	**17.3 ± 1.7**	117.1 ± 10.1	129.9 ± 25.5
Cholesterol	11.0 ± 1.1	11.1 ± 1.3	61.2 ± 3.1	65.4 ± 10.5
Total	**1061 ± 33.3**	**951.5 ± 20.3**	1767 ± 179.4	1870.2 ± 89.3

* SG = Steryl glycosides; ASG = Acylated steryl glycosides

** Data represent the mean (µg/g dry weight) of three biological replicates ± SE. Major differences are highlighted in bold font.

was concluded that the *HCR1* gene is abundantly expressed in the regions undergoing rapid cell division and expansion.

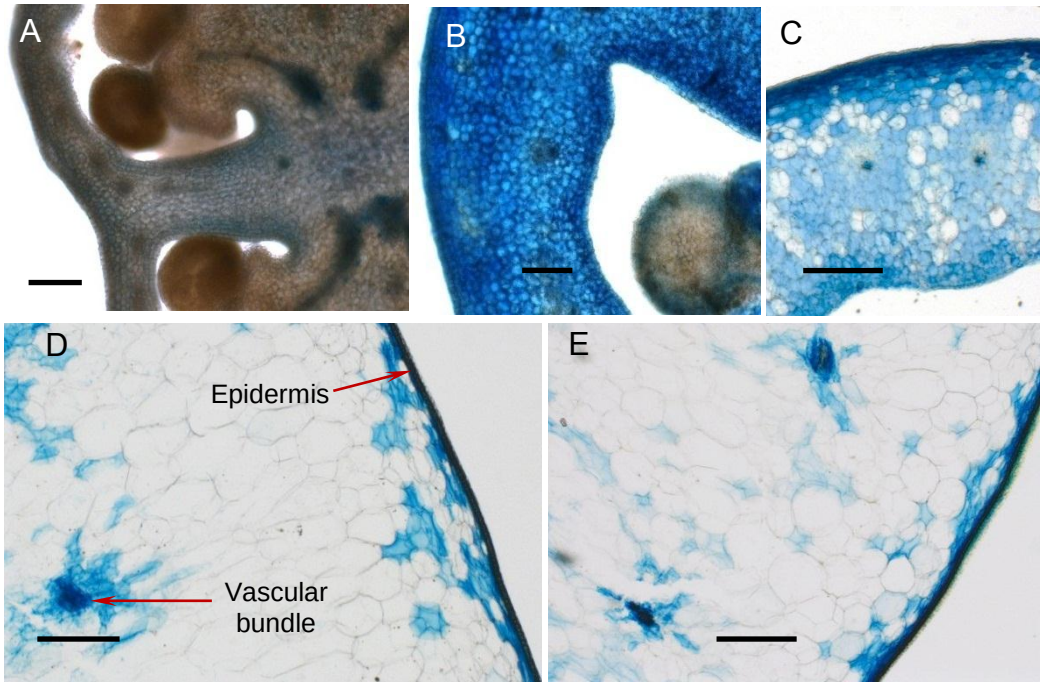

Figure 4.8 Spatial and developmental expression analysis of *HCR1* gene in fruit pericarp using the GUS reporter system. GUS staining of fruit pericarp at different stages: 1 DAP (A), 4 DAP (B), 12 DAP (C), mature green (MG) (D) and red ripe (RR) (E). Scale bars (A,B) = 100 µm, (C, D, E) = 500 µm.

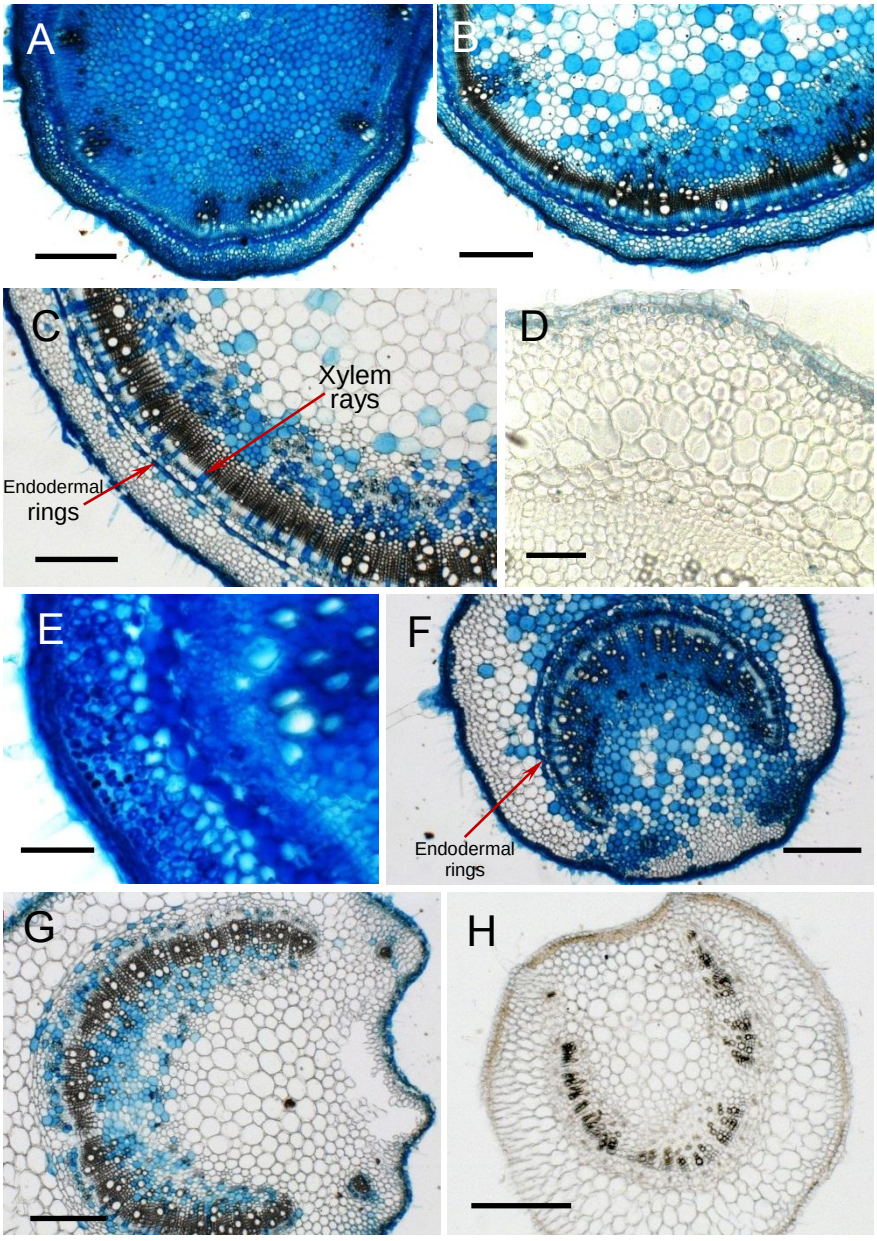

Figure 4.9 Spatial and developmental expression analysis of *HCR1* gene in stems and petioles using the GUS reporter system. (A-D) A developmental stages of tomato stems from younger (A) to older (D). (E-H) Petioles at different stages from younger (E) to older (H). Scale bars (D, E) = 100 μm, Scale bars of others = 500 μm

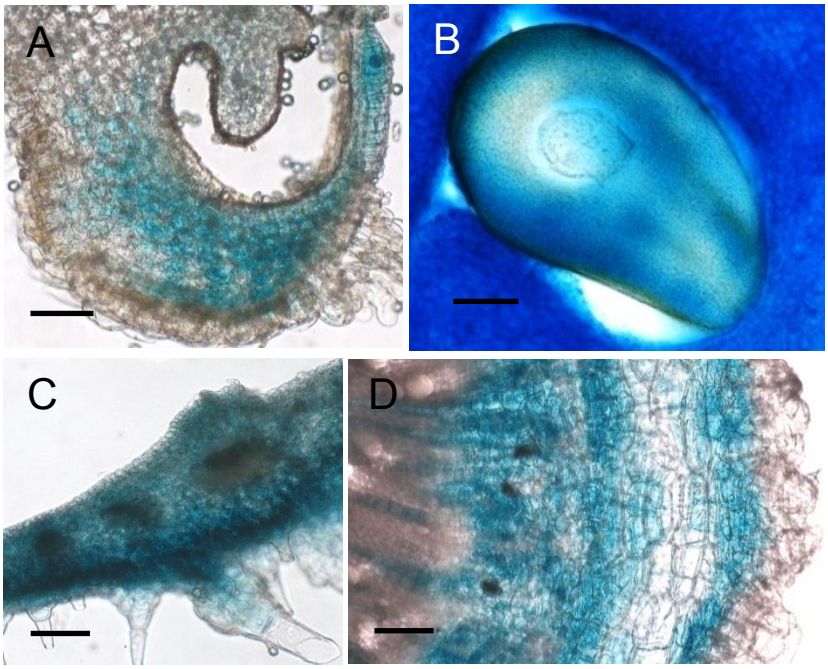

Figure 4.10 *HCR1* gene expression analysis in other tomato organs and tissues using the GUS reporter system. GUS staining in anther (A), ovule (B), sepal (C) and root (D). Scale bars = 100 μm.

Developmental expression analysis of the *HCR1* and *HCR2* genes was also carried out by quantitative PCR. Two sets of *HCR1* specific primers were designed (Fig. 4.11A): the hcr1-1 primers, matching two specific region on the ninth and tenth exon (spanning the ninth intron), were used to detect all *HCR1* cDNA species and the hcr1-2 primers, matching two specific regions on seventh and eighth exon (spanning the seventh intron), were used to detect the presence or absence of the deleted seventh exon of the *hcr1* gene. The qPCR result showed that the *hcr1* transcripts in *hcr1* plant were reduced to only about 10% of that of M82 at 3~9 DAP (Fig 4.11B); however, low levels of wild type *HCR1* transcripts with the seventh exon region intact were detected,

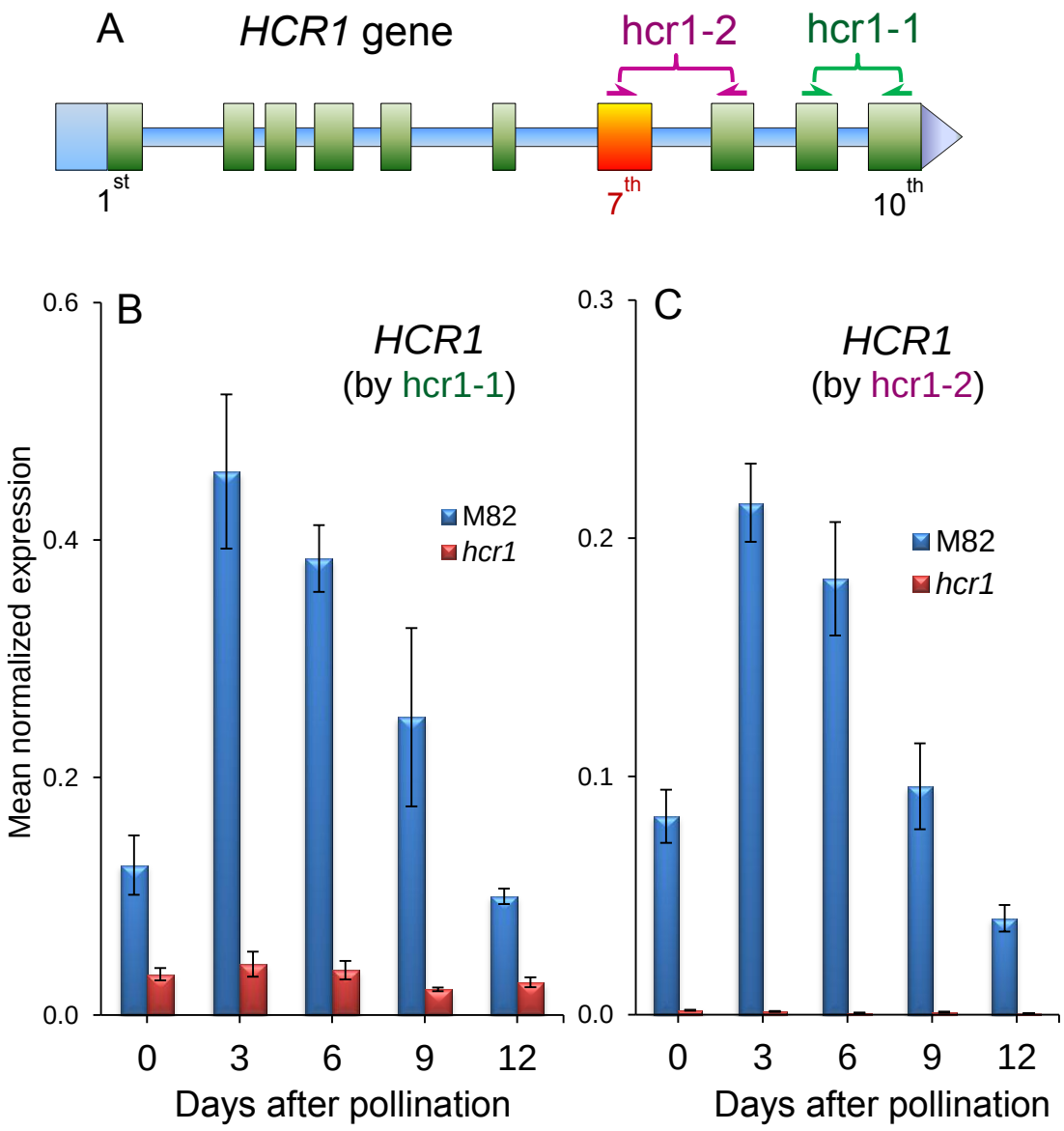

Figure 4.11 Developmental expression analyses of *HCR1* transcripts in fruit pericarp by qPCR. (A) The primer design schematic for *HCR1* gene expression analysis. (B) *HCR1* gene expression was determined using the hcr1-1 primer set, which is near to the 3'UTR region of the cDNA to detect all cDNA species. (C) *HCR1* gene expression using the hcr1-2 primer set, which is designed to detect the presence of the deleted seventh exon in cDNA of *hcr1* mutant.

albeit only at 0.5~1% of wild-type levels (Fig 4.11C). A possible explanation for this result is that most *hcr1* mRNAs (about 90%) without the 7th exon were eliminated by cellular quality control machineries due to the instability of the defective mRNA, but that very small amounts (0.5~1%) of functional *HCR1* mRNA accumulated in the *hcr1* mutant because of fault-tolerant splicing during mRNA transcription. It is noteworthy that the gene expression pattern in M82 fruit probed by the two sets of PCR primers showed a similar pattern: *HCR1* gene expression levels peaked at 3 DAP then declined gradually during fruit development and were reduced to about 20% of peak values at 12 DAP. This result is consistent with the expression pattern of the *HCR1* gene observed by the GUS reporter assay.

The *HCR2* gene displayed relatively consistent expression profiles across all time-points, but expression was slightly reduced in the *hcr1* mutant (Fig. 4.12).

4.3.6 Several metabolism processes related to fruit development were affected by the *hcr1* mutation.

The wide range phenotypic traits shown by *hcr1*, including fruit discoloration, suberin deposition, abnormal cuticle development and cell division and expansion, suggested that many metabolism pathways were altered by the *hcr1* mutation. To confirm this, the expression patterns of several marker genes related to these processes were investigated.

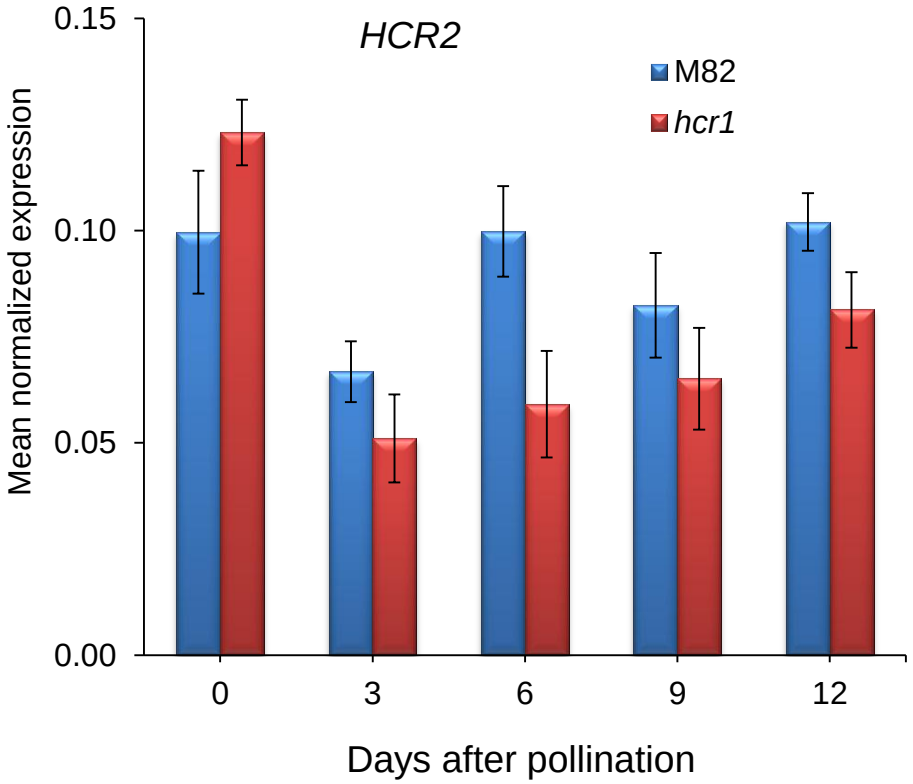

Figure 4.12 Developmental expression analysis of *HCR2* gene in fruit pericarp of M82 and *hcr1* mutant

Polyphenol oxidases (PPOs) catalyze the O_2-dependent oxidation of phenolics to quinones. The secondary reactions of quinones lead to the formation of polymeric brown or black pigments (Thipyapong et al., 1997, 2007). The previous study showed that mechanical wounding and pathogen infection can induce the expression of the *PPO-F* gene in tomato, suggesting that this gene may involve in the observed brown discoloration of the *hcr1* fruit. qPCR analysis of *PPO-F* expression (Fig. 4.13A) indicated that un-pollinated

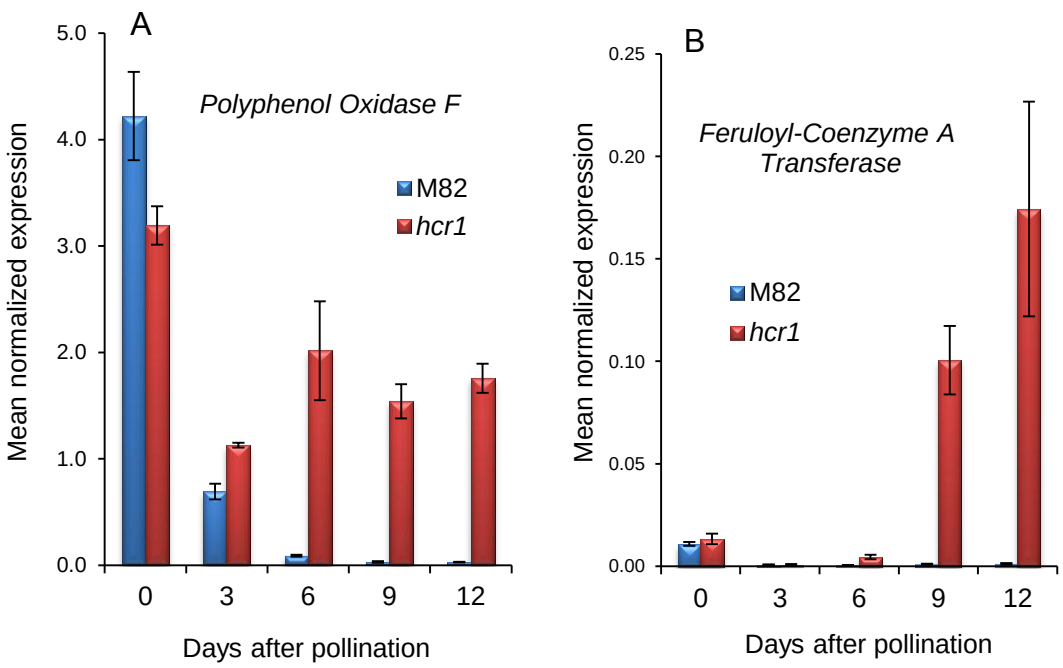

Figure 4.13 The expression patterns of marker genes related to fruit discoloration and suberization by qPCR. The expression of (A) *Polyphenol Oxidase F* and (B) *Feruloyl-Coenzyme A Transferase* by qPCR was used as a measure of phenolic compound formation and suberin biosynthesis, respectively, during M82 and *hcr1* fruit development.

tomato fruits have the most abundant *PPO-F* transcripts and that after pollination, *PPO-F* transcripts in M82 fruits decreased dramatically and by 6 DAP were reduced to only 1~4 % of the original levels at 0 DAP. In contrast, *PPO-F* transcript levels in *hcr1* fruit remained high during this period and were about 60-fold greater than that of the wild-type, which is consistent with *PPO-F* contributing to the fruit discoloration in *hcr1*.

Feruloyl-CoA transferase (AT5G41040) is essential for the incorporation of ferulate into suberin and has been identified as a key enzyme required for suberin synthesis in *Arabidopsis* (Molina et al., 2009). The expression pattern of the closest homolog of AT5G41040 in tomato (SGN-U562949, Solyc03g097500.2) was analyzed to gain insights into the suberin biosynthetic pathway during fruit development of M82 and *hcr1* fruit (Fig. 4.13B). qPCR results showed that this gene (SGN-U562949) was consistently expressed at a very low level in M82 plants, but was dramatically up-regulated in *hcr1* 6 days after pollination in comparison with the wild-type. These expression patterns are consistent with the observation that suberin synthesis lagged behind fruit discoloration and the first appearance of cracks.

Two marker genes which are associated with cutin and wax biosynthesis were selected for monitoring the cuticle formation of *hcr1* fruit. *CD1* catalyzes the polymerization of cutin *in situ* via successive trans-esterification of 2-MHG to the growing cutin polymers (see chapter 2).

LeCer6 encodes an essential enzyme of a very-long-chain fatty acid (VLCFA) elongase complex, which is required for aliphatic wax biosynthesis (Vogg et al., 2004; Leide et al., 2007) and so its expression would be expected to correlate with wax deposition. The qPCR results revealed that the expression patterns of *CD1* and *LeCer6* in M82 were quite similar with both genes were maximally expressed during the rapid expansion phase of fruits at 12 DAP or later (Fig. 4.14). In contrast, the expression of these two genes in

hcr1 fruit substantially lagged behind that of M82, suggesting that, as observed microscopically, cuticle development was apparently delayed in the *hcr1* mutant.

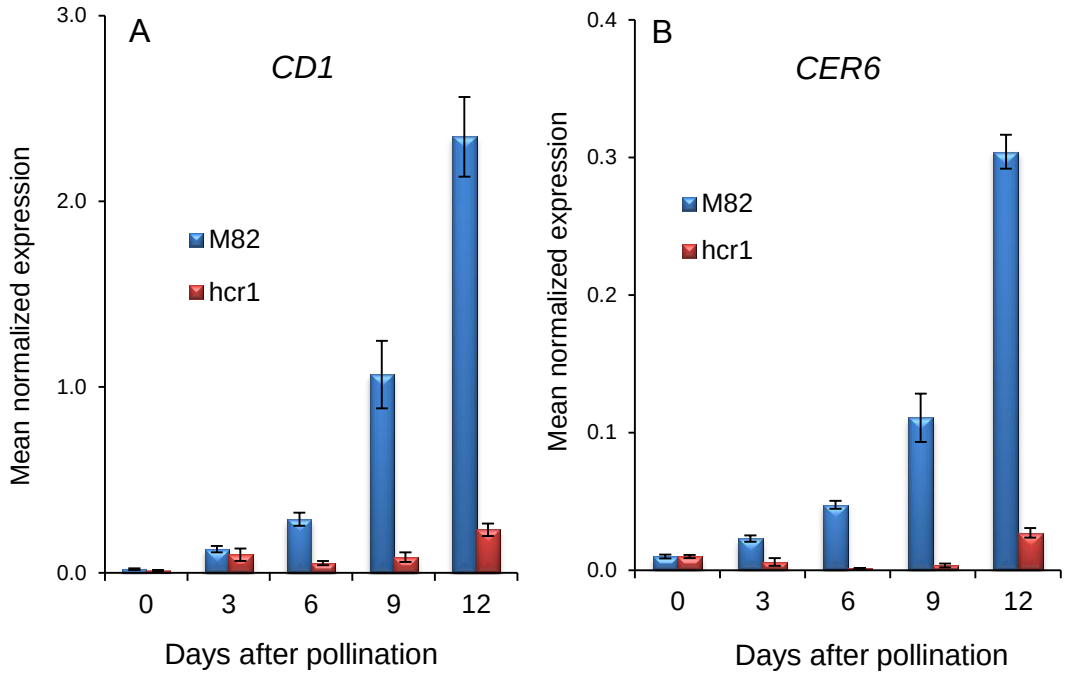

Figure 4.14 The expression patterns of marker genes related to fruit cuticle biosynthesis. The expression of (A) the cutin polymerase *CD1* gene and (B) the wax biosynthesis *CER6* gene during M82 and *hcr1* fruit development was quantified by qPCR.

4.3.7 *hcr1* mutant exhibit reduced levels of cellulose in fruit pericarp

Several studies have suggested that structural sterols may be involved in cellulose biosynthesis (Peng et al., 2002; Schrick et al., 2004; Bessueille et al., 2009). To examine the potential association between sterols and

cellulose biosynthesis in the *hcr1* mutant, the crystalline cellulose content in the pericarp of *hcr1* and wild type fruit at 12 DAP and the mature green stage was measured. The results showed that the crystalline cellulose levels in *hcr1* pericarp at both stages were reduced to 65% and 70% of that of the wild-type, respectively (Fig. 4.15), suggesting significant cell-wall cellulose deficiency in both stages. This result was consistent with the studies of three other sterol biosynthesis mutants from *Arabidopsis*, *fk*, *hyd1* and *smt1/cph* (Schrick et al., 2004).

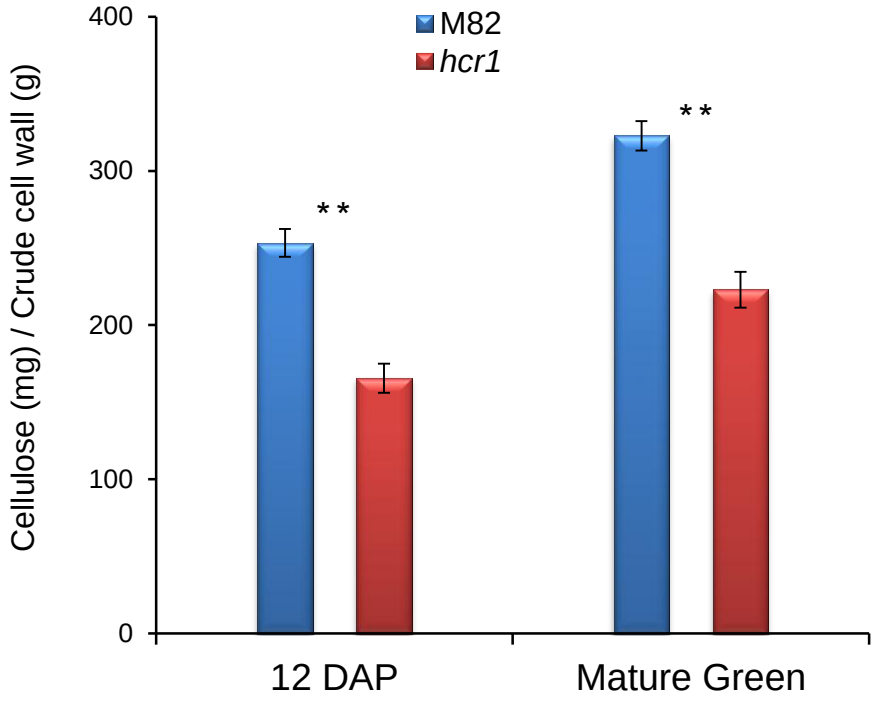

Figure 4.15 Crystalline cellulose content of *hcr1* and M82 fruit pericarp at 12 DAP and mature green stages.
(Mean ± SD of N = 4; ** P < 0.01 by two-tailed t-test.)

4.3.8 The gene expression of three subunits of cellulose synthase complex

It was hypothesized that the observed decrease of cellulose levels in cell wall extracts from *hcr1* pericarp could have resulted from reduced expression of cellulose synthase. To test this, we assessed the transcript levels of three subunits of cellulose synthase using qPCR (*SlCesA1, SlCesA3*, and *SlCesA2*/ *SlCesA6*). Through phylogenetic analysis, *SlCesA1* and *SlCesA3*, which appear to be orthologous to *Arabidopsis* CesA1 and CesA3, respectively, were identified in the tomato genome. But *SlCesA6* and *SlCesA2* could not be unambiguously distinguished form each other because the similarity of these two genes was too high. The result showed that the difference in expression levels of *SlCesA1* and *SlCesA3* (Fig. 4.16A, B) between M82 and *hcr1* mutant were small, but statistical differences were detected in gene expression level of CesA6-like subunit (Fig. 4.16C). However, considering that this difference was small (0.5~1 fold only) and the function of CesA6-like subunit can be compensated by other CesAs, the function of the cellulose synthase complex for primary cell wall formation may not be substantially affected by *hcr1* lesion at the level of transcript abundance.

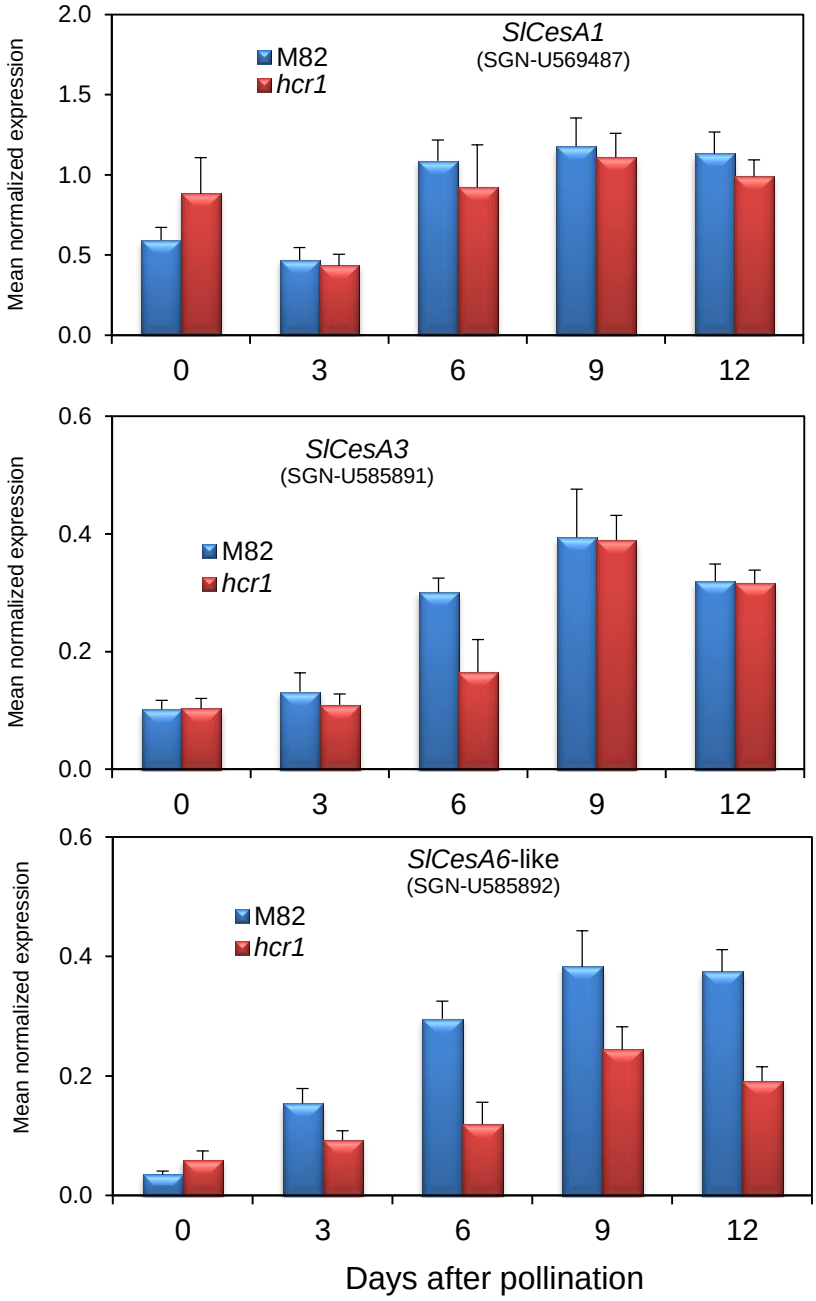

Figure 4.16 The expression patterns of marker genes related to cellulose biosynthesis. The expression patterns of *SlCesA1*(A), *SlCesA3*(B) and *SlCesA6*-like (C) during M82 and *hcr1* fruit development were quantified by qPCR.

4.3.9 Subcellular localization of HCR1 protein

HCR1 protein possesses the putative ER retrieval signal KXKXX-COOH at the C-terminus. In order to verify subcellular localization, confocal imaging analysis was performed of HCR1 fused to the tdTOMATO fluorescent reporter protein following transient expression in onion epidermal cells. The HCR1: tdTOMATO fusion protein co-localized with a GFP–ER marker protein, but not with a cytoplasmic GFP marker (Fig. 4.11). This result confirmed that HCR1 resides in ER membranes, in agreement with the current model that the ER is the site of sterol synthesis (Carland, et al., 2010).

4.4 Discussion

4.4.1 A function for 3β-hydroxysteroid-dehydrogenase/C4-decarboxylase in the plant sterol biosynthetic pathway.

Map based cloning revealed that the *HCR1* gene encodes a predicted 3β-hydroxysteroid-dehydrogenase/C4-decarboxylase, a bifunctional enzyme that catalyzes the demethylation of two C-4 methyl groups in the sterol biosynthesis pathway (Rehier etl al., 2006). This pathway has been well-defined in plants by biochemical and molecular studies of sterol mutants (Benveniste, 2004; Boutte and Grebe, 2009). Sterols become functional

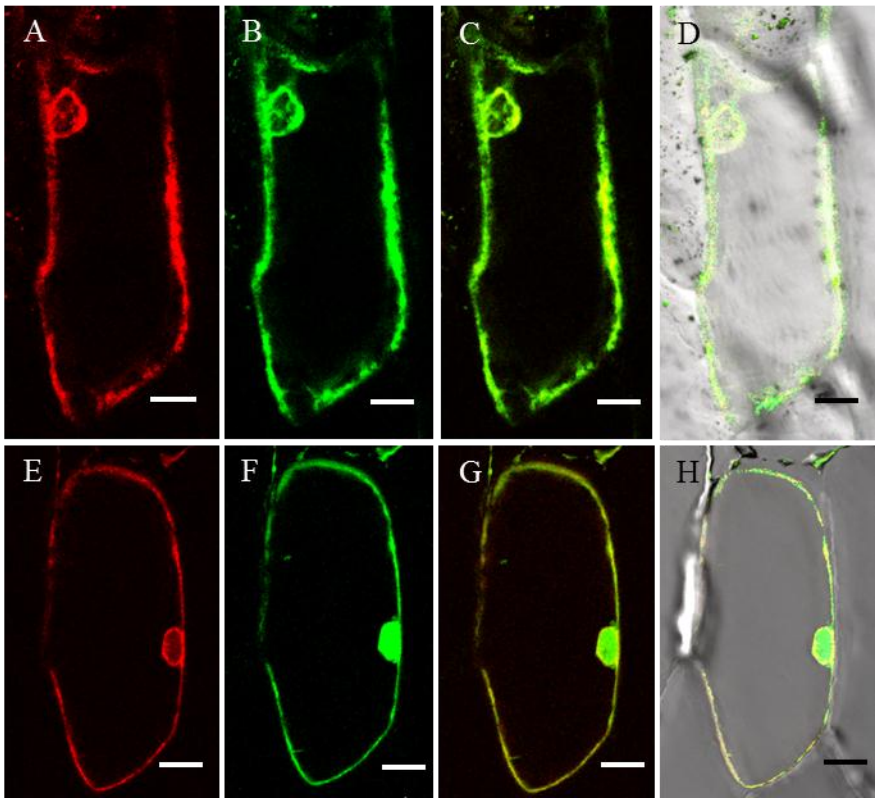

Figure 4.17 ER localization of HCR1-tdTOMATO fusion protein in onion epidermal cells (A-D) HCR1-tdTOM protein (A) showed co-localization with GFP–ER marker (B), with the corresponding merged (C) and the bright-field image (D). (E-H) Localization of a cytoplasmic GFP marker (F) was compared to that of HCR1-tdTOM (E), with the corresponding merged (G) and bright-field images (H). Scale bars = 25 μm.

molecules only after the removal of two methyl groups from the C-4 position of sterol precursors. The metabolic enzymes, catalytic mechanism and the structure of multienzyme complex for sterol C-4 demethylation in higher plants have been thoroughly reviewed (e.g. Rahier, 2011). In brief, three individual enzymes, including a sterol methyl oxidase (SMO) (Lees et al., 1995; Darnet

and Rahier, 2004), a 3β-hydroxysteroid-dehydrogenase/C4-decarboxylase (3β-HSD/D) (Rahier et al., 2006, 2009) and a 3-ketosteroid reductase (SR), are likely tethered as a membrane-bound multienzyme complex and sequentially participate in each C-4 demethylation step. Two 3β-HSD/D genes were identified from *Arabidopsis* and their functions have been well-characterized (Rahier et al., 2006, 2009). Substrate screening studies showed that these two isoenzymes require free 3β-hydroxyl and C-4-carboxyl groups for the enzymatic reaction, but are quite tolerant of structural variations in the sterol nucleus and side chains. An enzymatic activity assay revealed that the apparent catalytic rates of At3β-HSD/Ds are very high compared to those of other enzymes in the postsqualene sterol pathway, suggesting they are not rate-limiting steps in the overall sterol biosynthesis.

4.4.2 Sterols and plant growth

Sterols are essential lipid components of cell membranes that provide stability to the phospholipid bilayer and play a critical role in maintaining membrane integrity and function. They may directly or indirectly modulate the activity of integral membrane proteins, including enzymes, ion channels and signal transduction components (Schaller, 2003, 2004; Boutte and Grebe, 2009). Plant sterols are also the precursors of the brassinosteroid (BR) hormones and so have considerable influence on various plant physiological processes (Asami et al., 2005; Wang et al., 2006; Li, 2010). Molecular and

biochemical approaches to characterize sterol mutants with altered sterol profiles, or genetic manipulation of sterol-related genes in *Arabidopsis* have revealed pleiotropic roles of sterols in plant growth and development. These include patterning of organs (e.g. embryo, vein, shoot and root), cell expansion/ elongation, cell polarity and proliferation, reactive oxygen species (ROS) regulation, cellulose biosynthesis, root hair initiation and hormone signaling (Diener et al., 2000; Jang et al., 2000; Schrick et al., 2000, 2004; Carland et al., 2002, 2010; Peng et al., 2002; Souter et al., 2002, 2004; Willemsen et al., 2003; Men et al., 2008; Pose and Botella, 2009; Ovecka et al., 2010). However, the molecular mechanism underlying the specific phenotypes observed in many sterol-deficient mutants remain obscure and molecular downstream targets of sterols are largely unknown.

A common phenotype noted in many sterol synthetic mutants is a dwarfism, which is thought to be caused by an inhibition of cell expansion and division (Schrick et al., 2000, 2004; Pose et al., 2009; Carland et al., 2010). Brassinosteroids (BRs), derived from campesterol, are involved in numerous plant developmental processes, such as cell expansion and elongation, cell division and cell wall regeneration (Clouse and Sasse 1998; Cano-Delgado et al., 2004; Nemhauser et al., 2004). However, the dwarfed phenotype of most sterol biosynthetic mutants cannot be rescued by exogenous BR treatment, indicating that structural sterol molecules are also crucial for cell expansion and division (Fujioka and Yokota, 2003; Schaller, 2003; Carland et al., 2010).

Gene expression analysis demonstrated that exogenous application of both typical (sitosterol and stigmasterol) and atypical (e.g. 8, 14-diene sterols) sterols can activate the expression of genes involved in cell expansion and division, while sterol biosynthetic genes are regulated by several growth-promoting hormones, including BRs and auxin (He et al., 2003). This suggests the existence of a signaling crosstalk among sterols, hormones and the genes involved cell growth; however, knowledge of the regulatory role of sterols in transcriptional regulation of cell growth-related genes is still extremely limited.

Plant cell expansion and division require coordinated biosynthesis and restructuring of the cell wall, the major load bearing component of which is the cellulose/xyloglucan network (Rose and Bennett, 1999). Various studies have indicated that sterols are involved in cellulose biosynthesis, which in turn suggests that perturbations in sterol biosynthesis may adversely affect cell wall formation and lead to impaired cell division and expansion. Peng et al. (2002) reported that a CesA glucosyltransferase may initiate glucan polymerization using sitosterol-β-glucoside (SG) as a primer (Peng et al., 2002). This proposed model, however, could not adequately explain the causal relations between sterol-deficiency and cellulose deficiency in some sterol mutants, as the primer role of SG may be easily fulfilled by residual levels of steryl glycosides (DeBolt et al., 2009). In a comparative study of three sterol mutants, it was found that the *fackel*, *hydra1* and *smt1/cph*

mutants shared similar cellular ultrastructural features, such as incomplete cell walls, aberrant wall thickenings and ectopic callose or lignin deposits, despite distinct variances in their sterol profiles. In addition, all three mutants exhibited a cellulose deficiency in in the seedling cell walls, but normal levels of pectins and sugars, leading the authors to speculate that sterols are involved in cellulose synthesis (Schrick et al., 2004).

In recent years, the structure, composition, and possible functions of membrane raft-like domains of the plant PM have been studied (Peskan et al., 2000; Bessueille et al., 2009; Mongrand et al., 2010; Carmona-Salazar et al., 2011). Sterols and sphingolipids are enriched in these raft-like plasma membrane domains and the self-associating properties of these two types of lipids are considered to be the main driving force for the formation of stable membrane domains (Silvius, 2005). It was reported that detergent-resistant membranes (DRMs) isolated from the PM of hybrid aspen contain key wall polysaccharide synthases, including callose synthase and cellulose synthases (Bessueille et al., 2009). Indeed, more than 70% of the total glucan synthase activities in the PM were associated with this sterol-enriched DRM fraction (Bessueille et al., 2009). These results further support the possible involvement of structural sterols in cellulose biosynthesis. In addition, proteomic analyses have indicated that a high proportion of other proteins, such as ABCB19, OsRac1 and REMORIN protein, are associated with the DRM fraction, prompting speculation that DRMs may be involved in various

physiological processes such as signaling, immunity and environmental stress response etc. (Morel et al., 2006; Fujiwara, et al., 2009; Raffaele et al., 2009; Titapiwatanakun et al., 2009). Although detergent-resistant membranes may not explicitly define functional membrane rafts in plants (Boutte and Grebe, 2009; Tanner et al., 2011), such research has considerably increased our knowledge of the role of sterols in plant growth and development.

Several recent studies have demonstrated that the growth-suppressed phenotypes of two sterol synthetic mutants may be associated with the altered ROS production (Pose et al., 2009a, 2009b; Kim et al., 2010). ROS are important in the regulation of many biological processes, such as stress responses and systemic signaling and abnormal ROS accumulation can trigger oxidative stress and inhibition of cell growth, further inducing programmed cell death in relatively severe cases (Gill and Tuteja, 2010; Torres, 2010). The *sqe1-5*/*dry2 Arabidopsis* mutant shows pleiotropic developmental defects including a dwarfed appearance and pale green leaves, and was identified as a sterol synthetic mutant with a point mutation in the *Squalene Epoxidase 1* (*SQE1*) gene. Notably, the strong developmental defects were not correlated with changes in sterol composition, but rather with the altered production of ROS. In addition, this mutation caused the mislocalization of the RHD2 NADPH oxidase and induced ectopic accumulation of ROS in root hair cells, leading to the suggestion that sterols play an essential role in ROS regulation (Pose et al., 2009a, 2009b). In

another study, the *Arabidopsis cyp51a2* mutant, which displays pleiotropic defects, such as stunted hypocotyls, short roots, reduced cell elongation and seedling lethality (Kim et al., 2005) was shown to have a defect in a gene encoding an obtusifoliol 14α-demethylase enzyme, which performs the 14α-demethylation step in the sterol biosynthetic pathway. Transcriptome and proteome profiling analyses suggested that changes in membrane sterol composition in the *cyp51a2* mutant trigger the generation of ROS and ethylene, and eventually cause seedling senescence and death (Kim et al., 2010). Other possible roles of sterols in cell expansion and division have also been proposed. For example, the cell expansion defects of the *smt* mutants may be related to the regulatory roles of sterols in cell cycling (Carland et al., 2010).

It is apparent that sterols are involved in many and diverse aspects of plant cell function, through multiple complex mechanisms. This is reflected in the presence of a broad array of major sterols, numerous intermediates and a range of structural modifications (e.g. glycosylation and acylation), perturbations of which have been identified in different sterol mutants (Chaturvedi et al., 2011; Schrick et al., 2011; Wewer et al., 2011). Considering the pleiotropic phenotypes, the presence of many sterol molecular species and diverse molecular downstream targets of different sterols, the functional characterization of plant sterol remains challenging.

4.4.3 The sterol profile of *hcr1* fruit may be partially complemented by *HCR2*

It is common that redundancy among enzymes or even pathways ensures a balanced sterol composition and maintains sterols at adequate levels in plants (Carland et al., 2010). This homeostasis mechanism underscores the crucial role of sterols on plant growth and development. In *Arabidopsis,* two 3β-HSD/D isoenzymes can catalyze the demethylation without obvious preference *in vitro* between substrates with one or two substituents at C-4 position, suggesting that the enzymes have enzymes complementary characteristics (Rahier, 2011). Similarly, in this study, the two tomato 3β-HSD/D isoenzymes (HCR1 and HCR2) share a high level of sequence identity (84%) (Fig. 4.5), suggesting that they may functionally compensate for each other. Most *hcr1* gene transcripts (>99%) were defective, but the *hcr1* mutant plants were phenotypically normal and the sterol profiles of the *hcr1* leaves were unaffected. A possible explanation for this result is that the function of *HCR1* gene is complemented by *HCR2*.

Redundancy between *HCR1* and *HCR2* is also consistent with relatively small differences in fruit sterol composition between *hcr1* and M82: only an 11-16% reduction in total sterols was detected in *hcr1* pericarp samples at three developmental stages. The expression pattern analysis of the two genes provides further support for such redundancy as *HCR1* was expressed

at low levels at 0 DAP, but quickly peaked at 3 DAP, and then gradually reduced to about of 20% of the peak level at 12 DAP (Fig. 4.9). In contrast, *HCR2* was expressed at low levels with a relatively stable expression pattern (Fig. 4.10) during early fruit development. A comparison of the relative transcript levels of the two genes showed that the ratio of normalized expression values of *HCR1* to *HCR2* was about 6-fold at 3DAP, but almost zero at 12DAP. Transcript abundance analysis using an RNA-Seq digital expression database of the Ailsa Craig tomato variety showed that the number of normalized reads of *HCR1* was about two-fold higher than that of *HCR2* at 10 DAP (Matas et al., 2011). This result is in agreement with the assessment of relative transcript abundance of the two genes based on qPCR.

4.4.4 Evidence that sterols influence cellulose synthesis in *hcr1* fruit

Cellulose is the dominant structural component of plant cell walls. However, despite considerable progress made over the last decade, many fundamental questions related to the mechanisms of cellulose synthesis and our knowledge of its regulation and modulation is very limited (Mutwil et al., 2008; Endler and Persson, 2011; Guerriero et al., 2010).

As mentioned above, studies of sterol synthetic mutants (Schrick et al., 2004) and biochemical association of cellulose synthase activity with sterol rich PM extracts (Bessueille et al., 2009) provide indirect evidence that sterols are important for cellulose synthesis. The crystalline cellulose content in the

pericarp of *hcr1* fruit at 12 DAP or the mature green stage was only about 65-70% of that in wild-type, which is a similar reduction to that reported for the three sterol-deficient *Arabidopsis* mutants (Schrick, et al., 2004). This suggests a possible causal relationship between sterol deficiency in the *hcr1* fruit and the reduction in crystalline cellulose, which could in turn lead to an inhibition of cell division/expansion, impaired pericarp development and fruit cracking. Unlike *fk*, *hyd1* and *smt1/cph* mutants, the levels of bulk sterols in the pericarp of *hcr1* mutant is only 11-16% less than those of wild-type, while the reduction of crystalline cellulose content in the pericarp of *hcr1* fruit is substantial. However, redundancy of function between HCR1 and HCR2 provides a possible explanation for this discrepancy.

4.4.5 Is the *hcr1* growth inhibition phenotype associated with other physiological disorders?

Rapid and transient generation of ROS is considered to be an important component of the resistance response of plants to various abiotic and biotic stresses (Neill et al., 2002). ROS can serve as direct protective agents through their toxicity, but may also regulate many physiological processes such as stress responses, systemic signaling and programed cell death (Gill and Tuteja, 2010; Torres, 2010). ROS generation in plant cells is normally counterbalanced by the action of antioxidant enzymes or other redox molecules. However, abiotic or biotic stresses may lead to the overproduction

of ROS, which are highly reactive and toxic to proteins, lipids and DNA, resulting in oxidative stress. Recently, studies of two sterol synthetic mutants, *dry2/sqe1-5* and *cyp51A2,* revealed that the reduction of the sterol biosynthetic enzyme activities can trigger the ectopic accumulation of ROS and eventually cause abnormal phenotypes (Pose et al., 2009b; Kim et al., 2010), although the underlying molecular mechanism remain unclear.

In *hcr1* mutant, some phenotypic traits, including leaf necrosis and fruit discoloration are similar to several physiological stresses (e.g. programed cell death) triggered by ROS accumulation. In an experiment involving *3βHSD/D* gene silencing using virus induced gene silencing (VIGS), 4-carboxysterol, an atypical sterol derivative which account for 2-3% of the total sterol content was detected in infected *Nicotiana benthamiana* plants (Rahier et al., 2006, 2011). Hence we cannot rule out the possibility that some of the *hcr1* phenotypes are associated with ROS accumulation or abnormal sterols due to the reduced enzymatic activities of 3βHSD/D.

4.4.6 Proposed model of *hcr1* mutation

Based on the information gathered from morphological, cytological, biochemical and molecular experiments, a model is proposed to explain how the *HCR1* gene lesion causes the observed fruit phenotypes (Figure 4.18.) In this model, a nucleotide substitution (G to A) at the 3' splice site of the *HCR1* gene leads to the loss of the enzymatic activity of 3β-HSD/D, which consequently results in the sterol deficiency of *hcr1* fruit, especially during the

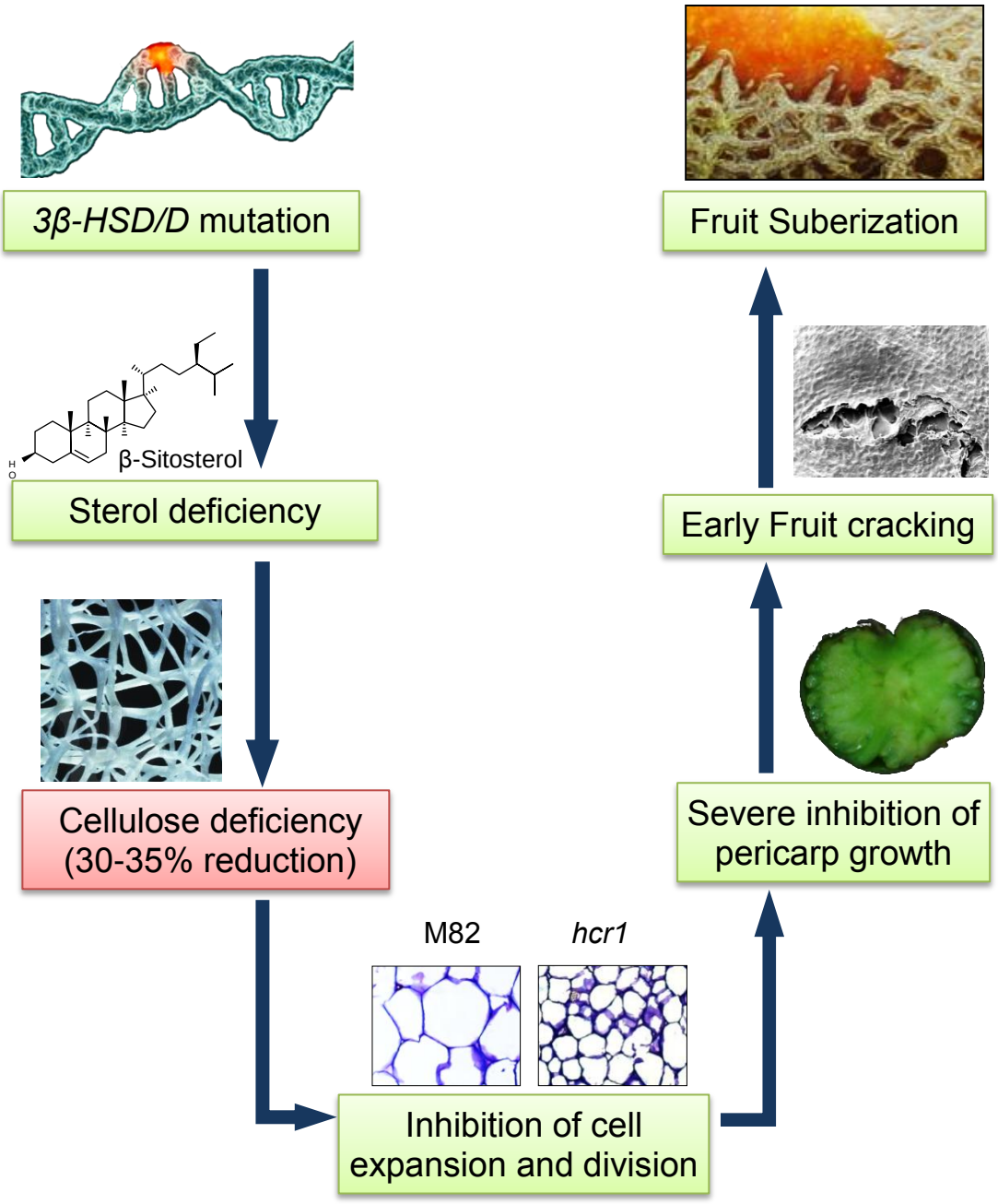

Figure 4.18 Proposed model for the relations between phenotypes and *hcr1* mutation

high expression of *HCR1* gene at 3 to 9 DAP. The sterol deficiency further causes reduced cellulose synthesis in the fruit pericarp cells walls, resulting in inhibited the cell division and expansion. The mechanically weak pericarp cracks during early fruit expansion and the observed fruit suberization is a normal wound-healing response to this cracking.

REFERENCES

Asami, T., Nakano, T. and Fujioka, S. (2005) Plant brassinosteroid hormones. *Vitam. Horm.,* **72**, 479-504.

Benveniste P. (2004) Biosynthesis and accumulation of sterols. *Annu. Rev. Plant Biol.*, **55**, 429-57.

Bessueille, L., Sindt, N., Guichardant, M., Djerbi, S., Teeri, T. T. and Bulone, V. (2009) Plasma membrane microdomains from hybrid aspen cells are involved in cell wall polysaccharide biosynthesis. *Biochem J.,* **420**(1), 93-103.

Bishop, G.J., Nomura, T., Yokota, T., Harrison, K., Noguchi, T., Fujioka, S., Takatsuto, S., Jones, J. D. and Kamiya, Y. (1999) The tomato DWARF enzyme catalyses C-6 oxidation in brassinosteroid biosynthesis. *Proc. Nat.l Acad. Sc.i U S A,* **96**(4), 1761-6.

Blakeney A. B. and Mutton L. L. (1980) A simple colorimetric method for the determination of sugars in fruit and vegetables. *J. Sci. Food Agric.*, 31:889-97

Boutte, Y. and Grebe, M. (2009) Cellular processes relying on sterol function in plants. *Curr. Opin. Plant Biol.,* **12**(6), 705-713.

Buda, G.J., Isaacson, T., Matas, A. J., Paolillo, D. J. and Rose, J. K. (2009) Three-dimensional imaging of plant cuticle architecture using confocal scanning laser microscopy. *Plant J.,* **60**(2), 378-385.

Cano-Delgado, A., Yin, Y., Yu, C., Vafeados, D., Mora-Garcia, S., Cheng, J. C., Nam, K. H., Li, J. and Chory, J. (2004) BRL1 and BRL3 are novel brassinosteroid receptors that function in vascular differentiation in *Arabidopsis*. *Development,* **131**(21), 5341-5351.

Carland, F., Fujioka, S. and Nelson, T. (2010) The sterol methyltransferases SMT1, SMT2, and SMT3 influence *Arabidopsis* development through nonbrassinosteroid products. *Plant Physiol.,* **153**(2), 741-56.

Carland, F.M., Fujioka, S., Takatsuto, S., Yoshida, S. and Nelson, T. (2002) The identification of CVP1 reveals a role for sterols in vascular patterning. *Plant Cell,* **14**(9), 2045-58.

Carmona-Salazar, L., El Hafidi, M., Enriquez-Arredondo, C., Vazquez-Vazquez, C., Gonzalez de la Vara, L. E. and Gavilanes-Ruiz, M. (2011) Isolation of detergent-resistant membranes from plant photosynthetic and non-photosynthetic tissues. *Anal. Biochem.,* **417**(2), 220-227.

Chaturvedi, P., Misra, P. and Tuli, R. (2011) Sterol glycosyltransferases-the enzymes that modify sterols. *Appl. Biochem. Biotechnol.,* **165**(1), 47-68.

Cifuentes, C., Bulone, V. and Emons, A. M. (2010) Biosynthesis of callose and cellulose by detergent extracts of tobacco cell membranes and quantification of the polymers synthesized in vitro. *J. Integr. Plant Biol.,* **52**(2), 221-33.

Clouse, S.D. (2002) *Arabidopsis* mutants reveal multiple roles for sterols in plant development. *Plant Cell,* **14**(9), 1995-2000.

Clouse, S.D. and Sasse, J. M. (1998) BRASSINOSTEROIDS: Essential regulators of plant growth and development. *Annu. Rev. Plant Physiol. Plant Mol. Biol.,* **49**, 427-451.

DeBolt, S., Scheible, W. R., Schrick, K., Auer, M., Beisson, F., Bischoff, V., Bouvier-Nave, P., Carroll, A., Hematy, K., Li, Y., Milne, J., Nair, M., Schaller, H., Zemla, M. and Somerville, C. (2009) Mutations in UDP-glucose:Sterol glucosyltransferase in *Arabidopsis* cause transparent testa phenotype and suberization defect in seeds. *Plant Physiol.,* **151**(1), 78-87.

Duperon, R., Thiersault, M. and Duperon, P. (1984) High level of glycosylated sterols in species of solanum and sterol changes during the development of the tomato. *Phytochemistry (Oxford),* **23**(4), 743-746.

Endler, A. and Persson, S. (2011) Cellulose synthases and synthesis in *Arabidopsis*. *Mol. Plant,* **4**(2), 199-211.

Foreman, J., Demidchik, V., Bothwell, J. H., Mylona, P., Miedema, H., Torres, M. A., Linstead, P., Costa, S., Brownlee, C., Jones, J. D., Davies, J. M. and Dolan, L. (2003) Reactive oxygen species produced by NADPH oxidase regulate plant cell growth. *Nature,* **422**(6930), 442-446.

Foster, C.E., Martin, T. M. and Pauly, M. (2010) Comprehensive compositional analysis of plant cell walls (lignocellulosic biomass) Part II: Carbohydrates. *J. Vis. Ex.,* **37**, 1837.

Fujiwara, M., Hamada, S., Hiratsuka, M., Fukao, Y., Kawasaki, T. and Shimamoto, K. (2009) Proteome analysis of detergent-resistant

membranes (DRMs) associated with OsRac1-mediated innate immunity in rice. *Plant Cell Physiol.,* **50**(7), 1191-1200.

Galea, A.M. and Brown, A. J. (2009) Special relationship between sterols and oxygen: Were sterols an adaptation to aerobic life? *Free Radical Biology & Medicine,* **47**(6), 880-889.

Gill, S.S. and Tuteja, N. (2010) Reactive oxygen species and antioxidant machinery in abiotic stress tolerance in crop plants. *Plant Physiol. Biochem.,* **48**(12), 909-30

Gleave, A.P. (1992) A versatile binary vector system with a T-DNA organizational structure conducive to efficient integration of cloned DNA into the plant genome*. Plant Mol. Biol.,* **20**, 1203–1207.

Grille, S., Zaslawski, A., Thiele, S., Plat, J. and Warnecke, D. (2010) The functions of steryl glycosides come to those who wait: Recent advances in plants, fungi, bacteria and animals. *Prog. Lipid Res.,* **49**(3), 262-88.

Guerriero, G., Fugelstad, J. and Bulone, V. (2010) What do we really know about cellulose biosynthesis in higher plants? *J. Integr. Plant. Biol.,* **52**(2), 161-175.

He, J.X., Fujioka, S., Li, T. C., Kang, S. G., Seto, H., Takatsuto, S., Yoshida, S. and Jang, J. C. (2003) Sterols regulate development and gene expression in *Arabidopsis*. *Plant Physiol.,* **131**(3), 1258-69.

Jang, J., Fujioka, S., Tasaka, M., Seto, H., Takatsuto, S., Ishii, A., Aida, M., Yoshida, S. and Sheen, J. (2000) A critical role of sterols in embryonic patterning and meristem programming revealed by the *fackel* mutants of *Arabidopsis thaliana*. *Genes and Development,* **14**(12), 1485-1497.

Jaspers, P. and Kangasjarvi, J. (2010) Reactive oxygen species in abiotic stress signaling. *Physiol. Plant,* **138**(4), 405-13.

Jefferson, R.A., Kavanagh, T. A. and Bevan, M. W. (1987) Gus fusions beta glucuronidase as a sensitive and versatile gene fusion marker in higher plants. *EMBO (European Molecular Biology Organization) Journal,* **6**(13), 3901-3908.

Jornvall, H., Persson, B., Krook, M., Atrian, S., Gonzalez-Duarte, R., Jeffery, J. and Ghosh, D. (1995) Short-chain dehydrogenases/reductases (SDR). *Biochemistry,* **34**(18), 6003-13.

Kelley, B.S., Lee, S. J., Damasceno, C. M., Chakravarthy, S., Kim, B. D., Martin, G. B. and Rose, J. K. (2010) A secreted effector protein (SNE1) from phytophthora infestans is a broadly acting suppressor of programmed cell death. *Plant J.,* **62**(3), 357-66.

Kim, H.B., Lee, H., Oh, C. J., Lee, H. Y., Eum, H. L., Kim, H. S., Hong, Y. P., Lee, Y., Choe, S., An, C. S. and Choi, S. B. (2010) Postembryonic seedling lethality in the sterol-deficient *Arabidopsis* cyp51A2 mutant is partially mediated by the composite action of ethylene and reactive oxygen species. *Plant Physiol.,* **152**(1), 192-205.

Kim, H.B., Schaller, H., Goh, C. H., Kwon, M., Choe, S., An, C. S., Durst, F., Feldmann, K. A. and Feyereisen, R. (2005) *Arabidopsis* cyp51 mutant shows postembryonic seedling lethality associated with lack of membrane integrity. *Plant Physiol.,* **138**(4), 2033-2047.

Kim, T.W., Chang, S. C., Lee, J. S., Takatsuto, S., Yokota, T. and Kim, S. K. (2004) Novel biosynthetic pathway of castasterone from cholesterol in tomato. *Plant Physiol.,* **135**(3), 1231-42.

Koka, C.V., Cerny, R. E., Gardner, R. G., Noguchi, T., Fujioka, S., Takatsuto, S., Yoshida, S. and Clouse, S. D. (2000) A putative role for the tomato genes DUMPY and CURL-3 in brassinosteroid biosynthesis and response. *Plant Physiol.,* **122**(1), 85-98.

Leide, J., Hildebrandt, U., Reussing, K., Riederer, M. and Vogg, G. (2007) The developmental pattern of tomato fruit wax accumulation and its impact on cuticular transpiration barrier properties: Effects of a deficiency in a beta-ketoacyl-coenzyme A synthase (LeCER6). *Plant Physiol.,* **144**(3), 1667-79.

Li, J. (2010) Regulation of the nuclear activities of brassinosteroid signaling. *Curr. Opin. Plant Biol.,* **13**(5), 540-547.

Lindsey, K., Pullen, M. L. and Topping, J. F. (2003) Importance of plant sterols in pattern formation and hormone signalling. *Trends Plant Sci.,* **8**(11), 521-525.

Matas, A.J., Yeats, T. H., Buda, G. J., Zheng, Y., Chatterjee, S., Tohge, T., Ponnala, L., Adato, A., Aharoni, A., Stark, R., Fernie, A. R., Fei, Z., Giovannoni, J. J. and Rose, J. K. (2011) Tissue- and cell-type specific transcriptome profiling of expanding tomato fruit provides insights into metabolic and regulatory specialization and cuticle formation. *Plant Cell,* .

Mayer, A.M. (2006) Polyphenol oxidases in plants and fungi: Going places? A review. *Phytochemistry,* **67**(21), 2318-31.

Menda, N., Semel, Y., Peled, D., Eshed, Y. and Zamir, D. (2004) In silico screening of a saturated mutation library of tomato. *Plant J.,* **38**(5), 861-872.

Molina, I., Li-Beisson, Y., Beisson, F., Ohlrogge, J. B. and Pollard, M. (2009) Identification of an *Arabidopsis* feruloyl-coenzyme A transferase required for suberin synthesis. *Plant Physiol.,* **151**(3), 1317-28.

Mongrand, S., Stanislas, T., Bayer, E. M., Lherminier, J. and Simon-Plas, F. (2010) Membrane rafts in plant cells. *Trends Plant Sci.,* **15**(12), 656-63.

Montoya, T., Nomura, T., Farrar, K., Kaneta, T., Yokota, T. and Bishop, G. J. (2002) Cloning the tomato curl3 gene highlights the putative dual role of the leucine-rich repeat receptor kinase tBRI1/SR160 in plant steroid hormone and peptide hormone signaling. *Plant Cell,* **14**(12), 3163-76.

Montoya, T., Nomura, T., Yokota, T., Farrar, K., Harrison, K., Jones, J. D., Kaneta, T., Kamiya, Y., Szekeres, M. and Bishop, G. J. (2005) Patterns of dwarf expression and brassinosteroid accumulation in tomato reveal the importance of brassinosteroid synthesis during fruit development. *Plant J.,* **42**(2), 262-9.

Morel, J., Claverol, S., Mongrand, S., Furt, F., Fromentin, J., Bessoule, J. J., Blein, J. P. and Simon-Plas, F. (2006) Proteomics of plant detergent-resistant membranes. *Mol. Cell. Proteomics,* **5**(8), 1396-1411.

Muller, P.Y., Janovjak, H., Miserez, A. R. and Dobbie, Z. (2002) Processing of gene expression data generated by quantitative real-time RT-PCR. *BioTechniques,* **32**(6), 1372-4, 1376, 1378-9.

Mutwil, M., Debolt, S. and Persson, S. (2008) Cellulose synthesis: A complex complex. *Curr. Opin. Plant Biol.,* **11**(3), 252-257.

Nemhauser, J.L., Mockler, T. C. and Chory, J. (2004) Interdependency of brassinosteroid and auxin signaling in *Arabidopsis*. *PLoS Biol.,* **2**(9), E258.

Oppermann, U., Filling, C., Hult, M., Shafqat, N., Wu, X., Lindh, M., Shafqat, J., Nordling, E., Kallberg, Y., Persson, B. and Jornvall, H. (2003) Short-chain dehydrogenases/reductases (SDR): The 2002 update. *Chem. Biol. Interact.,* **143-144**, 247-53.

Orozco-Cardenas, M.L., Narvaez-Vasquez, J. and Ryan, C. A. (2001) Hydrogen peroxide acts as a second messenger for the induction of defense genes in tomato plants in response to wounding, systemin, and methyl jasmonate. *Plant Cell,* **13**(1), 179-191.

Ovecka, M., Berson, T., Beck, M., Derksen, J., Samaj, J., Baluska, F. and Lichtscheidl, I. K. (2010) Structural sterols are involved in both the initiation and tip growth of root hairs in *Arabidopsis thaliana*. *Plant Cell,* **22**(9), 2999-3019.

Palta, J.P., Whitaker, B. D. and Weiss, L. S. (1993) Plasma membrane lipids associated with genetic variability in freezing tolerance and cold acclimation of *Solanum* species. *Plant Physiol.,* **103**(3), 793-803.

Peng, L., Kawagoe, Y., Hogan, P. and Delmer, D. (2002) Sitosterol-beta-glucoside as primer for cellulose synthesis in plants. *Science,* **295**(5552), 147-50.

Pose, D. and Botella, M. A. (2009) Analysis of the *Arabidopsis* dry2/sqe1-5 mutant suggests a role for sterols in signaling. *Plant Signal Behav.,* **4**(9), 873-4.

Pose, D., Castanedo, I., Borsani, O., Nieto, B., Rosado, A., Taconnat, L., Ferrer, A., Dolan, L., Valpuesta, V. and Botella, M. A. (2009) Identification of the *Arabidopsis* dry2/sqe1-5 mutant reveals a central role for sterols in drought tolerance and regulation of reactive oxygen species. *Plant J.,* **59**(1), 63-76.

Potocka, A. and Zimowski, J. (2008) Metabolism of conjugated sterols in eggplant. part 1. UDP-glucose : Sterol glucosyltransferase. *Acta Biochim. Pol.,* **55**(1), 127-34.

Potocka, A. and Zimowski, J. (2008) Metabolism of conjugated sterols in eggplant. part 2. phospholipid: Steryl glucoside acyltransferase. *Acta Biochim. Pol.,* **55**(1), 135-40.

Raffaele, S., Bayer, E., Lafarge, D., Cluzet, S., German Retana, S., Boubekeur, T., Leborgne-Castel, N., Carde, J. P., Lherminier, J., Noirot, E., Satiat-Jeunemaitre, B., Laroche-Traineau, J., Moreau, P., Ott, T., Maule, A. J., Reymond, P., Simon-Plas, F., Farmer, E. E., Bessoule, J. J. and Mongrand, S. (2009) Remorin, a *Solanaceae* protein resident in membrane rafts and plasmodesmata, impairs potato virus X movement. *Plant Cell,* **21**(5), 1541-1555.

Rahier, A. (2011) Dissecting the sterol C-4 demethylation process in higher plants. from structures and genes to catalytic mechanism. *Steroids,* **76**(4), 340-52.

Rahier, A., Darnet, S., Bouvier, F., Camara, B. and Bard, M. (2006) Molecular and enzymatic characterizations of novel bifunctional 3beta-hydroxysteroid dehydrogenases/C-4 decarboxylases from *Arabidopsis thaliana*. *J. Biol. Chem.,* **281**(37), 27264-77.

Rose, J.K. and Bennett, A. B. (1999) Cooperative disassembly of the cellulose-xyloglucan network of plant cell walls: Parallels between cell expansion and fruit ripening. *Trends Plant Sci.,* **4**(5), 176-183.

Sagi, M., Davydov, O., Orazova, S., Yesbergenova, Z., Ophir, R., Stratmann, J. W. and Fluhr, R. (2004) Plant respiratory burst oxidase homologs impinge on wound responsiveness and development in lycopersicon esculentum. *Plant Cell,* **16**(3), 616-28.

Sato, S., Kato, T., Kakegawa, K., Ishii, T., Liu, Y. G., Awano, T., Takabe, K., Nishiyama, Y., Kuga, S., Sato, S., Nakamura, Y., Tabata, S. and Shibata, D. (2001) Role of the putative membrane-bound endo-1,4-beta-glucanase KORRIGAN in cell elongation and cellulose synthesis in *Arabidopsis thaliana*. *Plant Cell Physiol.,* **42**(3), 251-63.

Schaller, H. (2003) The role of sterols in plant growth and development. *Prog. Lipid Res.,* **42**(3), 163-175.

Schaller, H. (2004) New aspects of sterol biosynthesis in growth and development of higher plants. *Plant Physiol. Biochem.,* **42**(6), 465-476.

Schrick, K., Fujioka, S., Takatsuto, S., Stierhof, Y., Stransky, H., Yoshida, S. and Jurgens, G. (2004) A link between sterol biosynthesis, the cell wall, and cellulose in *Arabidopsis*. *Plant J.,* **38**(2), 227-243.

Schrick, K., Mayer, U., Horrichs, A., Kuhnt, C., Bellini, C., Dangl, J., Schmidt, J. and Jurgens, G. (2000) FACKEL is a sterol C-14 reductase required for organized cell division and expansion in *Arabidopsis* embryogenesis. *Genes Dev.,* **14**(12), 1471-84.

Schrick, K., Mayer, U., Martin, G., Bellini, C., Kuhnt, C., Schmidt, J. and Jurgens, G. (2002) Interactions between sterol biosynthesis genes in embryonic development of *Arabidopsis*. *Plant J.,* **31**(1), 61-73.

Schrick, K., Shiva, S., Arpin, J. C., Delimont, N., Isaac, G., Tamura, P. and Welti, R. (2011) Steryl glucoside and acyl steryl glucoside analysis of *Arabidopsis* seeds by electrospray ionization tandem mass spectrometry. *Lipids,*.

Shu, X., Shaner, N. C., Yarbrough, C. A., Tsien, R. Y. and Remington, S. J. (2006) Novel chromophores and buried charges control color in mFruits. *Biochemistry,* **45**(32), 9639-9647.

Silvius, J.R. (2005) Partitioning of membrane molecules between raft and non-raft domains: Insights from model-membrane studies. *Biochim. Biophys. Acta,* **1746**(3), 193-202.

Souter, M., Topping, J., Pullen, M., Friml, J., Palme, K., Hackett, R., Grierson, D. and Lindsey, K. (2002) Hydra mutants of *Arabidopsis* are defective in sterol profiles and auxin and ethylene signaling. *Plant Cell,* **14**(5), 1017-31.

Swanson, S. and Gilroy, S. (2010) ROS in plant development. *Physiol. Plant,* **138**(4), 384-92.

Tanner, W., Malinsky, J. and Opekarova, M. (2011) In plant and animal cells, detergent-resistant membranes do not define functional membrane rafts. *Plant Cell,* **23**(4), 1191-1193.

Thipyapong, P. and Steffens, J. C. (1997) Tomato polyphenol oxidase (differential response of the polyphenol oxidase F promoter to injuries and wound signals). *Plant Physiol.,* **115**(2), 409-418.

Thipyapong, P., Joel, D. M. and Steffens, J. C. (1997) Differential expression and turnover of the tomato polyphenol oxidase gene family during vegetative and reproductive development. *Plant Physiol.,* **113**(3), 707-718.

Thipyapong, P., Stout, M. J. and Attajarusit, J. (2007) Functional analysis of polyphenol oxidases by antisense/sense technology. *Molecules,* **12**(8), 1569-95.

Titapiwatanakun, B., Blakeslee, J. J., Bandyopadhyay, A., Yang, H., Mravec, J., Sauer, M., Cheng, Y., Adamec, J., Nagashima, A., Geisler, M., Sakai, T., Friml, J., Peer, W. A. and Murphy, A. S. (2009) ABCB19/PGP19 stabilises PIN1 in membrane microdomains in *Arabidopsis*. *Plant J.,* **57**(1), 27-44.

Tjellstrom, H., Hellgren, L. I., Wieslander, A. and Sandelius, A. S. (2010) Lipid asymmetry in plant plasma membranes: Phosphate deficiency-induced phospholipid replacement is restricted to the cytosolic leaflet. *Faseb. J.,* **24**(4), 1128-38.

Torres, M.A. (2010) ROS in biotic interactions. *Physiol. Plant,* **138**(4), 414-29.

Van Eck J., Kirk D. D., Walmsley A. M. (2006) Tomato (*lycopersicum esculentum*). *Methods in Molecular Biology,* **343**, 459-473.

Vogg, G., Fischer, S., Leide, J., Emmanuel, E., Jetter, R., Levy, A. A. and Riederer, M. (2004) Tomato fruit cuticular waxes and their effects on transpiration barrier properties: Functional characterization of a mutant deficient in a very-long-chain fatty acid beta-ketoacyl-CoA synthase. *J. Exp. Bot.,* **55**(401), 1401-10.

Vrebalov, J., Pan, I. L., Arroyo, A. J., McQuinn, R., Chung, M., Poole, M., Rose, J., Seymour, G., Grandillo, S., Giovannoni, J. and Irish, V. F. (2009) Fleshy fruit expansion and ripening are regulated by the tomato SHATTERPROOF gene TAGL1. *Plant Cell,* **21**(10), 3041-62.

Wang, Z.Y., Wang, Q., Chong, K., Wang, F., Wang, L., Bai, M. and Jia, C. (2006) The brassinosteroid signal transduction pathway. *Cell Res.,* **16**(5), 427-434.

Wewer, V., Dombrink, I., vom Dorp, K. and Dormann, P. (2011) Quantification of sterol lipids in plants by quadrupole time-of-flight mass spectrometry. *J Lipid Res,* **52**(5), 1039-54.

Whitaker, B.D. (1991) Changes in lipids of tomato fruit stored at chilling and non-chilling temperatures. *Phytochemistry (Oxford),* **30**(3), 757-762.

Whitaker, B.D. and Gapper, N. E. (2008) Ripening-specific stigmasterol increase in tomato fruit is associated with increased sterol C-22 desaturase (CYP710A11) gene expression. *J. Agric. Food Chem.,* **56**(10), 3828-35.

Yeats, T.H., Howe, K. J., Matas, A. J., Buda, G. J., Thannhauser, T. W. and Rose, J. K. C.(2010) Mining the surface proteome of tomato (*Solanum lycopersicum*) fruit for proteins associated with cuticle biogenesis. *J. Exp. Bot.,* **61**(13), 3759-3771.

CHAPTER 5

Conclusions and Future Directions

5.1 Conclusions

As described in the introduction, the structure, composition and other biological features of fruit cuticle have significant effects on many economically important traits, such as storability/shelf life, surface appearance and resistance to desiccation, microbial infection or cracking. Tomato is an ideal model species for fruit cuticle biology study, due to its economic importance, typical cuticle composition and the ease of cuticle isolation. Chapter two describes the mapping of three genes related to fruit cutin biosynthesis in this model system. The *CD1* gene encodes a GDSL-motif lipase/hydrolase, which catalyzes extracellular cutin polymerization at the cuticle formation site. The *CD2* gene encodes a putative transcription factor in the IV group of the homeodomain-leucine zipper family (HD-Zip IV). The *CD3* gene was identified as a homolog of Arabidopsis CYP86A, which catalyzes the ω-hydroxylation to C16 and C18 fatty acids that act a precursors for cutin formation.

In chapters three and four, the research focuses on the detailed characterization of the *hypercracking 1* (*hcr1*) mutant. The *HCR1* gene encodes a 3β-hydroxysteroid dehydrogenase/C-4 decarboxylase (3β-HSD/D1),

which is a key enzyme in the sterol biosynthesis pathway. The *hcr1* lesion results in a reduction in sterol levels in the *hcr1* fruit pericarp. Phenotypic and biochemical analysis of *hcr1* suggests that early fruit cracking is probably caused by severe inhibition of cell division and expansion and possibly defective polysaccharide cell wall biosynthesis, suggesting a role for sterols in cellulose synthesis. The observed extensive fruit suberization is likely a wound-healing response to early fruit cracking.

At least 50 genes are thought to be involved in cuticle biosynthesis, monomer transportation and regulation in *Arabidopsis*. In tomato, however, knowledge of fruit cuticle biology is less advanced. Although on the characterization of the four cuticle and fruit surface mutants presented here represents a significant contribution to the field, more effort is needed to gain a better understanding of the mechanism underlying biosynthesis, metabolism, assembly and regulation of tomato fruit cuticle.

5.2 Future Directions

5.2.1 Further study of the three *cutin-deficient* mutants

We have gained valuable information about the function of the *CD1* gene. However, a future challenge is to demonstrate the cutin polymerization activity of CD1 protein with the presumed native substrate, 2MHG, *in-vitro*.

CD2 is a promising candidate gene for developing new plant varieties with desired fruit traits via genetic manipulation. Knowledge about the function of the *CD2* gene is still limited, and it has yet to be shown to encode a *bona fide* transcription factor. If this is in fact the case, the target genes of CD2 should be identified, together with the molecular pathways involved in regulating cutin and cuticle related gene expression. With respect to the *CD3* gene, the functions of its homologs in *Arabidopsis* have been studied in some detail (Wellesen et al., 2001; Rupasinghe et al., 2007). However, it may be useful to valid the fatty acid hydroxylase activity of CD3 protein. The *cd3* mutant shows a dramatic cutin reduction in fruit cutin but no visible phenotypes in other organs. Therefore, genetic manipulation of the *CD3* gene is also a promising strategy for improving fruit quality.

5.2.2 Outline of future studies of the *hcr1* mutant

The studies of the *hcr1* mutant described here represent significant progress towards understanding the genetic and molecular mechanism underlying the cuticle cracking in the *hcr1* fruits. Briefly, the early fruit cracking of *hcr1* likely results from the developmentally abnormal and structurally weak pericarp as a consequence of the inhibition of cell expansion and division. The molecular link between sterol deficiency and this reduced cell expansions and division has still to be established; however, several sets of data, including some generated in the analysis of *hcr1* fruit, point to a connection between

abnormal sterol profiles and defective cellulose synthesis, which can be directly related to cell wall architecture and cell expansion or division.

As mentioned before, studies of the functional role of sterols in plants are still challenging, due to their pleiotropic nature and the diversity of sterol species. Currently, the following approaches might be valuable in order to explore possible mechanisms underlying the cell growth inhibition in *hcr1* fruit.

More accurate sterol profiling: In the sterol profiling experiment, only the total sterol content was measured. The transient substrate of the 3βHSD/D enzyme, 4-carboxysterol is a compound with a steroid-like structure. Unanswered questions include whether 4-carboxysterol or other abnormal sterols accumulate in *hcr1* fruit and whether such abnormal sterols are toxic to plant cells. In addition, with the development of new analytical technologies, the profile of sterol lipids can be more accurately quantified by Q-TOF mass spectrometry methods (Wewer et al., 2011). If the sterol content of M82 and *hcr1* were compared at an early fruit stage (e.g. at 3 DAP), it might provide new insights into the sterol deficiency in *hcr1* fruits at this critical stage.

RNA-Seq analysis: An array of distinct phenotypes was observed in *hcr1* fruits during the rapid expansion phase. Consequently, various physiological processes were likely perturbed in a specific *relative chronological order.* RNA-Seq is a valuable tool for transcriptomics and could be used to monitor these physiological changes at the transcriptional level. It is possible that the downstream targets affected by the *hcr1* mutation could be

identified through the differential expression analysis of genes at an early fruit growth stage (e.g. at 0-6 DAP).

5.2.3 Future directions for the study of fruit cuticle biology in tomato

Forward and reverse genetic study of fruit cuticle-related genes:

More than 50 genes involved in cuticle biosynthesis have been identified in *Arabidopsis*, maize or rice. Identifying the counterparts of those cuticle-related genes in the tomato genome via comparative analysis would lay the groundwork for genetic manipulation and for a better understanding of fruit cuticle biosynthesis. Some candidate genes in tomato may be identified by comparing sequence identities with cloned cuticle genes. For some members in a large gene family, phylogenetic analysis may provide important clues for candidate gene prediction. The confirmation of the function of candidate genes in tomato can be carried out by gene targeted mutagenesis approaches, such as RNAi, artificial miRNAs and gene overexpression.

Several tomato mutant collections based on EMS or fast neutron mutagenesis approaches have been released by different research labs. This information is accessible online and seeds of these mutants are available upon request to the tomato scientific community (http://zamir.sgn.cornell.edu/mutants/; http://tgrc.ucdavis.edu/; http://tomatoma.nbrp.jp/index.jsp). These mutant collections provide valuable genetic material for fruit cuticle biology study. For those mutants caused by the mutation of unknown genes, or with

important/ interesting phenotypic traits, map-based cloning is still an effective approach to identify the gene functions, especially in the post-genome era.

In addition, some high-throughput techniques such as “TILLING” and “FOX hunting” are powerful tools for fruit cuticle studies. Targeting Induced Local Lesions In Genomes (TILLING) platforms represent a high-throughput reverse genetic strategy for screening mutations of targeted genes. TILLING technology can discover a series of allelic mutations that are very useful for genetic analysis. With the progress of next-generation sequencing technology, detection of induced mutations in several TILLING populations (e.g. rice and wheat) have been performed on the Illumina platform (Tsai et al., 2011). The application of TILLING in tomato is still in its early stages. Rigola et al. (2009) described a KeyPoint approach to identify the mutants of the tomato eIF4E gene based on screening more than 3000 M_2 plants in a single 454 (GS FLX) sequencing run (Rigola et al., 2009). The project “TILLING resources for the tomato functional genomics community” is making substantial progress in the UCD Genome Center TILLING Laboratory (http://tilling.ucdavis.edu/index.php/Tomato_Tilling).

Another mutagenesis screen strategy, “FOX hunting” (Full-length cDNA Over-eXpressor gene hunting), can also be used to identify gene functions in plants. This gain-of-function approach is simple and effective, and allows functional analysis of genes whose action may be masked in conventional knockout approaches due to gene redundancy (Nakamura et al.,

2007; Kondou et al,. 2009; Higuchi et al,. 2011). This approach has another advantage in that the gene can be transferred to many different plants by transformation once gene function is known.

Genetic manipulation of cuticle related genes for fruit quality improvement: It has been suggested that the cuticle may affect fruit storability by providing structural support or reducing fruit water loss (Saladié et al., 2007; Kosma et al., 2010). Increased understanding of the molecular mechanisms underlying fruit cuticle biosynthesis would provide an efficient strategy to improve fruit shelf-life or other important quality traits by genetic engineering of cuticle-related genes. For example, the research described here demonstrated that the CD2 putative transcription factor may specifically regulate the expression of some cutin-related genes without interrupting other plant physiological processes. By manipulation of *CD2* gene expression via overexpression, RNAi or other genetic approaches, it may be possible to develop new tomato varieties with long shelf-life or other desired fruit traits.

APPENDIX I

Genetic markers for the mapping of the 4 cuticle mutants

(Tomato var. M82/*S. pimpinellifolium* population)

location on Chr. (Tomato-EXPEN 2000)	Marker Name	Marker category	Restriction Enzyme	Marker quality
Chromosome 1				
1.0155	5g51970	CAPS	Xba I	**
1.02	TG184	dCAPS	Ssp I	*
1.032	SSR98	SSR		**
1.0461	5g13700	CAPS	Cfo I	**
1.0467	4g02070	Indel		**
1.0474	3g08030	CAPS	Hinc II	***
1.0575	4g00090	CAPS	Rsa I	*
1.059	T1162	CAPS	Hinf I	***
1.061	cLEG-37-I19	CAPS	Hind III	**
1.062	tg59	CAPS	BstN I	***
1.065	cLES-5-J1	CAPS	Hinc II	**
1.0692	2g45620	CAPS	EcoR I	**
1.073	2g45910	CAPS	Mse I	***
1.077	T1409	dCAPS	Xmn I	**
1.081	d4g01210	dCAPs	Hind II	**
1.0925	2g38730	CAPS	Alu I	**
1.1156	1g56345	CAPS	Msp I	**
1.1283	1g10240	CAPS	Dpn II	**
1.1363	4g14110	CAPS	Hinc II (or Apo I)	***
1.165	2g16920	Indel		**
Chromosome 2				
2.002	TG608	dCAPS	Cfo I (=Hha I)	**
2.012	T1117	CAPS	Bgl II	**
2.0555	3g56210	dCAPS	HaeIII	***
2.0631	4g30930	dCAPS	BsiHK I	***
2.0701	1g11430	dCAPS	SspI	***
2.0747	1g65900	CAPS	Dde I	**
2.075	5g17410	CAPS	ApoI	**
2.0754	U223257	CAPS	Swa I	**
2.0772	3g07100	CAPS	XmnI	**
2.0785	4g35560	CAPS	Eco RI	***
2.0831	2g18030	dCAPS	PstI	***
2.0875	4g36380	CAPS	Rsa I	**
2.0908	3g01480	dCAPS	HincII	***
2.097	2g04700	CAPS	Bgl II	**

2.106	T1480	CAPS	Alu I	**
2.1095	3g02220	CAPS	Mse I	**
2.135	4g37280	CAPS	Dra I	**
Chromosome 3				
3.04	TG585	CAPS	Dra I	***
3.047	T1388	CAPS	Hinc II	**
3.0757	5g51110	Indel		**
3.081	4g17300	CAPS	Rsa I	*
3.1015	3g47990	CAPS	Spe I	**
3.139	T1621	CAPS	Hinf I	***
Chromosome 4				
4.022	3g17040	CAPS	Bgl II	***
4.046	Tg182	CAPS	Rsa I	***
4.055	T0635	CAPS	Alu I	**
4.056	3g62940	CAPS	Ssp I	***
4.0887	1g10030	CAPS	EcoR V	**
4.0975	3g16150	CAPS	Hinf I	**
4.105	TG443	Indel		**
4.129	2g45730	Indel		**
Chromosome 5				
5.019	TG441	CAPS	Taq I	**
5.025	1g30110	CAPS	Ase I	***
5.035	2g01275	Indel		**
5.0582	1g28140	CAPS	Alu I	***
5.0595	1g26670	CAPS	Dra I	***
5.119	2g01720	CAPS	Dra I	**
Chromosome 6				
6.014	T0892	dCAPS	Rsa I	**
6.044	1g73720	CAPS	Hinc II (or Sty I)	***
6.0627	1g24360	dCAPS	Taq I	**
Chromosome 7				
7.003	2g24270	CAPS	Hinf I	***
7.0235	1g19140	Indel		**
7.0433	2g20860	CAPS	Dra I	***
7.0637	U220926	CAPS	Alu I	***
7.068	3g15430	Indel		**
7.0855	1g50575	dCAPS	Hinc II	*
Chromosome 8				
8.0205	5g27390	CAPS	Rsa I	*
8.037	TG302	CAPS	Alu I	***
8.057	TG510	CAPS	Rsa I	*
8.0685	U233990	CAPS	Rsa I	**

8.072	4g11560	CAPS	Dpn II	**
8.0755	5g41350	CAPS	BsrG I	**
8.078	3g27530	CAPS	DraI	**
8.0795	1g64150	CAPS	AccI	*
8.087	TG294	CAPS	XmnI	**
Chromosome 9				
9.014	TG18	dCAPS	Rsa I	**
9.052	3g63190	Indel		**
9.062	TG348	CAPS	EcoR V	**
9.0723	1g04190	CAPS		**
9.077	T1190	CAPS	Rsa I	**
9.101	T0156	CAPS	Dpn II	***
Chromosome 10				
10.003	5g06430	Indel		**
10.014	5g60990	CAPS	Dra I (or Hinf I)	**
10.0435	1g67740	CAPS	Bfa I	**
10.06	T0615	CAPS	Hinf I (or Taq I)	**
10.0605	4g30220	CAPS	Hinf I	**
10.086	TG233	CAPS	Hinc II	***
Chromosome 11				
11.0005	5g64730	dCAPS	Hinf I	**
11.001	TG497	CAPS	TaqI	**
11.009	T1657	CAPS	HaeIII	*
11.01	3g52220	CAPS	MseI	**
11.015	5g04420	CAPS	Alu I/BgI I	***
11.0317	2g22570	CAPS	Dpn II	**
11.037	4g22260	CAPS	Hinf I	**
11.061	3g44880	dCAPS	Hha I (or Hae II)	**
11.062	3g44890	CAPS	Hinf I	**
11.089	T0302	CAPS	Msp I	***
11.103	TG393	CAPS	Dpn II	***
Chromosome 12				
12.009	TG180	CAPS	Dra I	**
12.021	TG68	CAPS	Dpn II	***
12.041	cLET-8-K4	CAPS	Taq I	***
12.0535	CT99	CAPS	Taq I	*
12.093	5g38530	CAPS	Nci I	***
12.105	1g48300	CAPS	ApoI (or Hind III)	**

Note: “Tomato-EXPEN 2000” map is used for the of marker location of genetic markers.
* OK, but not a good marker ** A good marker *** A very good marker

APPENDIX II

Phenotype and genotyping data of 4 cuticle mutants

Table 2.2 The phenotype and genotyping data for *cd1* (cm14) gene mapping

cm14(cd1)	Marker Name	TG497	54I23-DraI (HBa0054I23T7)	54I23-TaqI (HBa0054I23sp6)	T1968	18O03T7HindIII (HBa0118O03T7)	CT269	T1657	5g04420
Plant ID	Phenotype	11.001	11.003	11.003	11.005	11.005	11.006	11.009	11.015
08-105-005	Thin-cuticle	2	2	2	1	1	1	1	1
08-105-083	Thin-cuticle	2	2	2	1	1	1	1	1
08-105-048	Thick-cuticle	1	1	2	2	2	2	2	2
08-105-027	Thick-cuticle	1	1	2	2	2	2	2	2
08-105-028	Thick-cuticle	1	1	2	2	2	2	2	2
08-105-046	Thick-cuticle	1	1	1	2	2	2	2	2
08-105-023	Thick-cuticle	1	1	1	2	2	2	2	2
08-105-051	Thick-cuticle	1	1	1	2	2	2	2	2
08-105-072	Thick-cuticle	1	1	1	2	2	2	2	2
08-105-073	Thick-cuticle	1	1	1	2	2	2	2	2
08-105-081	Thick-cuticle	1	1	1	2	2	2	2	2
08-105-086	Thick-cuticle	2	2	2	2	2	2	1	1
08-105-110	Thick-cuticle	2	2	2	0	1	1	1	1

Table 2.3 The phenotype and genotyping data for *cd1* (cm14) gene fine mapping

Plant ID	Phonotype	54I23sp6 (11.003)	P190	P160	T1968 (11.005)	118003T7
08-105-110	Thick-cuticle	2	2	2	2	1
08-105-028	Thick-cuticle	1	2	2	2	2
08-105-023	Thick-cuticle	1	1	2	2	2
08-105-027	Thick-cuticle	1	1	1	2	2
08-105-046	Thick-cuticle	1	1	1	2	2
08-105-048	Thick-cuticle	1	1	1	2	2
08-105-051	Thick-cuticle	1	1	2	2	2
08-105-072	Thick-cuticle	1	1	2	2	2
08-105-073	Thick-cuticle	1	1	2	2	2
08-105-081	Thick-cuticle	1	1	2	2	2
08-105-005	Thin-cuticle	2	2	2	1	1
08-105-083	Thin-cuticle	2	2	1	1	1

Table 2.4 The phenotype and genotyping data for *cd2* (cm15) gene mapping

Plant ID	Phenotype	T1162 (1.059)	14A17T7 (1.0616)	1g65520 (1.0621)	cLES5J1 (1.065)	2g45620 (1.0692)	2g45910 (1.073)	T1409 (1.077)	d4g01210 (1.081)
cm15-44	Thick-cuticle	1	1	1	2	2	2	2	2
cm15-64	Thick-cuticle	1	1	1	2	2	2	2	2
cm15-19	Thick-cuticle	2	2	2	1	1	1	1	1
cm15-65	Thick-cuticle	2	2	2	1	1	1	1	1
cm15-103	Thick-cuticle	2	2	2	1	1	1	1	1
cm15-17	Thick-cuticle	2	2	2	1	1	1	1	1
cm15-42	Thin-cuticle	2	2	2	1	1	1	1	1
cm15-81	Thin-cuticle	2	2	2	1	1	1	1	1
cm15-71	Thin-cuticle	1	1	1	2	2	2	2	0
cm15-133	Thin-cuticle	1	1	1	2	2	2	2	2
cm15-63	Thin-cuticle	1	1	1	3	3	3	3	3
cm15-138	Thick-cuticle	3	3	3	2	2	2	2	2
cm15-93	Thick-cuticle	2	2	2	3	3	3	3	3
cm15-29	Thick-cuticle	2	2	2	3	3	3	3	3
cm15-106	Thick-cuticle	2	2	2	3	3	3	3	3
cm15-140	Thick-cuticle	2	2	2	3	3	3	0	3
cm15-75	Thick-cuticle	2	2	2	3	3	3	3	3

Table 2.5 The phenotype and genotyping data for *cd2* (cm15) gene fine mapping

Plant ID	Phenotype	1g65520 (1.062)	180M12 sp6	14D03 sp6	TG59 (1.062)	M14504 (BAC)	14A17 sp6	M35909 (BAC)	M44040 (BAC)	4g00740 (1.0623)	180M12 T7	P76	Cles5J1 (1.065)
cm15-44	Thick-cuticle	1	1	1	1	1	2	2	2	2	2	2	2
cm15-64	Thick-cuticle	1	1	1	1	1	2	2	2	2	2	2	2
cm15-19	Thick-cuticle	2	2	2	2	2	2	2	2	2	2	2	1
cm15-65	Thick-cuticle	2	2	2	2	2	2	2	2	2	2	1	1
cm15-103	Thick-cuticle	2	2	2	2	2	2	2	1	1	1	1	1
cm15-17	Thick-cuticle	2	2	2	2	2	2	1	1	1	1	1	1
cm15-42	Thin-cuticle	2	2	2	2	1	1	1	1	1	1	1	1
cm15-81	Thin-cuticle	2	2	2	2	2	1	1	1	1	1	1	1
cm15-71	Thin-cuticle	1	1	1	1	1	1	1	2	2	2	2	2
cm15-133	Thin-cuticle	1	1	1	1	1	1	1	1	1	2	2	2
cm15-63	Thin-cuticle	1	1	1	1	1	1	1	1	1	1	1	3

Note: M14504, M35909 and M44040 three makers are designed according the BAC sequence of **C01SLm0026F20.1 (134kb).**

Table 2.6 The phenotype and genotyping data for *cd3* (cm20) gene mapping

Plant ID	Phenotype	T302 (8.037)	TG510 (8.057)	U233990 (8.0685)	5g41350 (8.0775)	TG294 (8.087)
cd3-22_22	Thin_cuticle	2	1	1	1	1
cd3-22_27	Thin_cuticle	2	1	1	1	1
cd3-22_2	Thin_cuticle	2	1	1	1	1
cd3-22_22	Thin_cuticle	2	1	1	1	1
cd3-22_38	Thin_cuticle	2	1	1	1	1
cd3-22_35	Thin_cuticle	2	2	1	1	1
cd3-22_10	Thin_cuticle	3	2	1	1	1
cd3-22_39	Thin_cuticle	2	2	1	1	1
cd3-22_21	Thin_cuticle	2	2	2	1	1
cd3-22_19	Thick_cuticle	2	0	2	2	1
cd3-22_9	Thick_cuticle	1	0	2	2	2
cd3-22_25	Thick_cuticle	1	0	2	2	2
cd3-22_13	Thick_cuticle	2	0	3	3	3
cd3-22_16	Thick_cuticle	3	0	2	2	2
cd3-22_11	Thick_cuticle	2	0	2	2	3
cd3-22_23	Thick_cuticle	2	0	3	3	3

Table 2.7 The phenotype and genotyping data for *hcr1* (cm17) gene mapping

sample ID	phenotype	CfoI	Hae III	BsiHK I	SspI	Dde I	BslI	RsaI	HincII	Bgl II	Mse I
		dt608	d3g65210	d4g30930	d1g11430	1g65900	2g18030	4g36380	d3g11480	2g04700	1n3g02220
		2.002	2.055	2.0631	2.0701	2.0747	2.0831	2.0875	2.0908	2.097	2.1095
24_39	CM17	2	2	1	1	1	1	1	1	1	1
24_38	CM17	2	2	2	1	1	1	1	1	1	1
24_44	CM17	3	3	2	1	1	1	1	1	1	1
23_16	CM17	2	2	2	2	1	1	1	1	1	1
24_45	CM17	3	1	1	1	1	1	1	2	2	2
23_18	CM17	1	1	1	1	2	2	2	3	3	3
23_14	CM17	1	1	1	1	1	3	3	3	3	3
24_35	CM17?	2	1	1	1	1	2	2	2	2	2
24_53	Pimp	3	2	2	2	2	2	1	1	1	1
24_22	Pimp	3	2	2	2	2	1	1	1	1	1
24_8	Pimp	2	3	3	3	2	1	1	1	1	1
24_24	Pimp	1	1	1	1	1	2	2	2	2	2
24_55	Pimp	1	1	1	2	2	2	2	2	2	1
24_59	Pimp	1	1	1	2	2	2	2	2	2	2

Table 2.8 The phenotype and genotyping data for *hcr1* (cm17) gene fine mapping

sample ID	phenotype	2.0747								2.0754	2.0772
		DdeI	Dde	RsaI	PstI	TaqI	PvuII	pcr	HinfI	Swa I	XmnI
		1g65900	U315890	near 318141	U327923	U322331	UDP-4F	U321734	U344725	U223257	3g07100
32E2	cm17	2	2	2	2	2	2	1	1	1	1
33C11	cm17	2	2	2	1	1	1	1	1	1	1
23A11	cm17	1	1	1	1	1	1	1	1	2	2
28F4	pimp	2	2	2	2	2	2	1	1	1	1
28A11	pimp	2	2	2	2	2	2	1	1	1	1
27F4	pimp	2	2	2	2	2	3	3	3	3	3
30A1	pimp	2	2	3	3	3	3	3	3	3	3
20G7	pimp	3	3	3	3	3	2	2	2	2	2
28E1	pimp	2	3	3	3	3	3	3	3	3	3
35D2	pimp	3	3	3	3	3	3	2	2	2	2